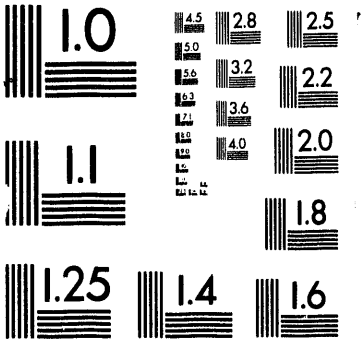
1.0
4.5
2.8
2.5
5.0
3.2
2.2
5.6
6.3
3.6
7.1
4.0
2.0
1.1
1.8
1.25
1.4
1.6

1 of 1

NIPER-724
Distribution Category UC-122

Data from Selected Almond Formation Outcrops
Sweetwater County, Wyoming

Topical Report

By
Susan R. Jackson
Viola Rawn-Schatzinger

December 1993

Work Performed Under Cooperative Agreement No. DE-FC22-83FE60149

Prepared for
U. S. Department of Energy
Assistant Secretary for Fossil Energy

Edith Allison, Project Manager
Bartlesville Project Office
P.O. Box 1398
Bartlesville, OK 74005

Prepared by
IIT Research Institute
National Institute for Petroleum and Energy Research
P.O. Box 2128
Bartlesville, OK 74005

MASTER

DISTRIBUTION OF THIS DOCUMENT IS UNLIMITED

TABLE OF CONTENTS

Page

Introduction 1
Acknowledgement 1
I Paleography of the Almond Formation 5
Depositional Environments 5
II Facies Descriptions and Facies Profiles 16
III Petrographic, Permeability and Porosity Data 34
Mineralogical Composition of the Almond Formation 34
Grain Size and Sorting (Almond Outcrop) 35
Grain Size and Porosity (Almond Outcrop) 36
Grain Size and Permeability (Almond Outcrop) 37
IV. Fractures Azimuth Measurements 46
REFERENCES 52
APPENDIX A 55

TABLES

1 Age and major shoreline movements in Upper Cretaceous Formations, south central Wyoming 7
2 Common shapes and dimensions of major tide related facies in Recent and Ancient mesotidal barrier systems 8
3 Whole rock x-ray diffraction analysis in weight percent, for samples from the upper Almond in Patrick Draw field and Rock Springs Uplift outcrops 38
4 Permeability, porosity and grainsize data measured from coreplugs drilled horizontally from Almond outcrop RG (profile 7) and RH (profile 2) localities 39

ILLUSTRATIONS

1 Locations of oil fields studies. Note the location of Patrick Draw Field, Washaskie Basin, WY. 2
2 Map of the east flank of the Rock Springs Uplift, Sweetwater County, WY 3
3 Circles indicate the location of Almond outcrops and corehole number 2 (CH#2) in Sweetwater County, Wyoming, addressed in this report 4
4 Generalized stratigraphic column of the Patrick Draw Field area, WY 9
5 East-west stratigraphic cross section of the Upper Almond Formation showing landward stepping shoreline deposits that become younger to the east 10
6 Paleogeographic setting of the Almond Formation shoreline/barrier island system 11
7 Isopach map of interval from the "A" bentonite to the top of the lower Almond outcrop 12
8 Paleogeographic map of Upper Almond Formation barrier bar G and associated facies 13
9 Dimensions and geometries of barrier island facies 14
10 Facies distribution within barrier bar G in the study area 15
11a Measured section RH-2 Almond Sandstone 0 to 40 ft 17
11b Measured section RH-2 Almond Sandstone 40 to 80 ft 18
11c Measured section RH-2 Almond Sandstone 80 to 120 ft 19
11d Measured section RH-2 Almond Sandstone 120 to 160 ft 20
12a Measured section RH-3 Almond Sandstone 0 to 40 ft 21
12b Measured section RH-3 Almond Sandstone 40 to 80 ft 22
12c Measured section RH-3 Almond Sandstone 80 to 120 ft 23
12d Measured section RH-3 Almond Sandstone 120 to 160 ft 24
13a Measured section RG-7 Almond Sandstone 0 to 40 ft 25
13b Measured section RG-7 Almond Sandstone 40 to 80 ft 26
13c Measured section RG-7 Almond Sandstone 80 to 120 ft 27
13d Measured section RG-7 Almond Sandstone 120 to 160 ft 28
13e Measured section RG-7 Almond Sandstone 160 to 200 ft 29
13f Measured section RG-7 Almond Sandstone 200 to 240 ft 30
13g Measured section RG-7 Almond Sandstone 240 to 260 ft 31
14 Cross sections of outcrops RH-2, RH-3 and RH-4, Sweetwater County, Wyoming 32
15 Legend for facies represented in Figure 14 33

TABLE OF CONTENTS

ILLUSTRATIONS (continued)

Page

16 Ternary plot of quartz-feldspar-rock fragment composition of outcrop and subsurface Almond and Muddy Formations 40
17 Grain size distribution for combined outcrop and subsurface facies in the Almond Formation 41
18 Comparison of outcrop and subsurface grain size distribution for various facies in the Almond Formation 41
19 Standard deviation for various outcrop and subsurface facies in the Almond Formation 42
20 Standard deviation versus mean grain size for outcrop and subsurface Almond Formation 42
21 Standard deviation versus mean grain size for subsurface Almond Formation facies 43
22 Standard deviation versus mean grin size for outcrop Almond Formation facies 43
23 Comparison of subsurface and outcrop facies porosity, Almond Formation 44
24 Natural log of permeability versus porosity for outcrop and subsurface Almond Formation 44
25 Comparison of subsurface and outcrop permeability distribution for Almond facies 45
26 Rose diagrams of fracture orientations and related statistics for: a) all outcrops measured in this study; b) all sandstone intervals in outcrop RG; and c) all sandstone intervals in outcrop RH 48
27 Rose diagrams of fracture orientations and related statistics for various facies in outcrop RG: a) Oyster Bed; b) Recurved Spit and Shoreface; and c) Tidal Channel facies 49
28 Rose diagrams of fracture orientations and related statistics for three major sandstone facies in outcrop RH: a) Flood Tidal Delta, Tidal Inlet and Tidal Channel; b) Tidal Channel and Delta; and c) Tidal Flat and Tidal Delta 50
29 Rose diagrams of fracture orientations and related statistics in: a) outcrop VH8; and b) "white sands" overlying bar G in outcrop RG 51
30 (a) Rose diagrams of fracture orientations and related statistics in: a) White Sandstone and Major White Sandstone northeast and north of outcrop RG; and b) sandstone (Lower Almond) underlying the marine sequence of the Upper Almond in outcrop RH 51

DATA FROM SELECTED ALMOND FORMATION OUTCROPS SWEETWATER COUNTY, WYOMING

Introduction

The data and analyses in this report resulted from work performed by NIPER for the U.S. Department of Energy under cooperative agreement DE-FC22-83FE60149, Base Program BE1, Reservoir Assessment and Characterization. The objectives of this research program are to: (1) determine the reservoir characteristics and production problems of shoreline barrier reservoirs; and (2) develop methods and methodologies to effectively characterize shoreline barrier reservoirs to predict flow patterns of injected and produced fluids.

Two reservoirs were selected for detailed reservoir characterization studies—Bell Creek field, Carter County, Montana, that produces from the Lower Cretaceous (Albian-Cenomanian) Muddy Formation, and Patrick Draw field, Sweetwater County, Wyoming that produces from the Upper Cretaceous (Campanian) Almond Formation of the Mesaverde Group (fig. 1). An important component of the research project was to use information from outcrop exposures of the producing formations to study the spatial variations of reservoir properties and the degree to which outcrop information can be used in the construction of reservoir models. A report similar to this one presents the Muddy Formation outcrtop data and analyses performed in the course of this study (Rawn-Schatzinger, 1993).

Two outcrop localities, RG and RH, previously described by Roehler (1988) provided good exposures of the Upper Almond shoreline barrier facies and were studied during 1990-1991 (fig. 2). Core from core well No. 2 drilled approximately 0.3 miles downdip of outcrop RG was obtained for study. The results of the core study will be reported in a separate volume. Outcrops RH and RG, located about 2 miles apart were selected for detailed description and drilling of core plugs (fig. 3). One 257-ft-thick section was measured at outcrop RG, and three sections ~145 ft thick located 490 and 655 feet apart were measured at the outcrop RH. Cross-sections of these described profiles were constructed to determine lateral facies continuity and changes.

This report contains the data and analyses from the studied outcrops. The outcrop data set includes: 4 measured sections and descriptions of outcrop exposures; grain-size distribution data from image analysis of 30 thin sections; permeability and porosity measurements from 25 1-inch diameter coreplugs drilled from the face of the outcrops; and 923 fracture azimuths measured from the outcrop face. This data is available in electronic format from the U.S. Department of Energy, Bartlesville Project Office. Figures and data taken from the literature have also been compiled in this report to provide background information on the outcrops described and sampled. An annotated bibliography of references on the geology and interpretation of the Almond Formation as well as general, petroleum-related papers on the greater Green River Basin is included as Appendix A. These results of the studies on the Almond Formation are reported in Szpakiewicz et al., (1991), Schatzinger et al., (1992); and Jackson et al., (1993).

ACKNOWLEDGEMENTS

The data collection and analyses contained in this report was performed by the reservoir characterization group at NIPER. Dr. Roderick W. Tillman provided valuable contributions to the description and interpretation of outcrop profiles. Editorial and technical reviews were provided by Mike Madden, Min Tham and Edith Allison. Computer graphical support was provided by Djaun Grissom and word processing by Edna Hatcher.

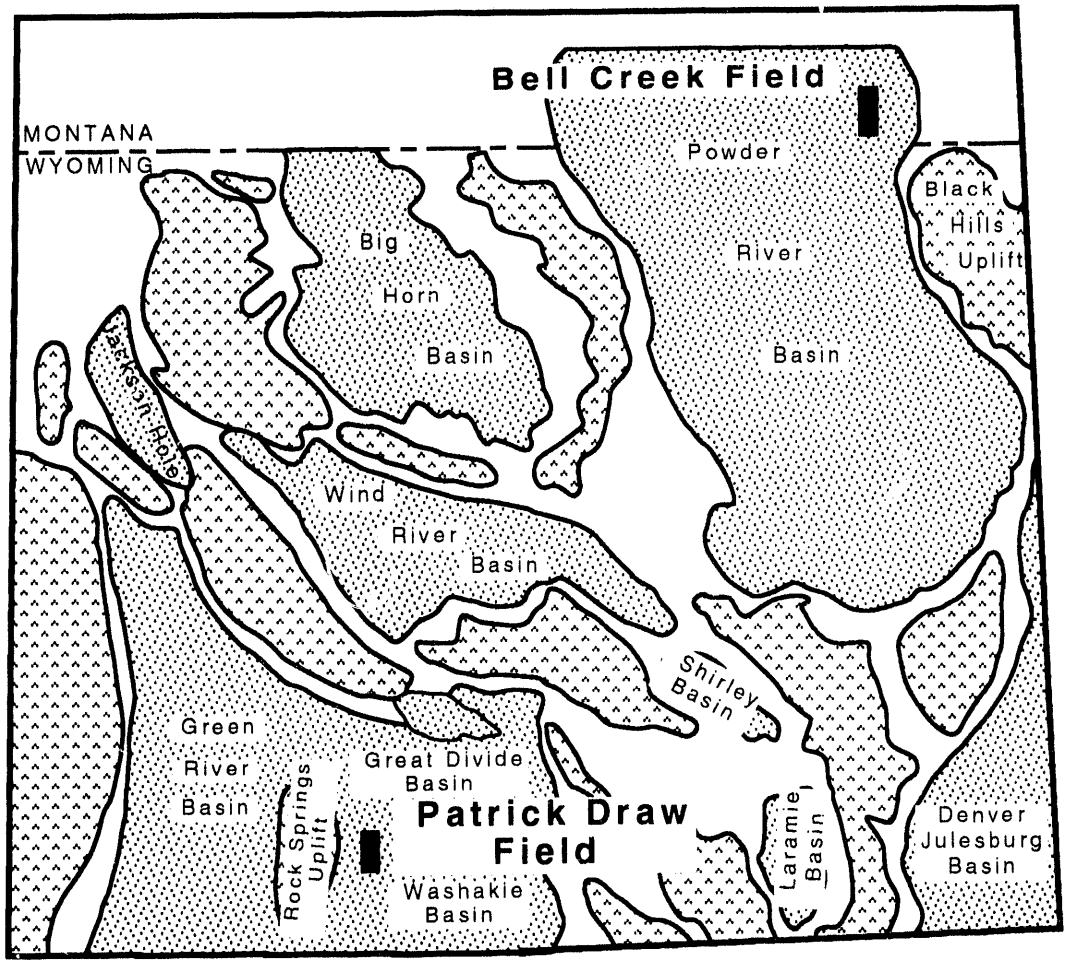

FIGURE 1 Location of oil fields studied. Note the location of Patrick Draw field, Washakie Basin, WY and Bell Creek field, Powder River Basin, MT. (After Schatzinger et al., 1992)

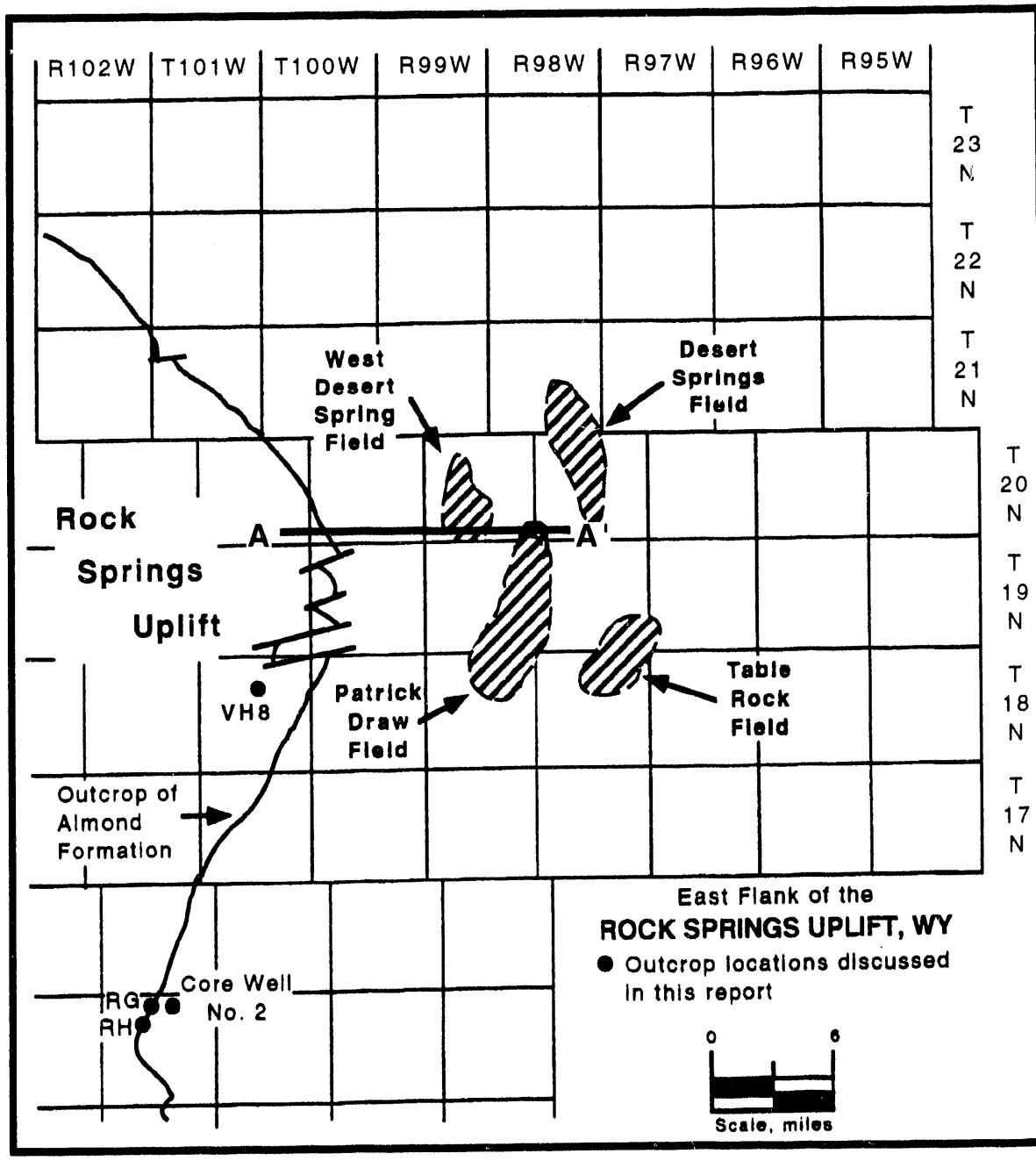

FIGURE 2 Map of the east flank of the Rock Springs Uplift, Sweetwater County, WY. Note locations of Almond outcrop exposures RG and RH, discussed in this report, and Patrick Draw field. (After Schatzinger et al., 1992). Cross-section A-A' presented in figure 5.

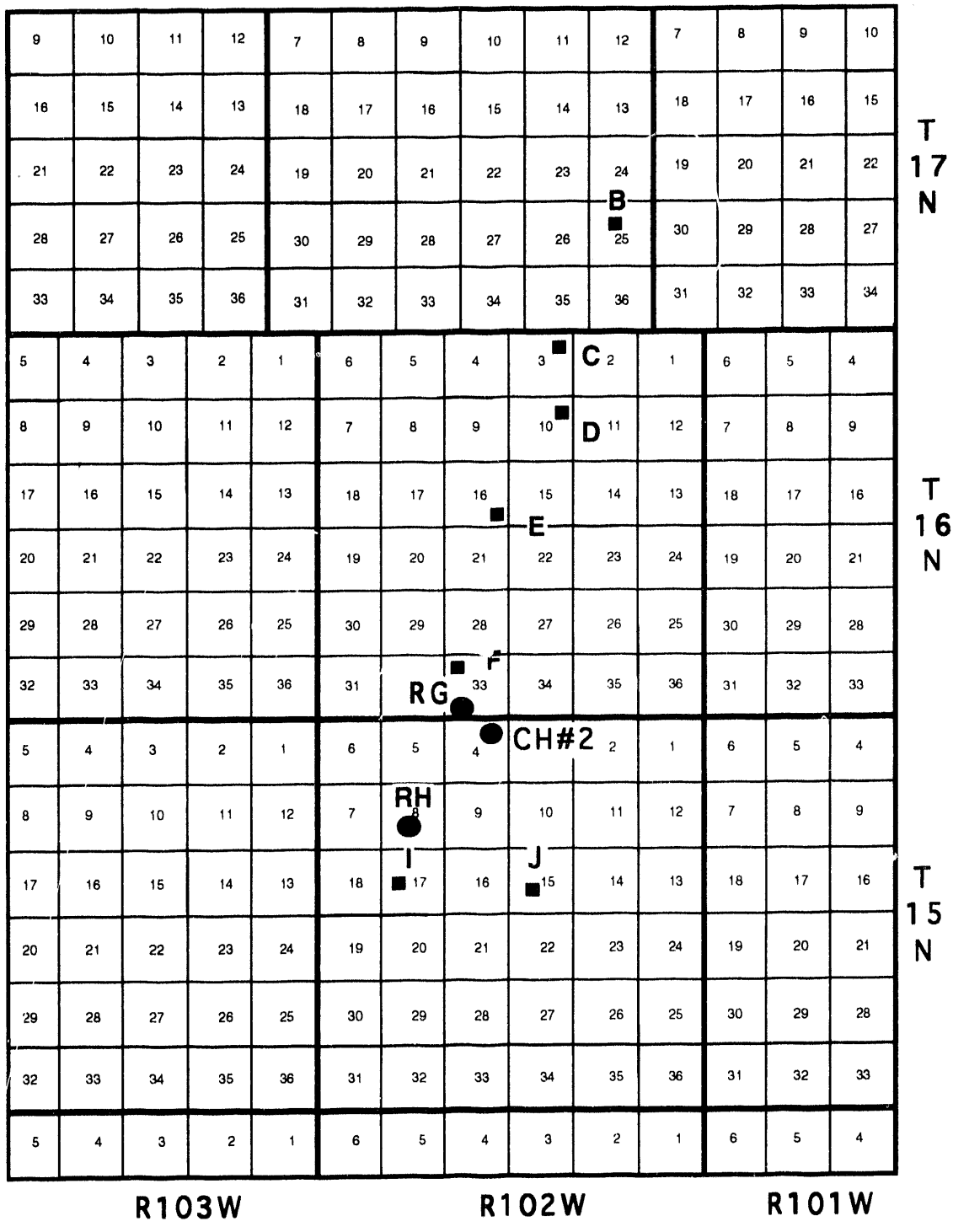

FIGURE 3 Circles indicate the location of Almond outcrops and corehole number 2 (CH#2) in Sweetwater County, Wyoming, addressed in this report. Other outcrops described in Roehler, 1988 are indicated by squares.

I Paleogeography of the Almond Formation

In the Rock Springs Uplift area, the Upper Cretaceous (Campanian) Almond Formation is the youngest formation in the Mesaverde Group (fig. 4). It ranges in thickness from 250 to 750 ft and is informally divided into lower and upper members. The lower Almond (100 to 600 ft thick) contains a fresh water fauna including dinosaur, crocodile, turtle, and fish fossils and consists of small, lenticular channel sandstones; thin, finer-grained levee; overbank and floodplain sandstones, siltstones and mudstones; and carbonaceous shales and coal beds deposited in a fresh water, coastal swamp environment (Meyers, 1977). The upper part of the lower Almond (125 to 250 ft thick) consists of a cyclic sequence of coals deposited in a fresh-water coastal-marsh environment and fossiliferous slightly carbonaceous shales, mudstones, siltstones and thin sandstones deposited in a brackish-water, salt-marsh tidal flat, estuarine setting. The paleogeographic and stratigraphic setting of the Almond Formation has been previously described (Meyers, 1977; Van Horn 1979; Roehler, 1988, Weimer, 1988; and Martinsen and Christiansen, 1992).

The Almond Formation was deposited during the early stages of the T4 transgression of Weimer (Weimer, 1960). The upper Almond consists of a series of landward stepping strandline sandstones separated by transgressive disconformities, that rise stratigraphically and become younger from east to west (Martinsen and Christiansen, 1992) (fig. 5).

In the Rock Springs/Patrick Draw area, barrier islands were deposited at the head of a large, east-west oriented embayment (Roehler, 1988) in an inter-deltaic area between the Red Desert delta (Van Horn, 1979; Jacka, 1970; Weimer, 1966; Asquith, 1970) to the north and an unnamed delta west of Craig in northwestern Colorado (fig. 6). Moderately high tides (greater than 3 ft) affected the development of the barrier islands and probably resulted from a focusing of tidal currents as they flowed westward and became constricted toward the head of the Rock Springs embayment (Roehler, 1988).

Surface and subsurface evidence indicate that the east- to northeast-trending normal faults in the study area were active during the Almond deposition (Van Horn, 1979). Strong evidence for syndepositional movement of the faults can be seen in figure 7, an isopach map of an interpreted time-stratigraphic interval between the "A" marker bentonite of the lower Lewis Shale and the top of the Almond sandstones (Van Horn, 1979). Differential movement of the fault blocks are indicated by variations in the direction of thinning between fault blocks (fig. 7).

Depositional Environments

The paleogeographic reconstruction of the Upper Almond outcrop exposures around the Rock Springs Uplift is presented in figure 8, and represents deposition in a mesotidal shoreline barrier setting (Roehler, 1988). In this environment, the major sandbodies are predominantly associated with the lateral migration of tidal inlets and consist of: (a) flood tidal delta, that forms on the landward (lagoonal) side of the inlet, interfingers with tidal flat and salt marsh deposits, and commonly contains oysters (*Crassostrea* sp.) at the base of the deposit; (b) tidal channel, characterized by scoured erosional bases, shell lags of abraded oyster valves and bimodal, ebb and flood oriented cross-stratification; and (c) ebb tidal delta, that forms on the seaward side of tidal inlets, and exhibits ebb oriented cross-strata where associated with tidal channel sandstones, and in a seaward direction, becomes massive and grades into marine sandstones.

Other sandbodies present in this environment are shallow marine sandstones deposited on the seaward side of the barrier islands, and consist of shoreface and foreshore (beach) deposits. Lower shoreface environments of interbedded sandstone, siltstone and shale are deposited below daily wave base and commonly contain the trace fossils, *Thalassinoides* and a miniature form of *Ophiomorpha*. The upper shoreface sandstones were deposited below low tide and above effective wave base and commonly contain burrows of deposit feeders in the lower part and low-angle cross-stratification and abundant *Ophiomorpha* burrows in the upper part. In the Rock Springs/Patrick Draw area, the laterally extensive shallow marine sands are truncated by tidal inlet/channel deposits resulting in rapid lateral facies changes and complex reservoir unit geometries.

Facies characteristics used in interpretations of the measured outcrop sections are listed in Table 1. Although the current status of the outcrop work does not permit facies geometry determination, maximum facies dimensions reported in 15 references was compiled to determine the geometry and volume differences of the facies within barrier island systems (Table 2, fig. 9). This data shows that the shoreface and foreshore facies have volumes over 10 times those of the tidal inlet, flood tidal delta and tidal channel/creek facies. In addition to greater volumes, reservoirs composed of shoreface and foreshore facies have much better reservoir continuity and therefor can be developed with greater well spacings. Reservoirs composed of tidal inlet, flood tidal delta and tidal channel/creek facies have much less continuity that indicates that closer well spacing, infill drilling, or horizontal wells will be most effective productive strategies.

The outcrops described in this study include two major episodes of shoreline barrier deposition that correspond to the Barrier bar G and F, using Roehler's (1988) nomenclature. Barrier bar G is part of a generally north trending shoreline deposit that is lenticular in cross section, more than 60 miles long, has a maximum thickness of 95 ft, and is about 3.5 miles wide. It is subdivided into tidal channel, tidal inlet, tidal delta, dune, washover fan, and shoreface facies (fig. 10).

TABLE 1

Sedimentological characteristics used to distinguish facies of the Almond Formation shoreline barrier system.

FLOOD TIDAL DELTA

sand, 125-225 microns moderately to poorly sorted
planar tabular beds
Ramp and Swashbar - subhorizontal to horizontal bedded and laminated, thinly bedded (to 1" thick)
Feeder Channels - deep erosive scours filled with
cross-bedded sandstone
trace of sand-filled burrows
flow directions - bimodal, landward on flood ramp, seaward on ebb shield and spit
disconformable base
geometry - lobate or wedge shaped

TIDAL CHANNEL

sand, 150-200 microns, moderate to well sorted
planar tabular bedding 1' thick, horizontal bedding, massive to subhorizontal bedding
carbonaceous drapes on bedding planes
20 to 50 ft wide, sharp basal contact
oyster channel lag (60% oysters) 3 ft thick
ebb flow
5-10% sand-filled burrows, trace *Ophiomorpha*

TIDAL INLET

sand, 250+ microns, moderate to poorly sorted
massive to large-scale local cut and fill (2.5 ft thick), horizontal bedding 1.5 ft thick, trough cross-bedding (0.5 ft thick)
erosive base often containing channel lag of shells (whole oyster shells, no preferred orientations and mudclasts)
geometry-laterally continuous - spit accretion beds
dip parallel to shore

MIDDLE SHOREFACE

sand, 100-150 microns, moderately sorted
horizontal to subhorizontally laminated, bedding 1-3", uniform thickness, minor amounts of cut and fill
alternating bioturbated and sub-horizontally laminated (wave deposits)
trace of burrowing with zones up to 90% bioturbated, trace *Ophiomorpha*
erosional base

TIDAL CREEK

sand, 175 microns moderate sorting
planar tabular bedding
rip-up clasts

TIDAL FLAT

50% sand, 66-125 microns, moderately-well to well sorted
thin bedded .05-6 inches thick
ripplebedded (up to 60%) current ripples
horizontal laminae (20%)
shale (20%) horizontal laminae and drapes (2mm) on ripples
slight soft-sediment deformation
burrowing 60%, oblique sand-filled burrows, locally abundant *Coropoides* (u-shaped burrows)

TABLE 2
Common shapes and dimensions of major reservoir facies in Recent and Ancient mesotidal shoreline barrier systems[1] (After Schatzinger et al., 1992)

Facies Name and shape	Thickness (ft)	Width (mi)	Length (mi)
Mesotidal Barrier (Shoreface & Foreshore Facies); elongated oval, drumstick	12.0 to 90.0	0.6 to 4.0	2.0 to 12.0
Washover Fan & Terrace; fan or terrace	0.5 to 6.0	0.4 to 1.6	0.8 to 1.8
Spit Platform; accreted cycles	3.0 to 15.0	0.5 to 3.0	0.3 to 1.0+
Tidal Inlet; strait or slightly curved	5.0 to 100.0+	0.1 to 1.0+	0.6 to 4.0+
Tidal Channel & Tidal Creek; convergent, sinuous	5.0 to 100.0+	0.02 to 0.8	1.0 to 3.0+
Flood Tidal Delta; lobate fan, tear-shaped	6.0 to 30.0	0.3 to 4.0	1.0 to 3.0
Ebb Tidal Delta & Shoal; lobate fan, oval	15.0 to 75.0	1.0 to10.0	1.5 to 6.0

[1]Data compiled from Bernard et al., 1959; Cuevas et al., 1985; Donselaar, 1984, 1990; Fitzgerald et al., 1984; Flores, 1978; Hayes and Sixton, 1989; Hoyt and Henry, 1965; Reinson, 1979; Roehler, 1979, 1988; Sha Li Ping, 1990; Sneider et al., 1984; Van Horn, 1979, and from NIPER's field observations (Szpakiewicz et al., 1986, 1990-91).

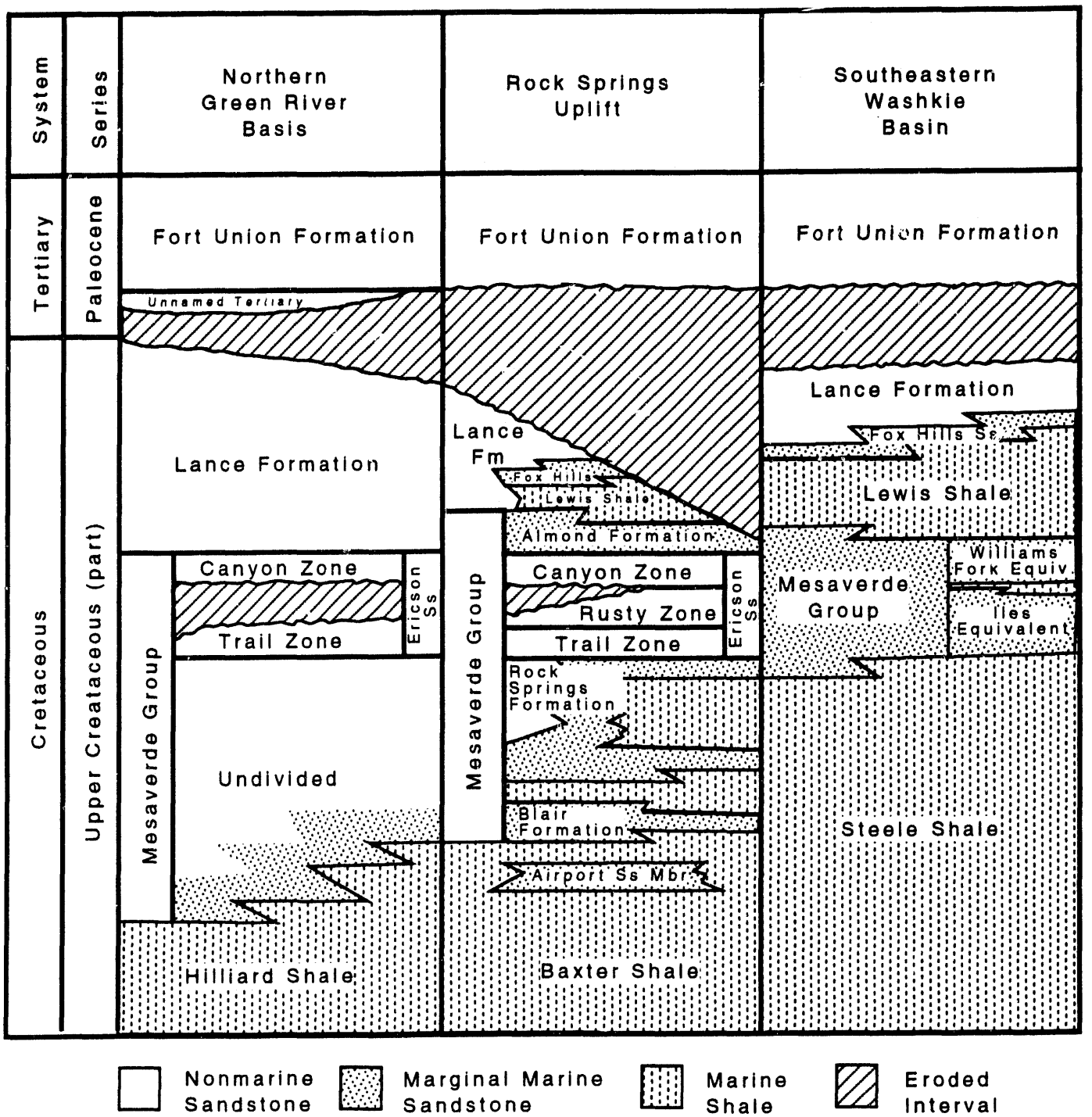

FIGURE 4 Generalized stratigraphic column of the Patrick Draw field area, WY. (After Law, 1984)

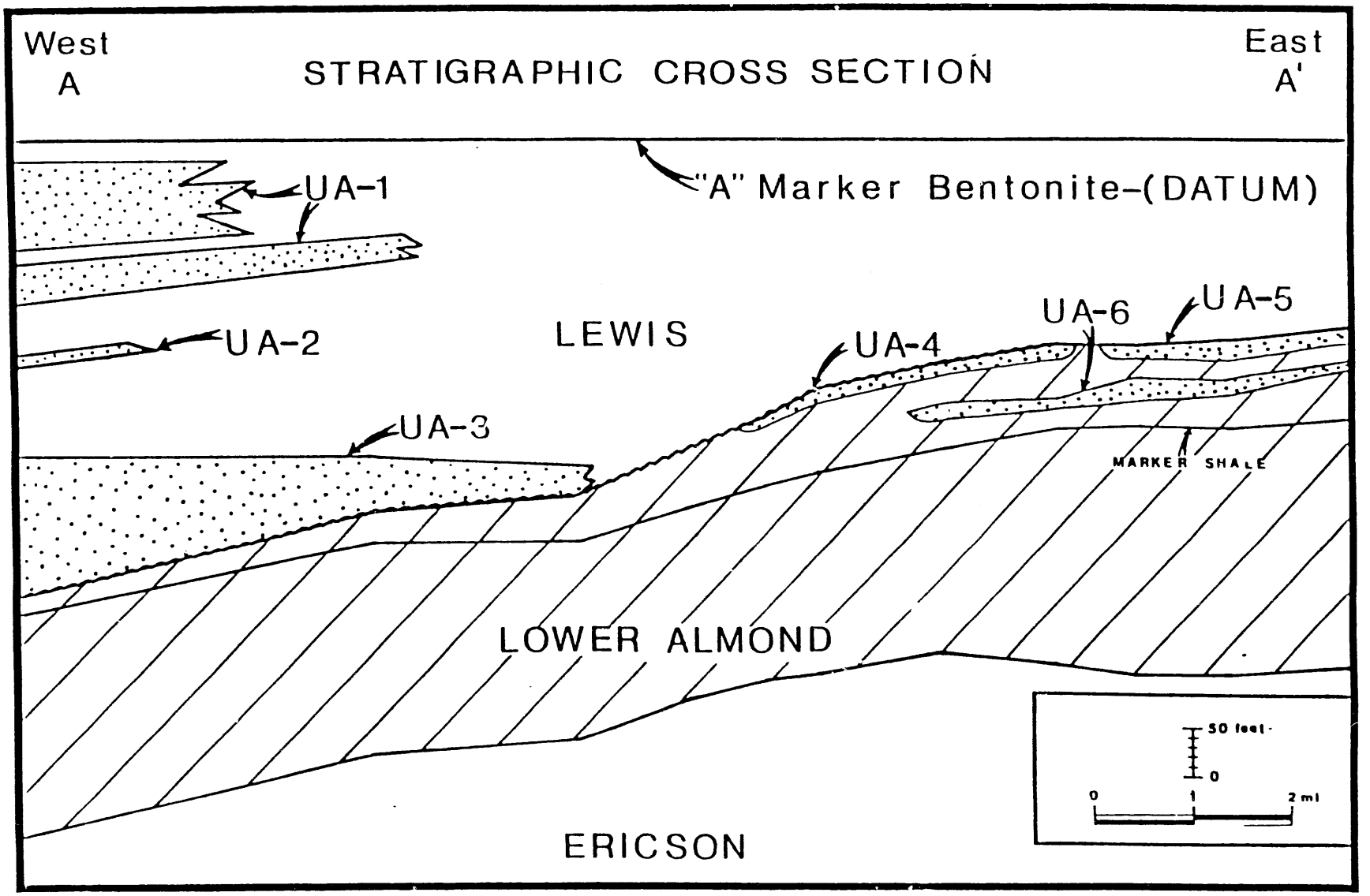

FIGURE 5 East-west stratigraphic cross section of the upper Almond Formation showing landward stepping shoreline deposits that become younger to the east. (After Van Horn, 1979). See figure 2 for location of cross-section.

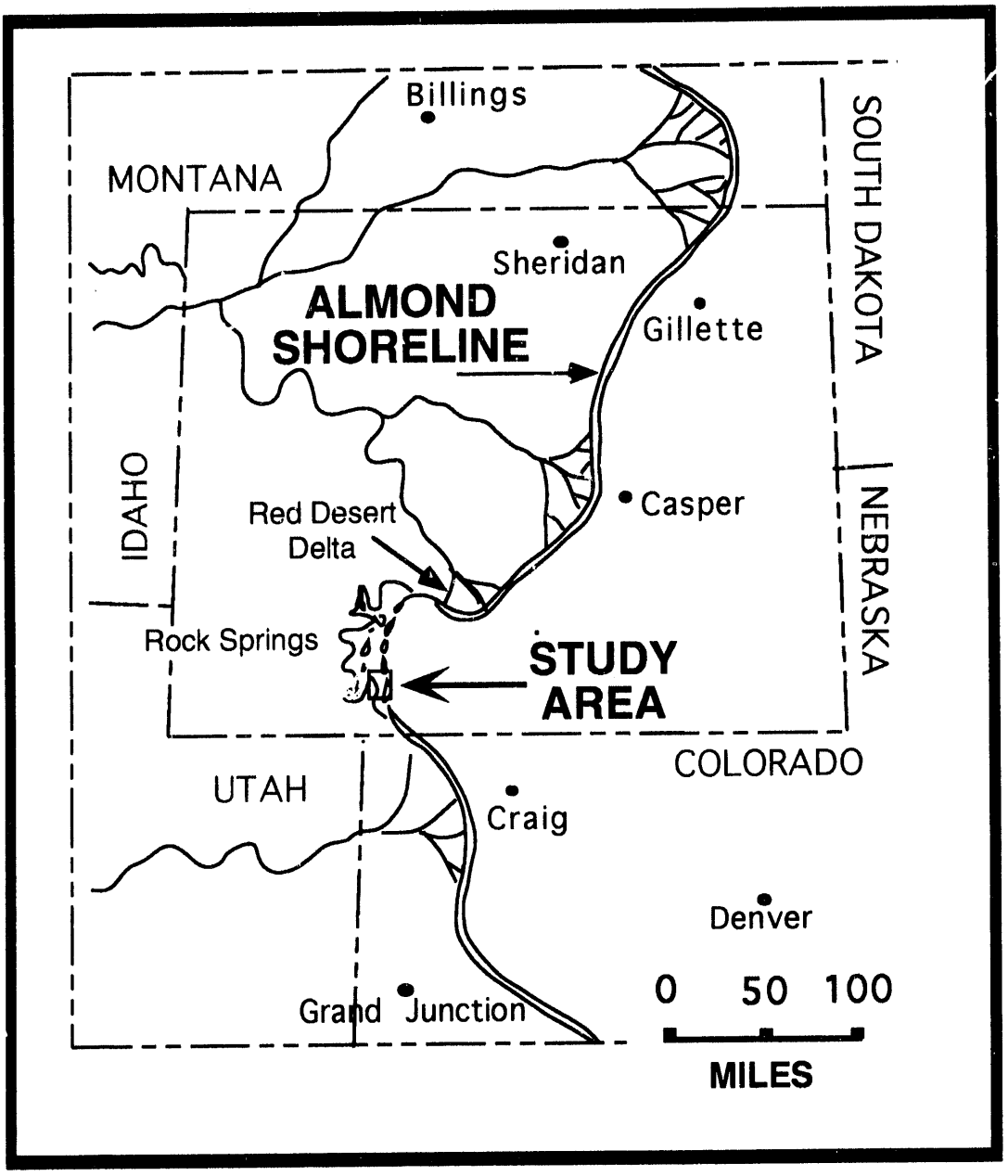

FIGURE 6 Paleogeographic setting of the Almond Formation shoreline barrier island system on the western shoreline of the Late Cretaceous epeiric sea. (After Roehler, 1988)

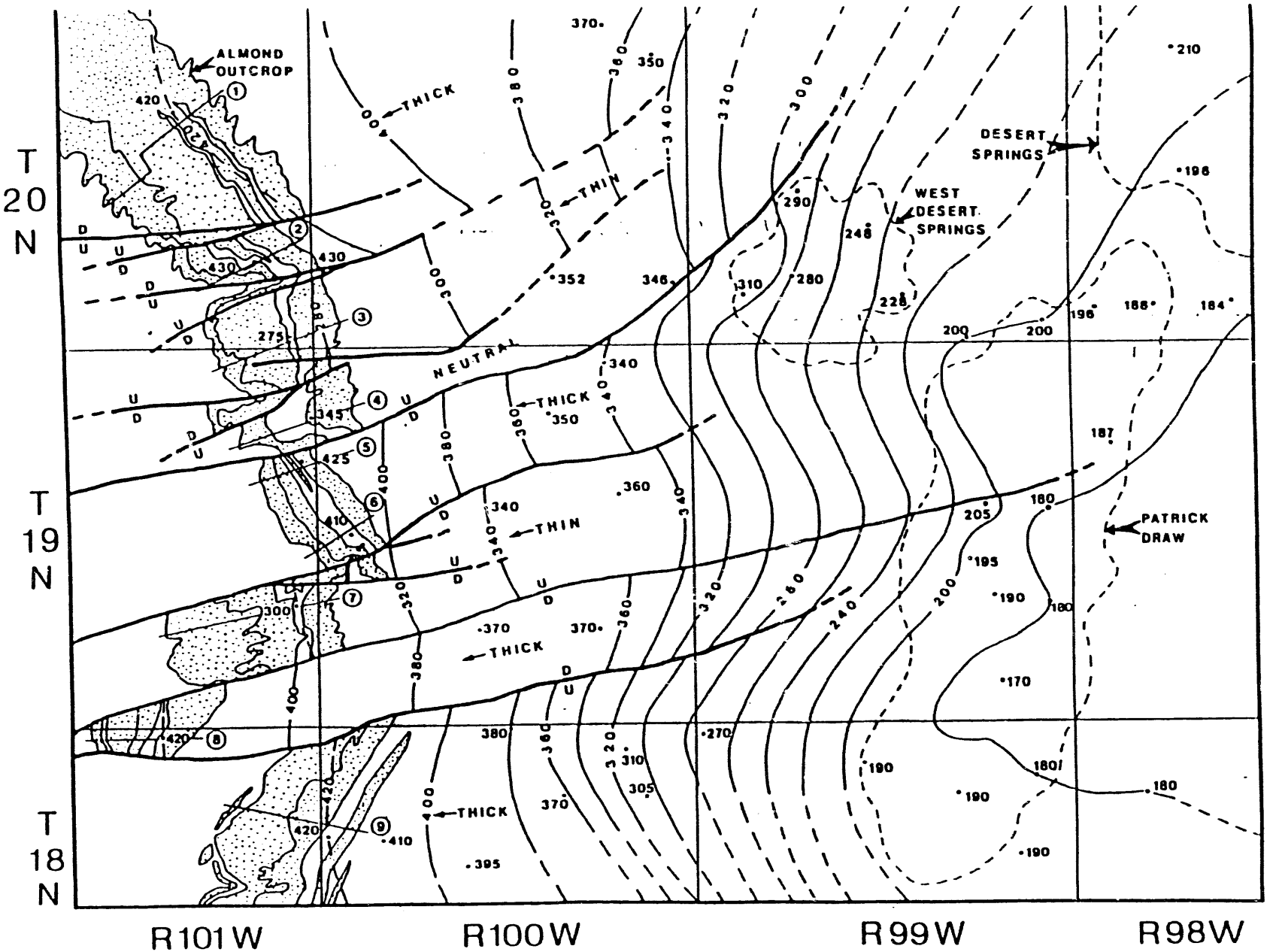

FIGURE 7 Isopach map of interval from the "A" marker bentonite to the top of the lower Almond outcrop. Syndepositional movement of the fault blocks are indicated by variations in the direction of thinning within fault blocks. Contour interval is 20 ft. (After Van Horn, 1979). Dashed lines indicate field outlines.

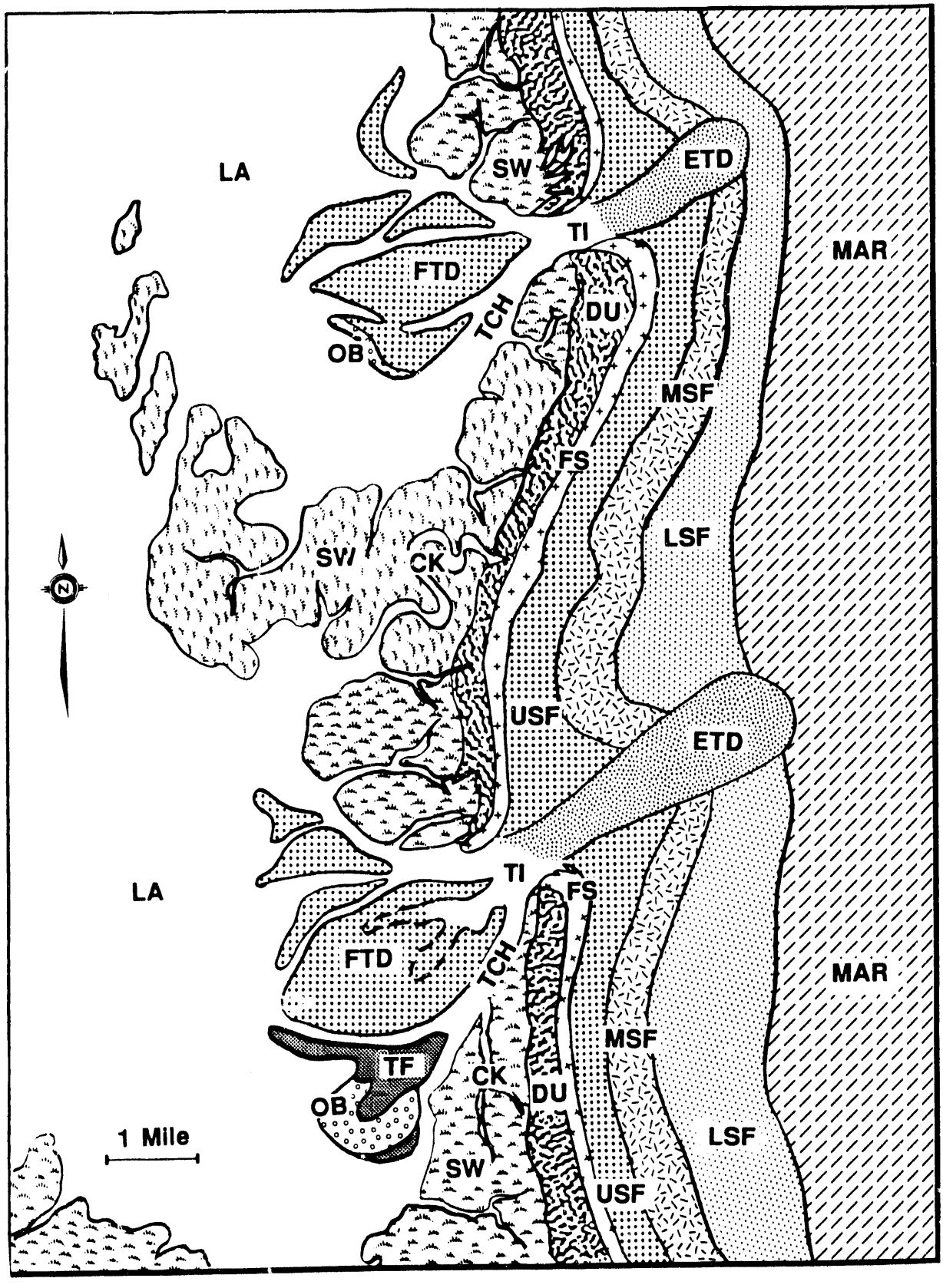

FIGURE 8 Paleogeographic map of upper Almond Formation barrier bar G and associated facies located in the study area. Abbreviations: CK, creek; DU, dunes; ETD, ebb tidal delta; FS, foreshore; FTD, flood tidal delta; LA, lagoon; LSF, lower shoreface; MAR, offshore marine; MSF, middle shoreface; OB, oyster bed; SW, swamp; TCH, tidal channel; TF, tidal flat; TI, tidal inlet; USF, upper shoreface. (Modified from Roehler, 1979 and 1988)

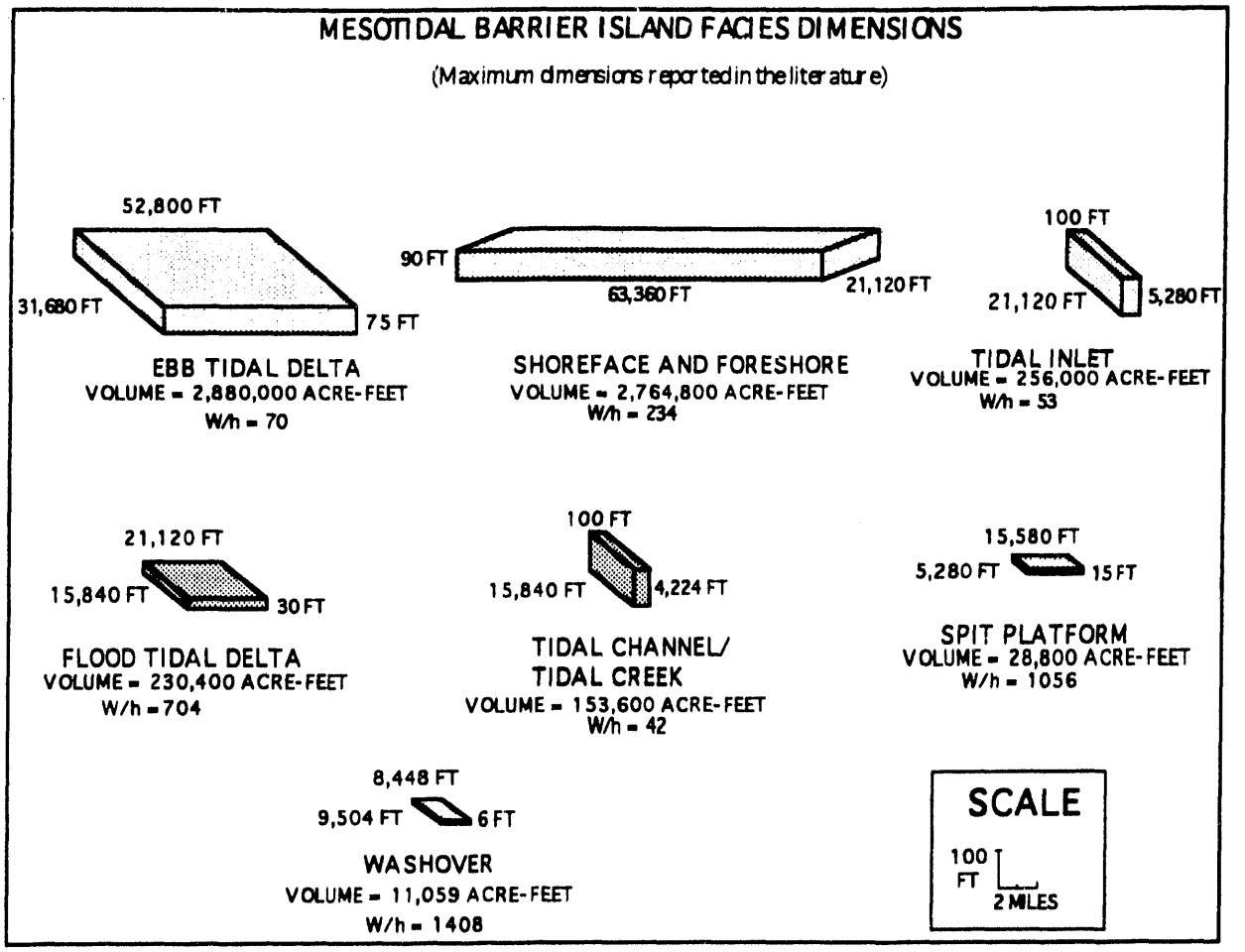

FIGURE 9 Dimensions and geometries of barrier island facies. Data from references listed in Table 2. (After Jackson, 1992)

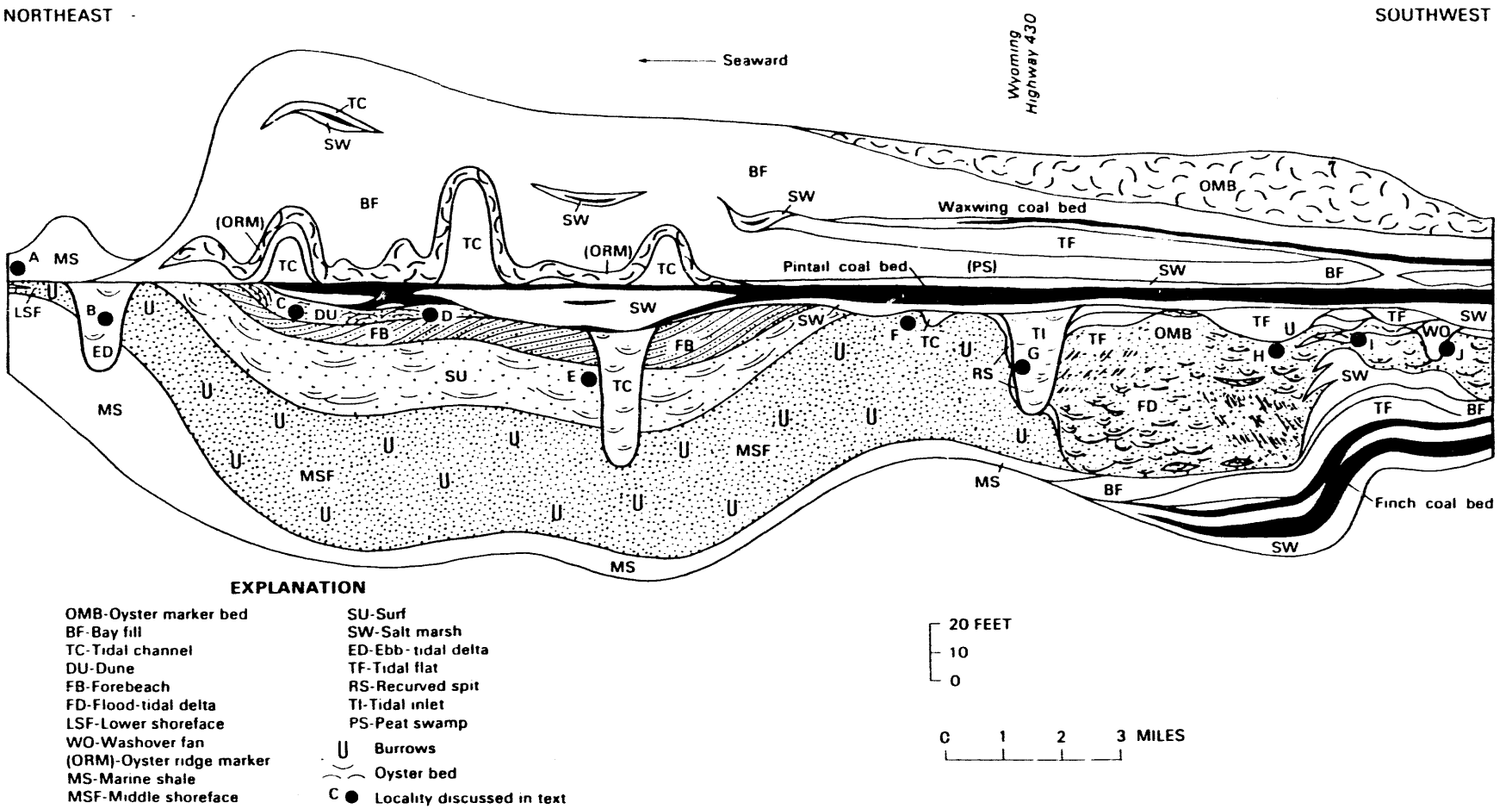

FIGURE 10 Facies distribution within barrier bar G in the study area. See Figure 3 for outcrop localities. (After Roehler, 1988)

II Measured Sections

Detailed measured sections of outcrop RH-2 (figs. 11a-d), RH-3 (figs. 12a-d) and RG-7 (figs. 13a-g) are provided to show the vertical sequence of facies in the Almond Formation. Grain size measurements were made at least every foot with a hand lens and grain-size comparitor. Outcrops RH-2 and RH-3 (figures 11 and 12) are located in section 8 T15N R102W in the Mud Springs Ranch Quadrangle of Sweetwater County, Wyoming. RG-7 (fig. 13) is located in section 33 T16N R102W of the Mud Springs Ranch Quadrangle of Sweetwater County, Wyoming (fig.3).

Figure 14 is a cross section of outcrops RH-2, RH-3 and RH4 in the Almond Formation, Sweetwater County, Wyoming. The facies legend for figure 14 is given in figure 15.

FIGURE 11a Measured section RH-2, Almond Sandstone. C NE SW sec. 8, T15N, R102W, Sweetwater County, Wyoming. O to 40 ft.

Described by: R. Tillman, R. Schatzinger
Date: 6/20/91
Measured at or near Rohler, 1988 Measured Section H in Bar G.
Measured on traverse of 3°, dip 4° to N.
2.2 miles, south of M.S. RG-7
Total interval measured 145'.
Mud Springs Ranch Quad (7 1/2")

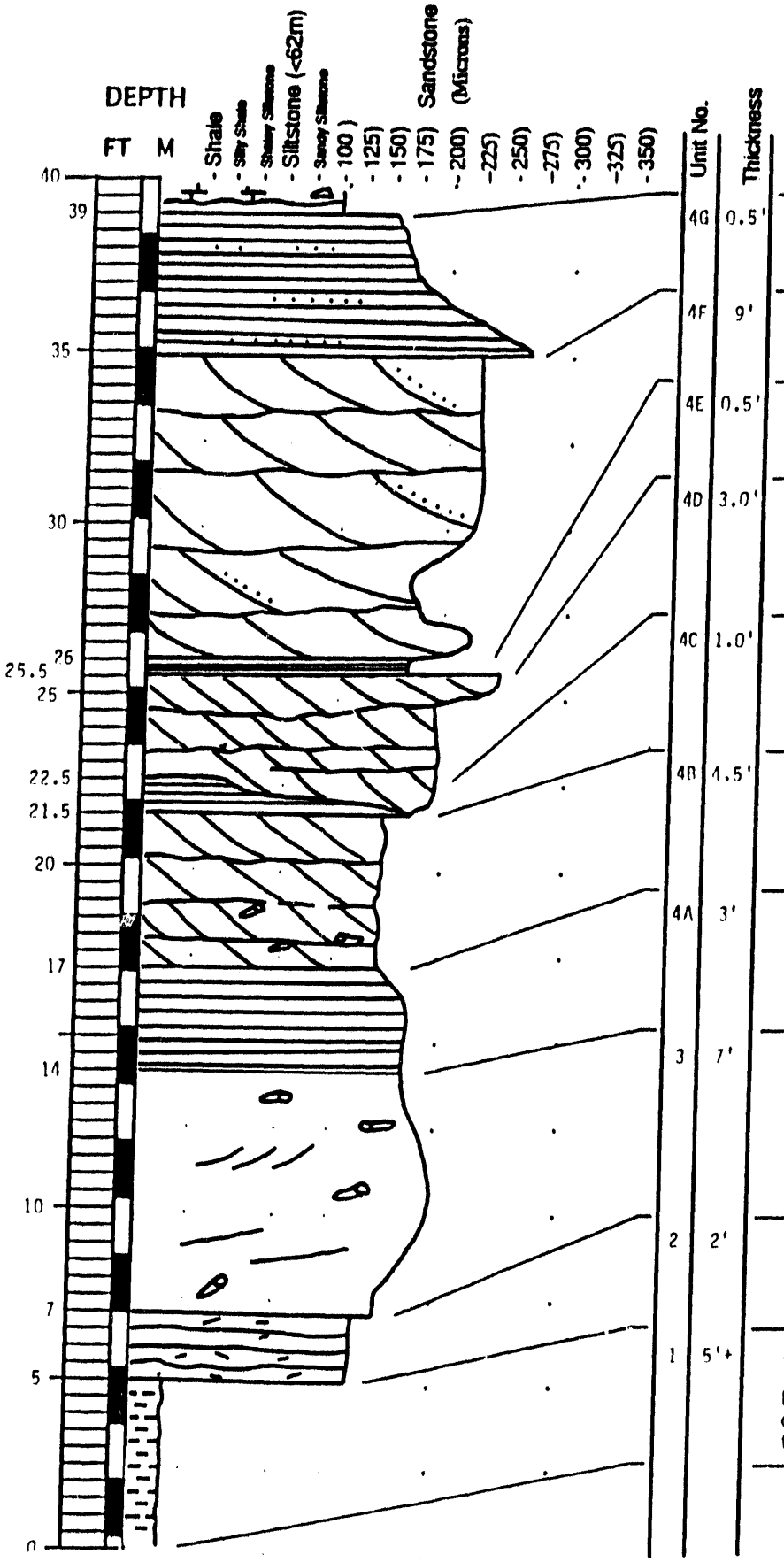

35.0-39.0' Sandstone. Horizontally laminated throughout. TIDAL SWASH BAR (90%).

26.0-35.0' Sandstone. Planar tangential laminae, 1' beds, ESE flow. No burrows.

25.5-26.0' Sandstone (175 microns). Horizontally laminated. TIDAL SWASH BAR (90%).

22.5-25.5' Sandstone (200-250 microns, moderate to poorly sorted). Planar tabular laminated (ESE flow and SW flow), base erosional, top sharp. TIDAL DELTA (90%).

21.5-22.5' Sandstone (175 microns, moderate sorting), horizontally laminated, cut out laterally by overlying unit. TIDAL SWASH BAR (90%).

17.0-21.5' Sandstone (150 microns, moderately poorly sorted), cross laminated. Up to 0.8' thick beds. Trace burrows. ESE flow. TIDAL DELTA.

14.0-17.0' Sandstone (150-175 microns, moderately sorted), horizontally bedded and laminated, sharp lower contact. TIDAL SWASH BAR (80%) or MIDDLE SHOREFACE (20%).

7.0-14.0 Sandstone (175-200 microns, moderately poorly sorted). Overall massive appearance. Diffuse bedding locally (cross laminated?, low angle planar?). Trace Ophimorpha. 2% carbonaceous drapes on cuts. TIDAL CHANNEL (75%).

5.0-7.0' Sandstone (125 microns) 2-8% carbonaceous fragments. Thin irregular(?) horizontal bedding; internally rippled.

0-5.0' Claystone, dark gray fissile, less than trace of silt size carbonaceous grains. Not silty. Lower contact covered. Sharp upper contact. BAY FILL SHALE (75%).

FIGURE 11b Measured section RH-2, Almond Sandstone. C NE SW sec. 8, T15N, R102W, Sweetwater County, Wyoming. 40 to 80 ft.

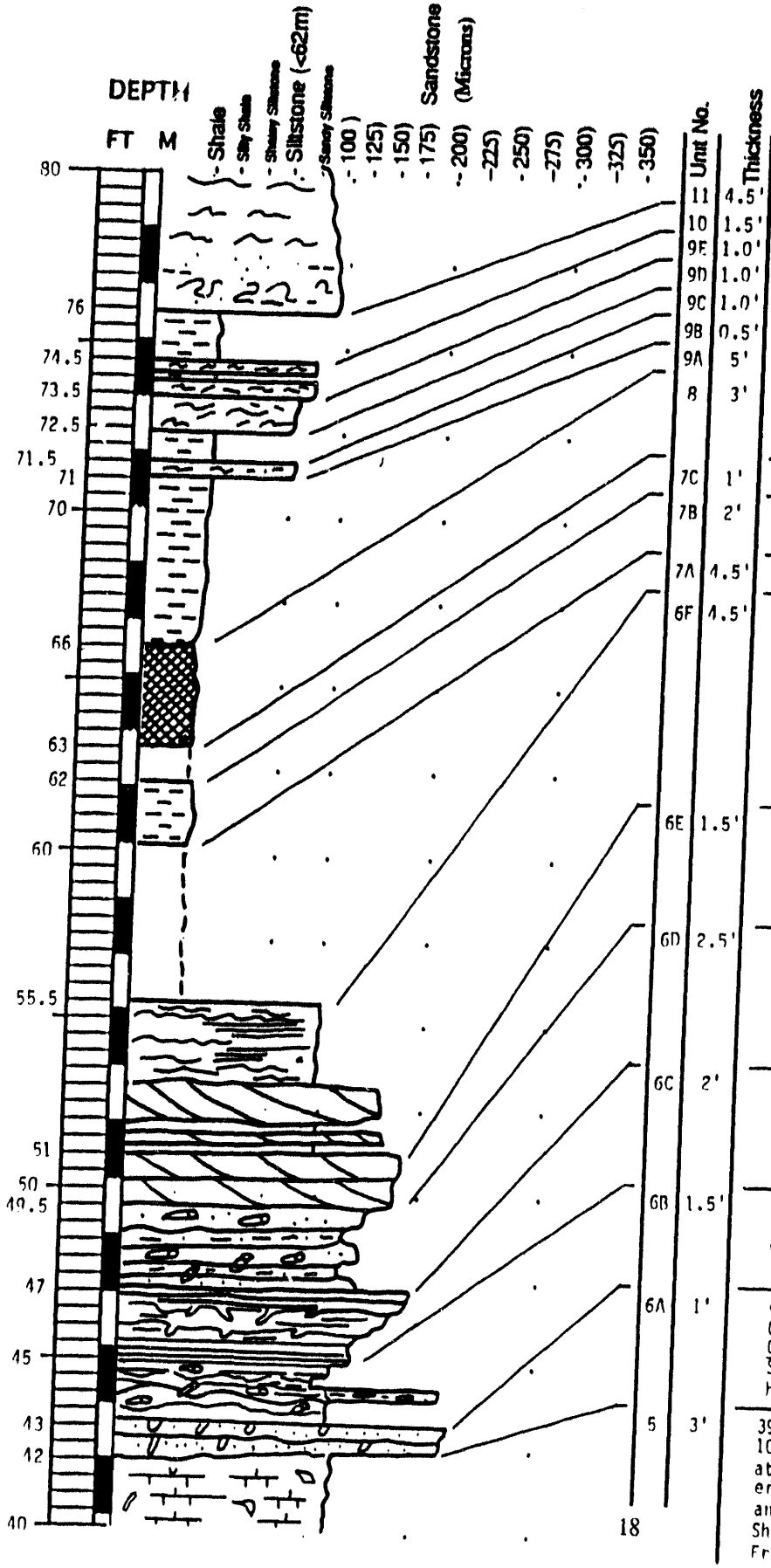

76.0-80.5' Sandstone (75-100 microns, moderate to well sorted). Trace-10% carbonaceous fragments. Lower 1/3 soft sediment deformed, remainder ripples and small troughs.

74.5-76.0' Claystone, black. 10%+ carbonaceous fragments. BAY SHALE (80%).

73.5-74.5' Sandstone (75 microns, poorly sorted), rippled 20% carbonaceous. Interbedded carbonaceous shale.

72.5-73.5' Siltstone, light tan. 5% carbonaceous, rippled.

71.5-72.5' Shale, carbonaceous.

71.0-71.5' Siltstone, rippled, red-brown. Well sorted, quartzose.

66.0-71.0' Shale, carbonaceous (10%+), brownish-black, fissile, slightly silty. BRACKISH(?) MARSH (80%).

63.0-66.0' Coal, vitreous, black. Non-clayey. Pintail coal. FRESH WATER MARSH (95%).

62.0-63.0' Covered, soil.

60.0-62.0' Shale, carbonaceous, brownish-black, slighly silty.

55.5-60.0' Covered, soil.

51.0-55.5' Sandstone (65-125 microns, moderately well to well sorted sandstone). Very thin bedded, 1/2-2". 50% current ripples (sandstone), 20% horizontal laminae (sandstone), 20% shale (horizontal laminae and drapes on ripples). 10% tidal creek sandstone deposits(1' thick). TIDAL FLAT and TIDAL CREEKS (90%).

49.5-51.0' Sandstone (100%, 175 microns, moderate sorting). 0.5-1' beds, planar tabular (flow NE). 5% clay rip-up clasts. 10% burrowed. TIDAL CREEK (90%).

47.0-49.5' Sandstone (50%, 150 microns, moderate sorting) interbedded with silty shale. 60% burrowed, oblique sand filled. Sand mostly slightly soft sediment deformed. TIDAL FLAT (90%).

45.0-47.0' Sandstone (80%, 175-200 microns, moderate sorting). Horizontally laminated (90%), 10% burrowed, vertical. High flow regime deposit. TIDAL FLAT (90%).

43.0-45.0' Sandstone (60%, 125 microns, poor sorting) interbedded with burrowed silty shale (40%). Sandstone beds 2-6" thick. TIDAL FLAT (90%).

42.0-43.0' Sandstone (150 microns). Calcareous cemented. Abundant Corophoides burrows ("U" shaped). Slightly irregular bedded, sub-horizontally laminated. TIDAL FLAT (80%).

39.0-42.0' Calcareous sandstone, 100-150 microns, very poorly sorted at base (100 microns), otherwise moderately sorted. Oxidized. Massive and mottled appearing. 5% shells. Sharp upper and lower contacts. Fractured. SANDY LAGOON (60%).

FIGURE 11c Measured section RH-2, Almond Sandstone. C NE SW sec. 8, T15N, R102W, Sweetwater County, Wyoming. 80 to 120 ft.

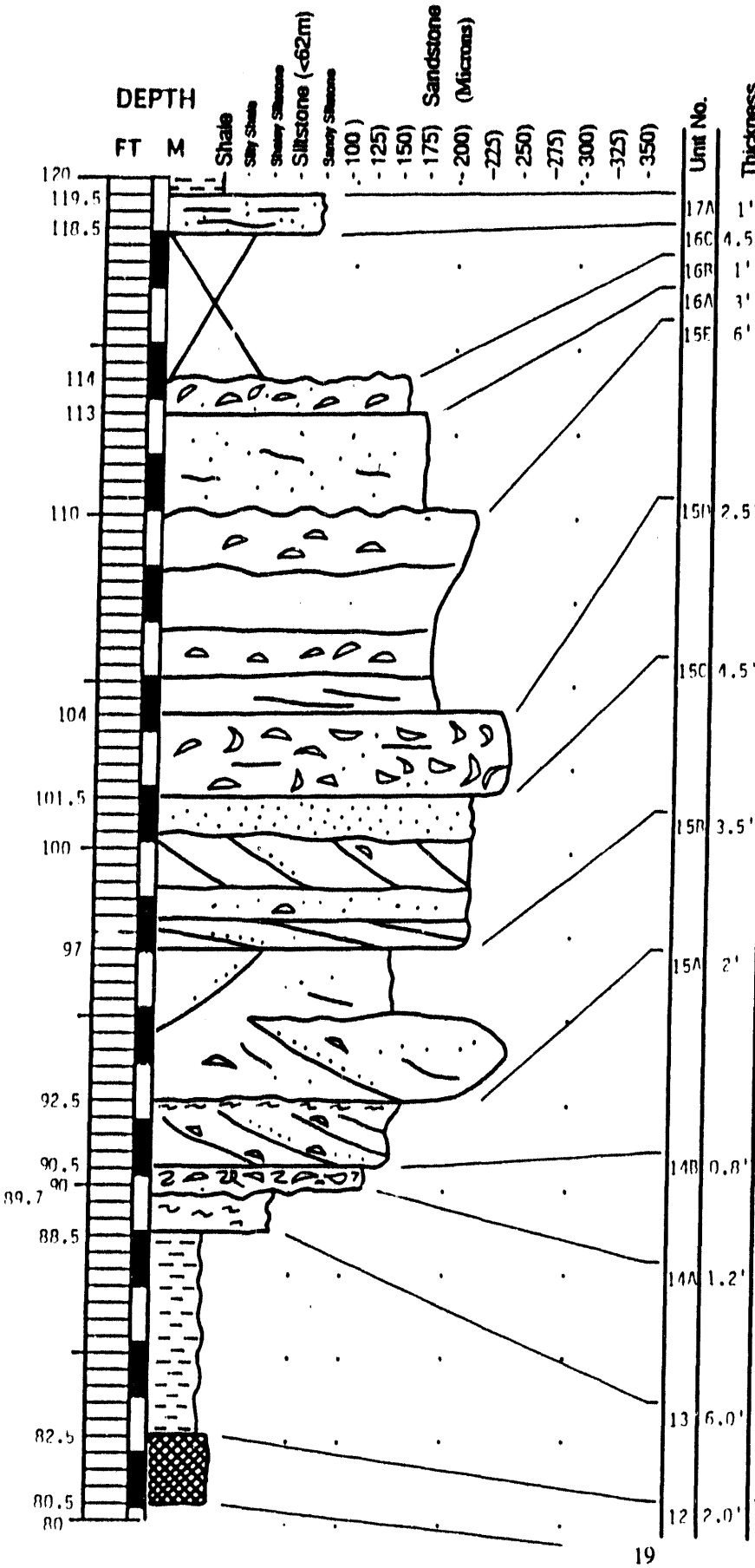

118.5-119.5' Sandstone (75 microns) thin platey bedded. Non-burrowed TIDAL CREEK (60%).

114.0-118.5' Covered, sandy, no outcrop laterally, non-resistant.

113.0-114.0' Sandstone (150 microns, poorly sorted). Locally 30% oyster fragments. Sharp upper and lower contacts. Very local sandstone, extends 20' laterally. TIDAL CHANNEL (85%).

110.0-113.0 Sandstone. Grey, massive appearing. Diffuse subhorizontal bedding? Local sandstone 50' lateral extent. Non-burrowed. TIDAL CHANNEL (75%).

104.0-110.0' Sandstone (175-225 microns, moderate to poor sorting). Interbeds of sandstone with abundant oysters (0.5-1.0' thick) and non-oyster bearing sandstone. Oysters mostly fragmented. At least 10% low angle planar laminae, remainder massive appearing. Extends 300' along outcrop to west.

101.5-104.0' Sandstone (250 microns, moderate sorting). 40% large 2-4" long whole oysters with no preferred orientations. 15% oyster fragments. Forms one amalgamated(?) bed with sharp upper and lower contacts. TIDAL INLET CHANNEL FILL (80%).

97.0-101.5' Sandstone (250 microns, moderate sorting). 1-1.5' thick horizontal beds, internally planar-tabular to planar tangential. SE flowing, cross-lamination (30%). 30% low-angle planar laminae, 40% "massive". TIDAL INLET FILL (90%).

92.5-97.0' Sandstone (150-250 microns, moderate sorting). Trace-5% oysters. Massive appearing. Some large scale local cut and fill (2.5'). Suggestion of troughs and horizontal laminae. TIDAL INLET CHANNEL FILL (90%).

90.5-92.5' Sandstone (150-175 microns, moderately to poorly sorted). Trace of carbonaceous material. Thick bedded (1.5'), bedding horizontal and rippled at top. Medium size troughs (0.5' thick) within beds. Trace of oysters. Uniform SE flow. Unit consistent but thickens to west. TIDAL INLET CHANNEL FILL (90%).

89.7-90.5' Sandstone (125 microns, moderate sorting). Shelter porosity filled with muddy silt. Thoroughly soft sediment deformed. Locally sharp upper contact.

88.5-89.7' Sandstone (100 microns, poorly to moderately well sorted, rippled and disturbed). 2% tiny very thin pelecypod shells. Trace carbonaceous, thin (0.1 mm thick) clay lenses. BRACKISH(?) BAY SANDSTONE (65%).

82.5-88.5' Claystone, medium grey, trace of carbonaceous fragments in lower half of unit. Non-silty. BAY FILL SHALE (65%).

80.5-82.5' Coal, vitreous, thin bedded, non-clayey. MARSH DEPOSIT (90%).

FIGURE 11d Measured section RH-2, Almond Sandstone. C NE SW sec. 8, T15N, R102W, Sweetwater County, Wyoming. 120 to 160 ft.

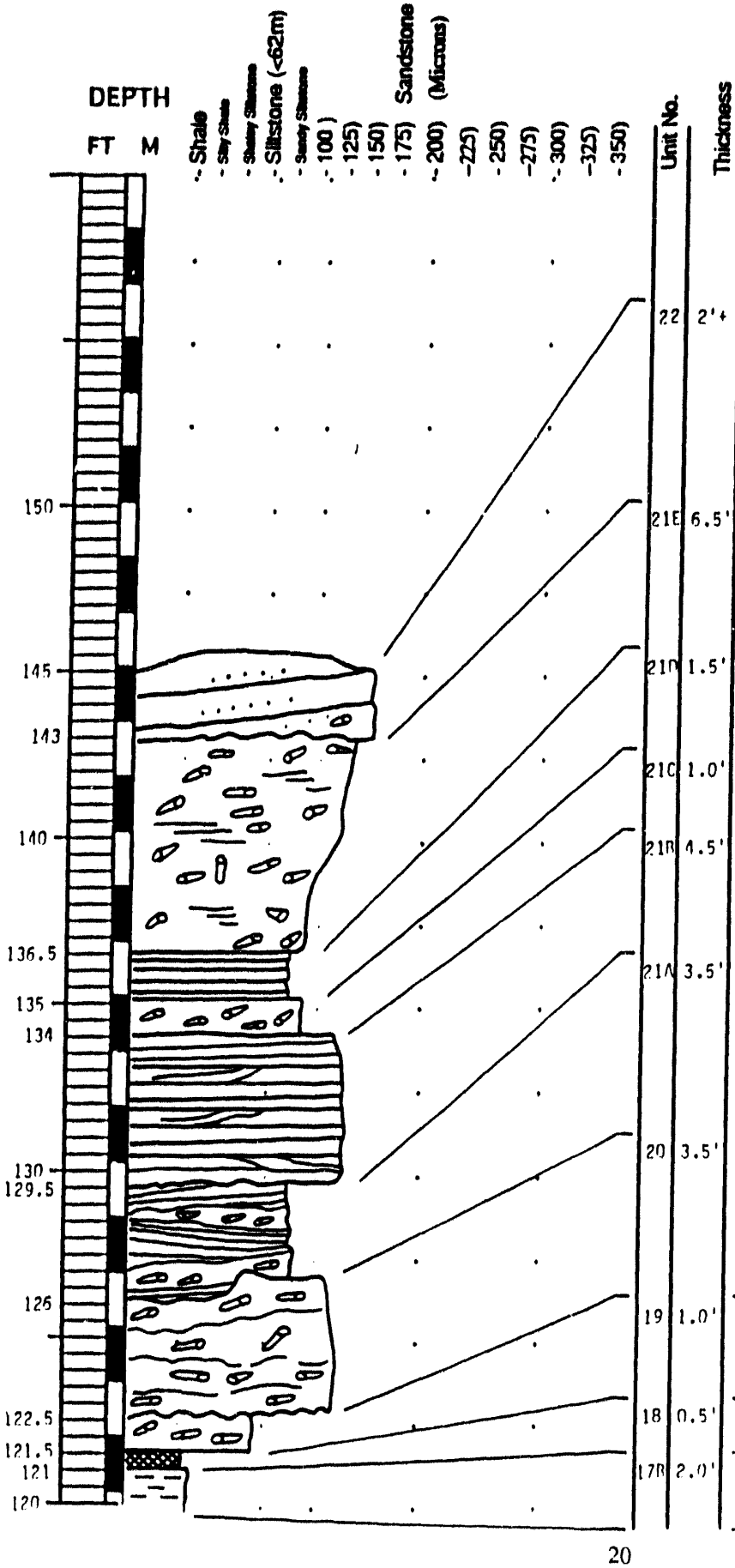

143.0-145.0'+ Sandstone (150 microns, moderately poor sorting). White sub-horizontal bedding surfaces in interior of beds. "Massive". Top of outcrop. Base disconformable. Note: The entire thickness of this white Tidal Delta complex outcrops across the valley to east. TIDAL DELTA (75%).

136.5-143.0' Sandstone (100-150 microns, poorly sorted). Thin bedded 10% horizontal laminae where not burrowed. Bioturbated. Uniform appearance throughout. 2% Ophiomorpha. MIDDLE SHOREFACE (90%).

135.0-136.5' Sandstone (80 microns, moderately well sorted). Low-angle to sub-horizontally laminated (wave deposited). MIDDLE SHOREFACE (90%).

134.0-135.0' Sandstone (100 microns, moderately well sorted). Bioturbated, 5% carbonaceous.

129.5-134.0' Sandstone (100-125 microns, moderate sorting). Sub-horizontally laminated, trace of burrowing. Wave deposited. MIDDLE SHOREFACE (90%).

126.0-129.5' Sandstone (80-100 microns, moderately sorted). Trace of Ophiomorpha. Thin bedded (0.1-0.8'). "Lam-Scram", alternating bioturbated and sub-horizontally laminated (wave deposited) beds. Base erosional, cut down 3'. MIDDLE SHOREFACE (90%).

122.5-126.0' Sandstone (75-125 microns, moderate sorting). Trace carbonaceous. 10% clay laminae. 85% burrowed (bioturbated). Irregular horizontal bedding (0.2-0.8' thick). Base a flooding surface. LOWER SHOREFACE (90%).

121.5-122.5' Silty claystone. Bioturbated. 20% carbonaceous. Unconformable upper surface. MARSH/LAGOON (65%).

121.0-121.5' Coal, vitreous, black non-clayey.

119.5-121.0' Claystone, dark grey, slightly silty, 3-5% carbonaceous fragments. BAY/LAGOON FILL (75%).

FIGURE 12a Measured section RH-3 Almond Sandstone. SW NW sec. 8, T15N, R102W, Sweetwater County, Wyoming. 0 to 40 ft.

Described by: R. W. Tillman,
R. Schatzinger, 6/21/91
Note: Located 2.1 miles south of Measured Section RG7, 1/2 mile NE of Measured Section H2. Used dip of 4° on transverse to east. Interval from 53-60' also measured 50' to north. Changed to apparent dip of 5° at 60'.
Measured Interval 140'.
Mud Springs Quadrangle (7 1/2")

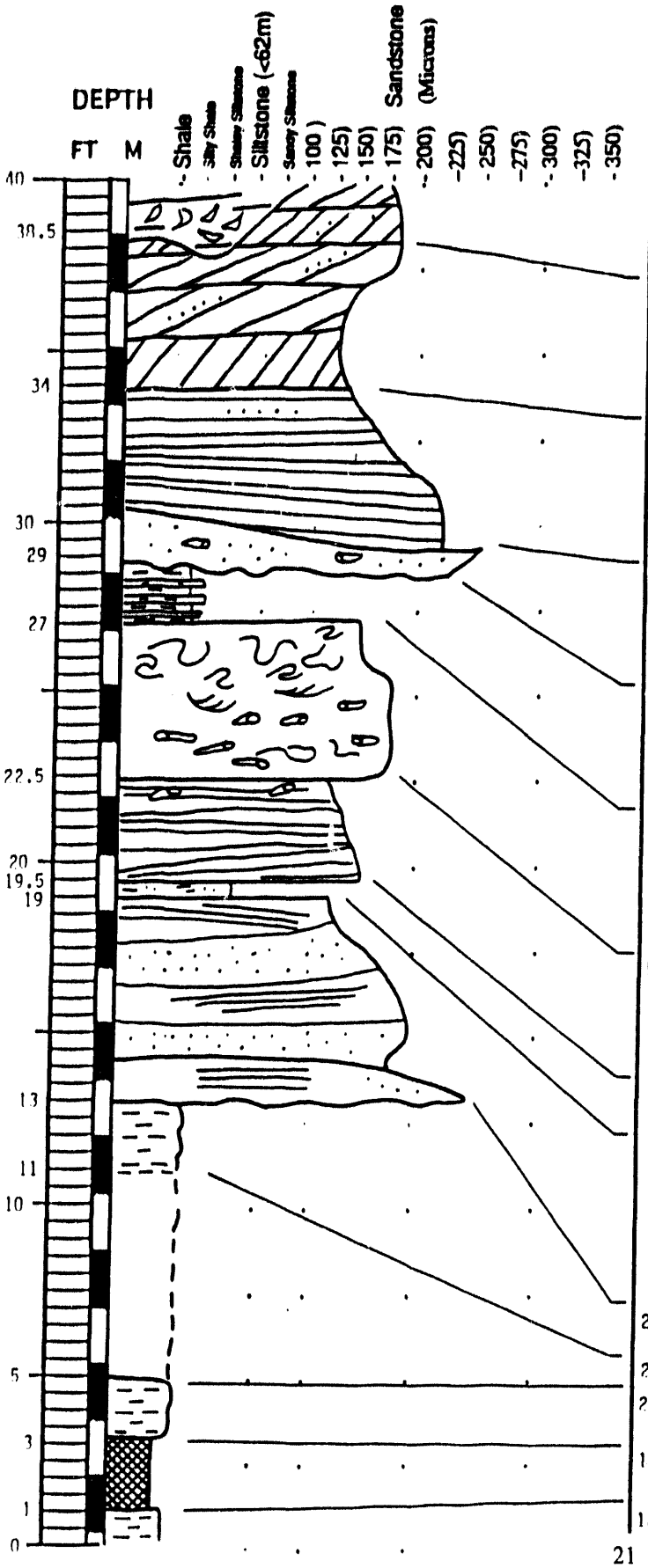

Unit No.	Thickness	
8A	2.5'	38.5-41.0' Sandstone (175 microns, moderately sorted). Massive appearing. 30% oysters. Cut down into planar tabular unit below. 2.5' cut down; cut is 10' wide. TIDAL CHANNEL (90%).
7C	4.5'	34.0-38.5' (Top of unit is at 41' laterally). White (125-175 microns, moderate sorting). Planar tabular laminae in horizontal beds; flow to south. Top cut into by oyster filled channel. TIDAL DELTA RAMP (80%).
7B	4.0'	30.0-34.0' Sandstone (125-225 microns, moderately sorted). Graded. Subhorizontal bedded and laminated dip up to 200 to west. Trace sand filled burrows. TIDAL DELTA RAMP (70%).
7A	1.0'	29.0-30.0' Sandstone (225-250 microns, moderately sorted). Massive appearing. Base erosional (0.5' relief). Trace of sand filled burrows.
6	2.0'	27.0-29.0' Silty (sandy) shale. Black. 40% thin silty sandstone (75 microns) lenses and siltstone lenses (gray). Upper surface cut down 0.5'. LAGOON (80%).
5B	4.5'	22.5-27.0' Sandstone (150-175 microns, moderate sorting). 40% burrowed (includes bioturbated intervals), 30% soft sediment deformed, 30% small troughs. TIDAL CHANNEL IN TIDAL DELTA (75%).
5A	3.0'	19.5-22.5' Sandstone (125-150 microns, moderate sorting). 0.5' thick sub-horizontal bedding; 100% sub-horizontal laminae. TIDAL DELTA SWASH BAR (90%).
4	0.5'	19.0-19.5' Clayey sandstone (100 microns). LAGOON (60%).
3	6.0'	13.0-19.0' Sandstone (125-250 microns, moderately sorted). Distinctly graded. Sub-horizontally bedded. Beds are internally sub-horizontally laminated (60%) to massive (40%). Base disconformable. TIDAL DELTA (90%).
2C	2'	11.0-13.0' Shale, gray, non-carbonaceous, fissile. BAY FILL SHALE (75%).
2B	6'	5.0-11.0' Covered.
2A	2'	3.0-5.0' Claystone, gray, non-carbonaceous. BAY FILL (75%).
1B	2'	1.0-3.0' Coal, vitreous, non-clayey. MARSH (90%).
1A	1'+	0-1.0' Shale, carbonaceous, dark gray. 10% carbonaceous fragments. LAGOON (50%).

FIGURE 12b Measured section RH-3 Almond Sandstone. SW NW sec. 8, T15N, R102W, Sweetwater County, Wyoming. 40 to 80 ft.

Note: Moved Measured Section to north. Discontinuous exposure above 50' at sight of 0-50'.

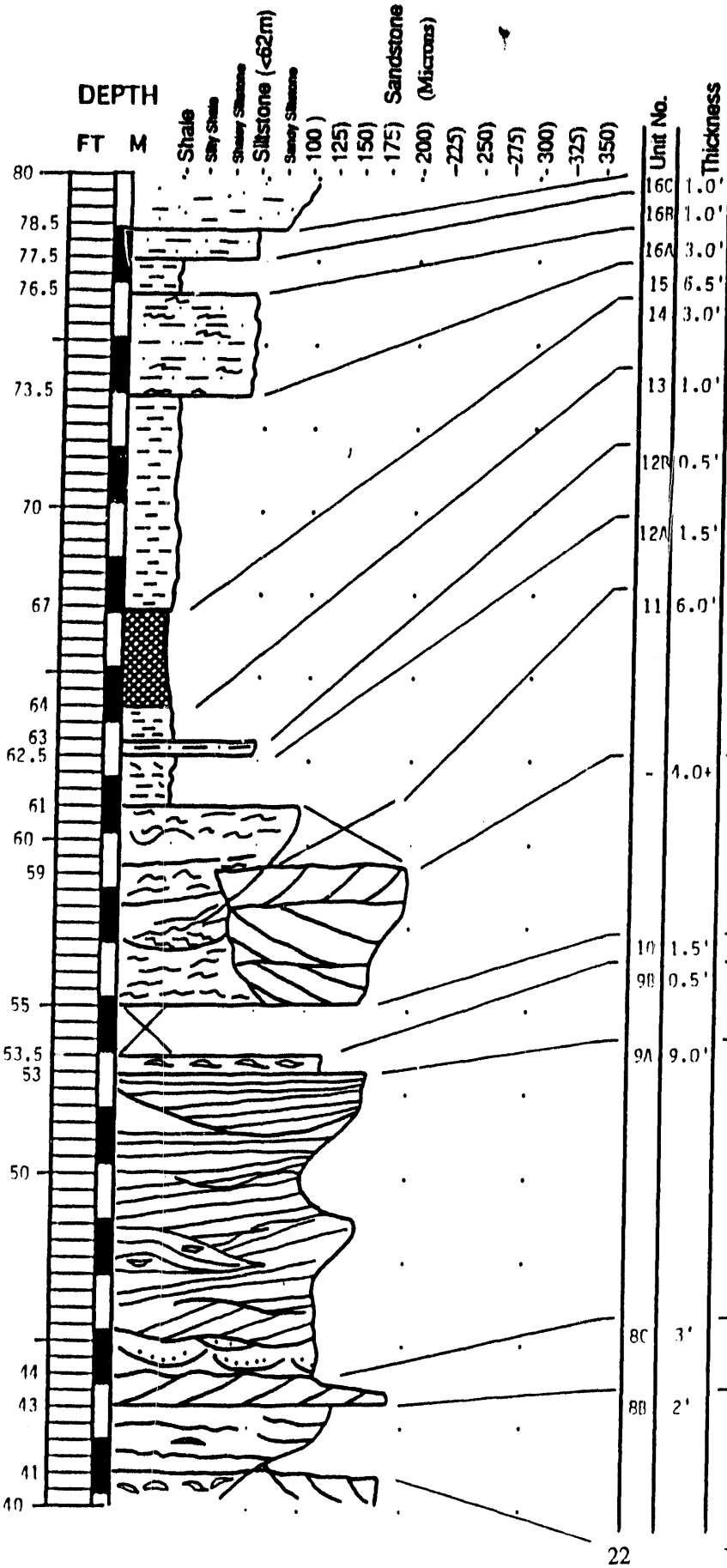

Unit No.	Thickness	
16C	1.0'	77.5-78.5' Siltstone.
16B	1.0'	76.5-77.5' Shale, gray. Trace carbonaceous. BAY FILL SHALE (90%).
16A	3.0'	73.5-76.5' Siltstone. Rippled; thin (1/2") rippled beds.
15	6.5'	67.0-73.5' Shale, dark gray, only slightly carbonaceous (<5%) fissile. BAY FILL SHALE (90%).
14	3.0'	64.0-67.0' Coal, black, vitreous non-clayey. Sharp upper and lower contacts. PINTAIL COAL, MARSH (95%).
13	1.0'	63.0-64.0' Claystone, gray, 25% carbonaceous fragments, fissile. MARSH (75%).
12B	0.5'	62.5-63.0' Siltstone (65 microns, moderately well sorted). Dark gray carbonaceous stained.
12A	1.5'	61.0-62.5' Shale, carbonaceous brown-black. 20%+ carbonaceous fragments. CONTINENTAL (95%).
11	6.0'	55.0-61.0(S)' Sandstone (65-100 microns, 70%). 30% silty shale in 1/2"-3" beds and drapes. Sandstone 65% ripples, 20% with 1 mm thick shale drapes. Trace? of burrows. This unit is cut out by tidal channel to north. TIDAL FLAT (95%).
-	4.0+	55.0-59.0(N)' Sandstone (150-200 microns, moderate to moderately well sorted). Planar tabular 1' thick beds; flow toward 80-140°. Trace of sand filled burrows. This unit erodes tidal flat in Unit 11. Located 50' N of 55' on Measured Section. TIDAL CHANNEL (Ebb Flow)(70%).
10	1.5'	53.5-55.0' Covered.
9B	0.5'	53.0-53.5' Sandstone (125 microns, moderate sorting). Thin (2") beds, 40% oysters. TIDAL CHANNEL FILL (70%).
9A	9.0'	44.0-53.0' Sandstone (125-150 microns, moderately sorted). Swaley cross stratified (SCS) (70%), and 30% medium troughs. Slightly deformed and fractured. Fracturing and slight bending (soft sediment?) obscure most bedding and lamination. Cut and fill within unit up to 1.5'. Fill of cuts commonly parallels 1-2" thick laminated swaley beds. Wave deposits filling channel? Trace of white clay fragments. MIDDLE SHOREFACE (70%).
8C	3'	43.0-44.0' Sandstone (175 microns). A single sand wave flowing NE, 1' thick. Top eroded.
8B	2'	41.0-43.0' Sandstone (175 microns, moderately poor sorting). Irregularly horizontally bedded; internally deformed to horizontally laminated. Top 0.7' massive. 3% oysters. 25' wide. Filling of upper part of tidal channel. TIDAL CHANNEL (90%).

FIGURE 12c Measured section RH-3 Almond Sandstone. SW NW sec. 8, T15N, R102W, Sweetwater County, Wyoming. 80 to 120 ft.

Note: Units 21-23 downlap on oyster Tidal Inlet Fill bed that truncates 50' to south.

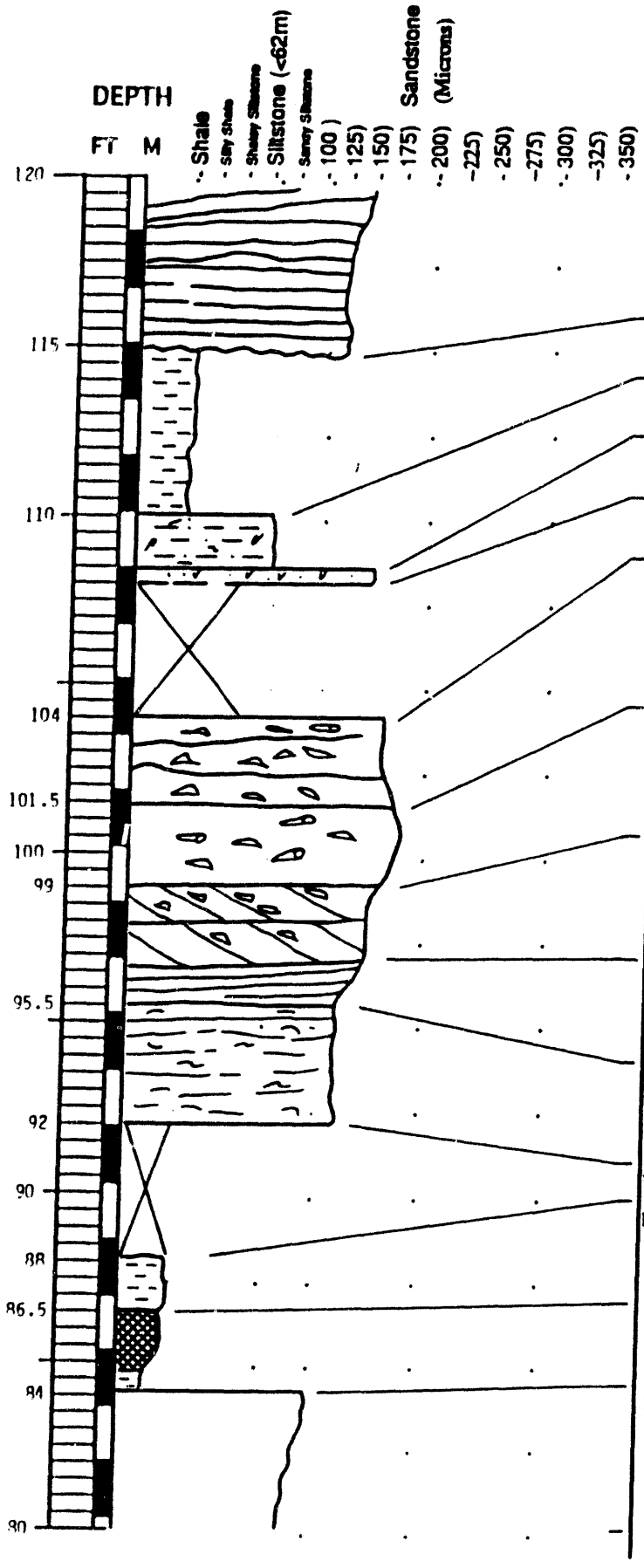

Unit No.	Thickness	
27	5.0'	110.0-115.0' Shale, gray, non-carbonaceous BAY FILL SHALE (75%).
26	1.5'	108.5-110.0' Siltstone, gray, abundant plant fragments. MARSH (90%).
25	0.5'	108.0-108.5' Sandstone (150 microns) poor sorting, rooted "SPLAY".
24	4.0'	104.0-108.0' Covered, probably friable sandstone.
23	2.5'	101.5-104.0' Sandstone (150-200 microns). (Local increases in thickness by 1.5' due to channeling). Oysters up to 60% of sandstone. Sub-horizontally bedded to massive. TIDAL CHANNEL LAG (80%).
22	2.5'	99.0-101.5' Sandstone (175 microns, poor sorting). Massive to sub-horizontally laminated (40%). 5-10% sand filled burrows. TIDAL CHANNEL?
21B	2.0'	97.0-99.0' Sandstone (150 microns, poorly sorted). Horizontal 1' beds. Planar tabular laminated. 30% oysters which form a drape on laminae. TIDAL DELTA RAMP (75%).
21A	1.5'	95.5-97.0' Sandstone (150 microns, moderate sorting). Sub-horizontally laminated. TIDAL DELTA SWASH BAR (75%).
20	3.5'	92.0-95.5' Sandstone (125 microns, moderate sorting). Partially rippled, 1-2" thick beds. Partially covered. Current deposited.
19B	4.0'	88.0-92.0' Covered.
19A	4.5'	86.5-88.0' Shale, fissile, gray, with trace micro-mollusca. Trace of carbonaceous material. BAY FILL SHALE (75%).
18	2.5'	84.0-86.5' Coal, black, vitreous. Basal 6" clayey. WAXWING COAL; MARSH (90%).
17	5.5'	78.5-84.0' Sandstone (75-100 microns, moderately well to well sorted). Irregular bedding planes. Massive appearing, 20% rippled. Sharp upper, gradational lower contact. SPLAY (75%).

FIGURE 12d Measured section RH-3 Almond Sandstone. SW NW sec. 8, T15N, R102W, Sweetwater County, Wyoming. 120 to 160 ft.

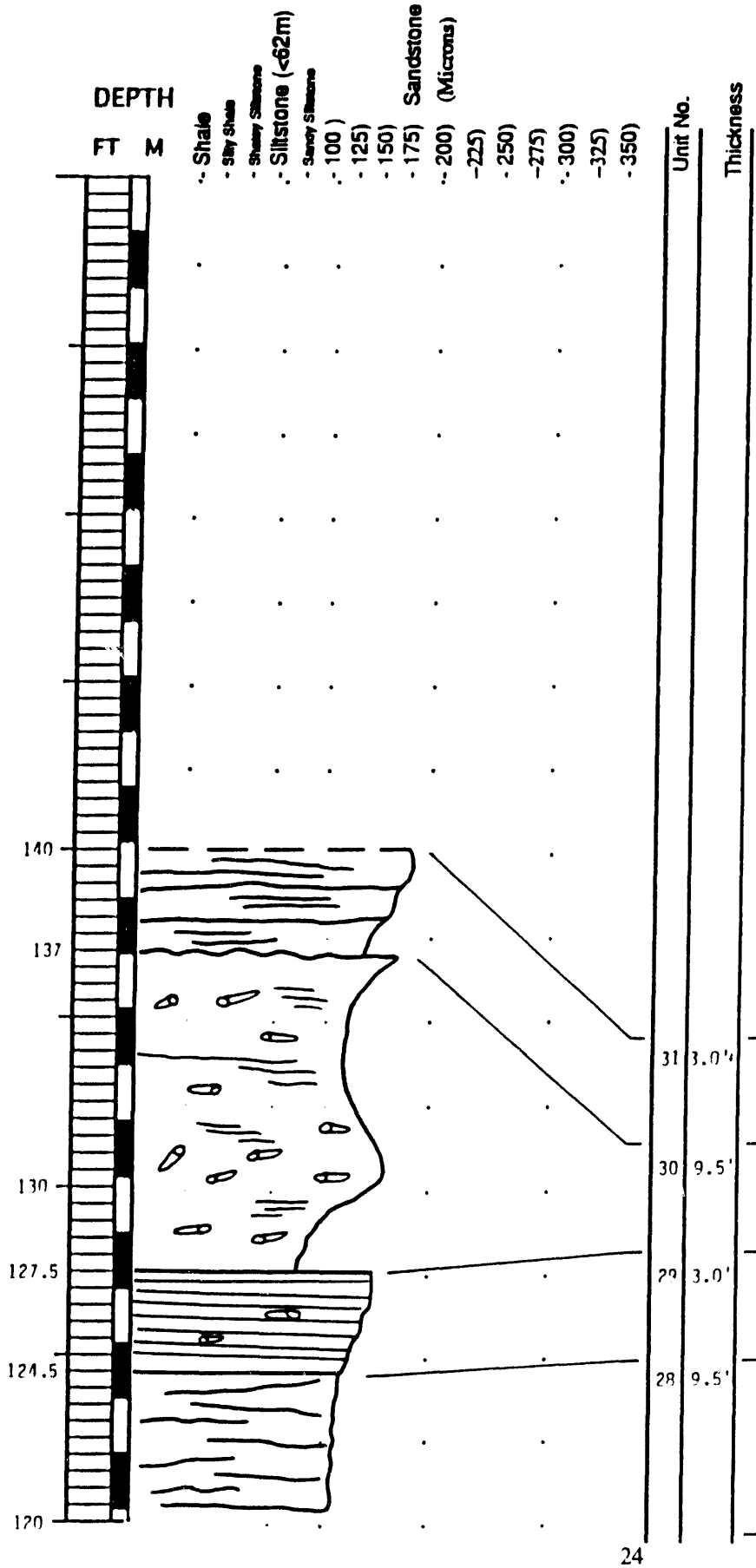

137.0-140.0+ Sandstone (150-175+ microns, moderate sorting). White. Sub-horizontally bedded and laminated. TIDAL DELTA SWASH BAR (75%).

127.5-137.0' Sandstone (100 microns at base to 150 microns). 90% bioturbated, 10% sub-horizontally laminated. MIDDLE SHOREFACE (95%).

124.5-127.5' Sandstone (125-150 microns). Horizontally laminated. Trace of burrowing. MIDDLE SHOREFACE (90%).

115.0-124.5' Sandstone (125-150 microns, moderate sorting). Trace of burrows. Bedding uniform thickness (1-3") throughout. Some cut and fill; filled with sub-horizontal laminae. (Wave deposit) MIDDLE SHOREFACE (80%).

FIGURE 13a Measured section RG-7 Almond Sandstone. SE SW SW sec. 33, T16N, R102W, Sweetwater County, Wyoming. 0 to 40 ft.

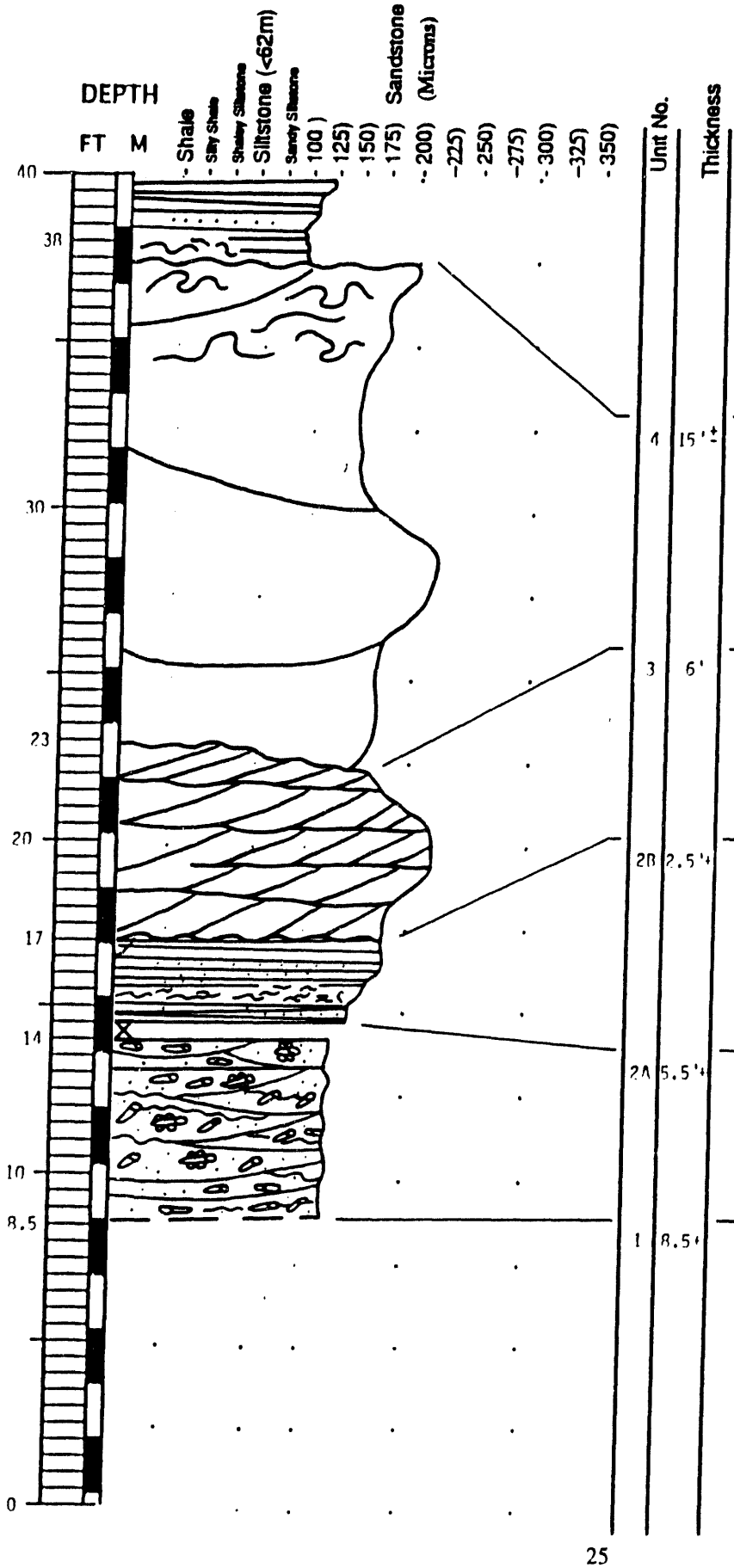

Described by R. W. Tillman & R. Schatzinger
Date: 6/18/91
Base of section measured from fence post approximately 50' north of Highway 430. Near southernmost outcrop of Rohler's Bar G (1988). Traverse 110° at apparent dip of 3° E. One and possibly two approximately N-S faults cut section above 216', total offset of fault(s) 80-130'±. Measured interval 216'. Measured section offset 20' to east at 92'. Traverse changed to north at 95'. Offset to east at 105', traverse 135°. Mud Springs Ranch Quadrangle (7 1/2").

4 — 15'± — 23.0-38.0' Sandstone (175-225 microns, moderately poor to moderately well sorted). Massive appearing throughout. Large scale cut and fill; cut 3'+. Non-burrowed? This abruptly to north; replaced by sub-horizontally laminated sandstone to north. Upper 3-4' soft sediment deformed. TIDAL CHANNEL (90%).

3 — 6' — 17.0-23.0' (175-225 microns, moderate sorting). Wedge sets with planar cross laminae throughout. Set boundaries dip north, cross-laminations dip east (Ebb tidal). Pinches out to south. Non-burrowed. Unit only 60' wide. TIDAL DELTA (90%).

2B — 2.5'+ — 14.5-17.0' Sandstone (150-175 microns. 175 microns at top, moderately sorted, 100%). 80% horizontally to sub-horizontally laminated. 20% large ripples, symetrical to asymetrical and small troughs (2" amplitude). Wave deposited. Trace of Ophiomorpha. MIDDLE SHOREFACE (80%).

2A — 5.5'+ — 8.5-14.0' Sandstone (125 microns, moderately sorted, 100%). Low relief swales with some internal trough cross-lamination. 10% sub-horizontally laminated. Bioturbated, 90% burrowed, trace of Ophiomorpha. MIDDLE SHOREFACE (75%).

1 — 8.5+ — 0-8.5' Covered.

FIGURE 13b Measured section RG-7 Almond Sandstone. SE SW SW sec. 33, T16N, R102W, Sweetwater County, Wyoming. 40 to 80 ft.

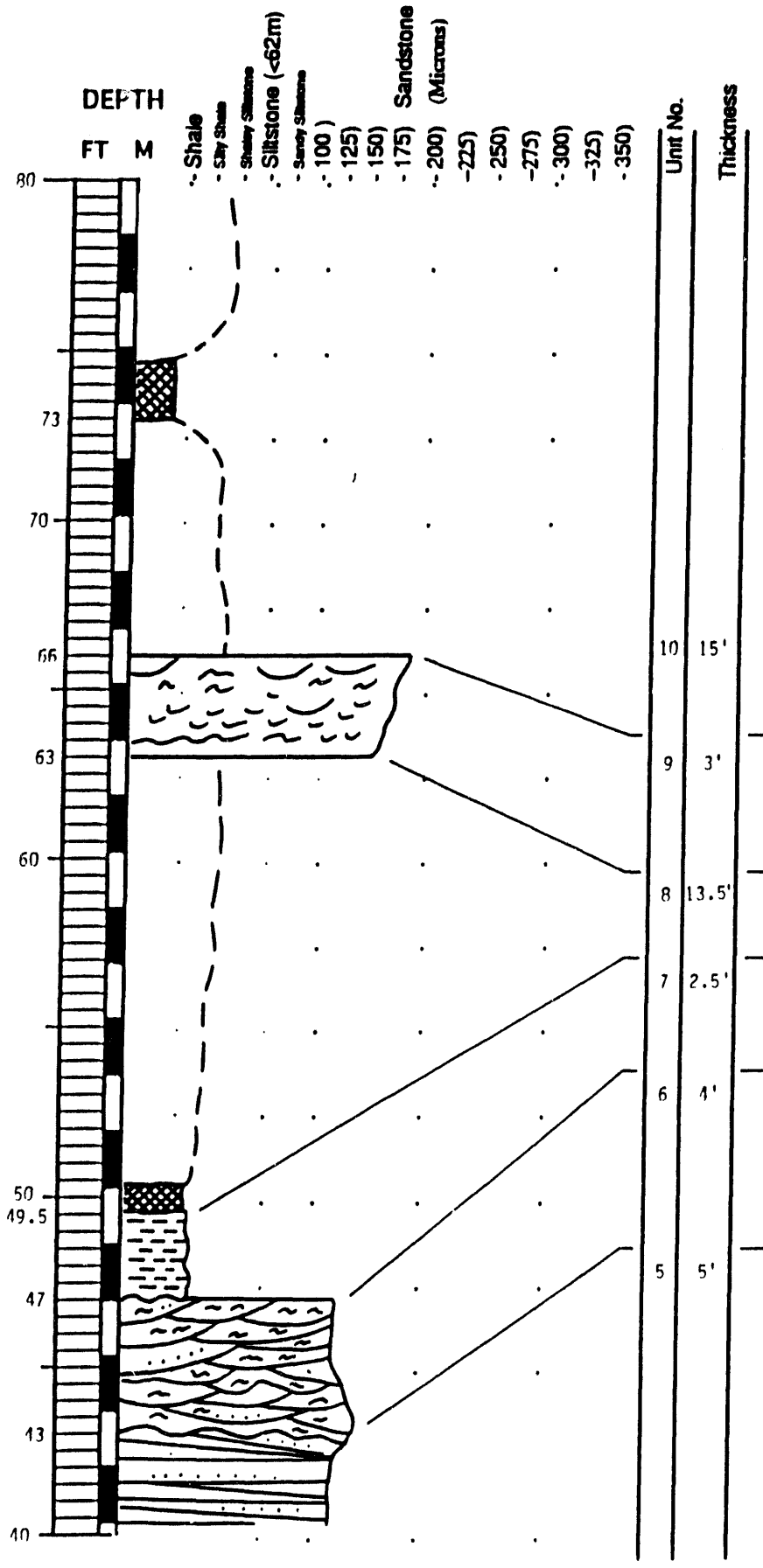

66.0-81.0' Covered (with oyster shell sandstone debris). 1.5'+ thick burned out coal 73.0-74.5'. Waxwing coal. MARSH (90%).

63-66' Sandstone (150-175 microns, moderately well sorted). Lenses out laterally, 50' wide, 80% rippled, 20% small troughs. CHANNEL SANDSTONE (TIDAL, 60%).

49.5-63.0' Covered, (shale?). At base burned out coal. Equivalent of Pintail coal of Rohler, 1988.

47-49.5' Shale, gray. Thin, 0.2' thick, siltstone in lower 1.0'. Gray slightly carbonaceous shale. BAY FILL (90%).

43-47' Sandstone (125 microns, moderately well sorted). Irregular to low-angle trough bedded, 35% small troughs, internally rippled (30%). Soft sediment deformed (30%), 5% carbonaceous shale rip-up-clasts. TIDAL CREEK (IN BACKSHORE)(70%).

38-43' Sandstone (100-125 microns, moderately well to well sorted). Sub-horizonatlly laminated, well sorted (greenish color). Base of unit unconformable. Locally lower 1' soft sediment deformed. BACKSHORE (70%) OR FORESHORE (BEACH) (30%).

FIGURE 13c Measured section RG-7 Almond Sandstone. SE SW SW sec. 33, T16N, R102W, Sweetwater County, Wyoming. 80 to 120 ft.

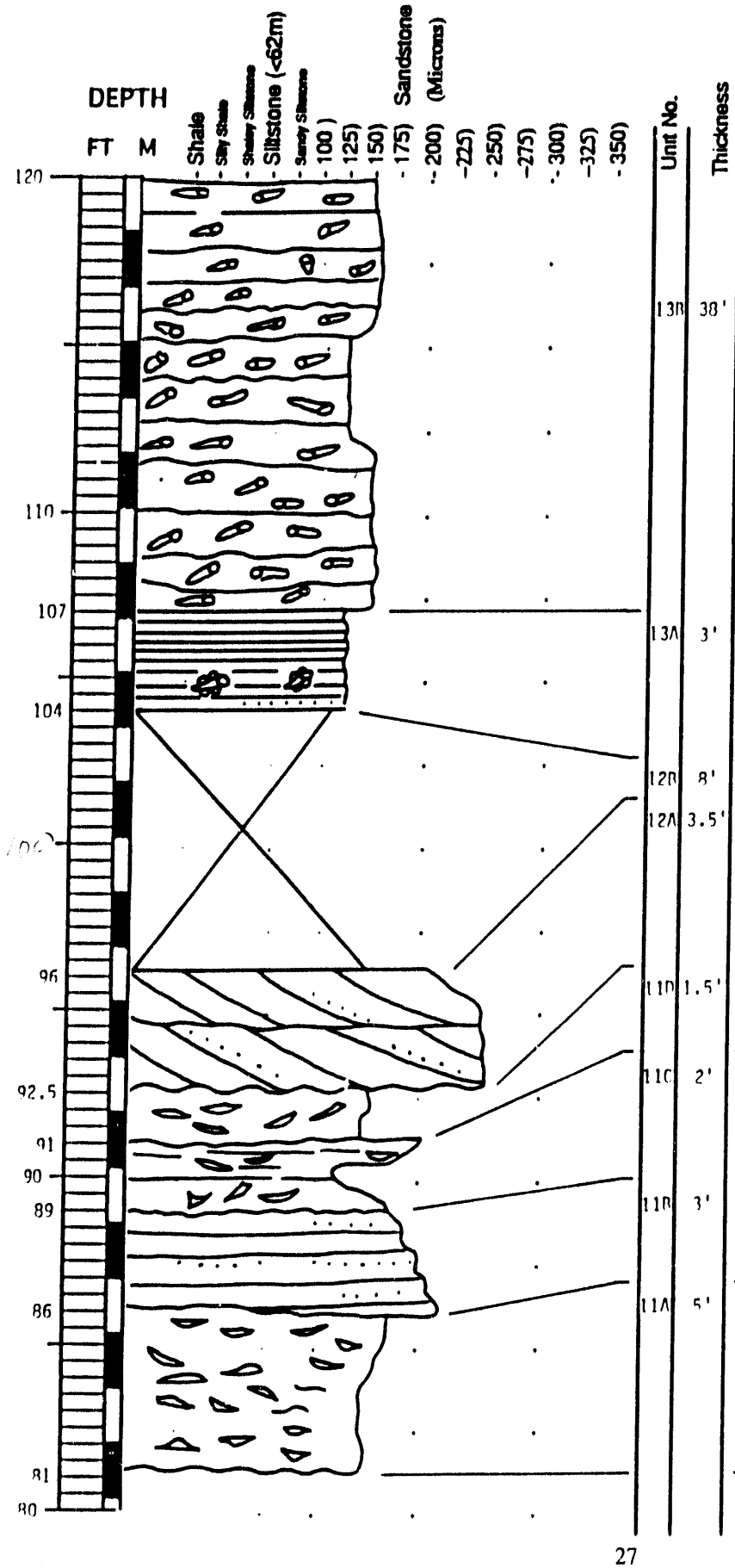

107-145' Sandstone (125-150 microns, moderately well to well sorted). 90% burrowed (bioturbated). 3-6" thick beds. Horizontal slightly undulating bedding planes, 10% horizontally laminated. Uniform appearance throughout. Most burrows less than 1/4" diameter, sand filled, oblique. Includes two covered intervals. Ophiomorpha burrows at top. Long horizontal offset of measured section to north at 121'; changed to 8° apparent dip to north. MIDDLE SHOREFACE (90%).

101-107' Sandstone (100-125 microns, moderate sorting). Horizontally laminated (95%). Trace of vertical 1" diameter Ophiomorpha burrows. Wave deposited. MIDDLE SHOREFACE (65%).

96.0-104.0' Covered.

92.5-96' Sandstone (200-250 microns, moderate to moderatly well sorted). 3% Ophiomorpha burrows, Large scale, 2'+ thick, troughs, flow to NNE, 5% scattered oysters. TIDAL DELTA (60%) OR TIDAL CHANNEL (40%).

91-92.5' Sandstone, oyster lag (175 microns, moderate sorting). 15% oysters.

89-91' Sandstone (125-175 microns, moderately sorted). Some oyster lag at base (15%) decreasing upward (2%). Subhorizontal bedding. Internally massive.

86-89' Sandstone (225 microns [base] to 175 microns, moderately sorted). "Horizontal" bedding, 2-3" thick. Internally massive.

81-86' Sandstone (oyster lag). Base of unit 150 microns, 175 microns at top, poor to moderate sorting). 2-3% carbonaceous fragments and grains. 10-20% fragmented oysters, highly calcite cemented. Bedding apparently irregularly horizontal.

FIGURE 13d Measured section RG-7 Almond Sandstone. SE SW SW sec. 33, T16N, R102W, Sweetwater County, Wyoming. 120 to 160 ft.

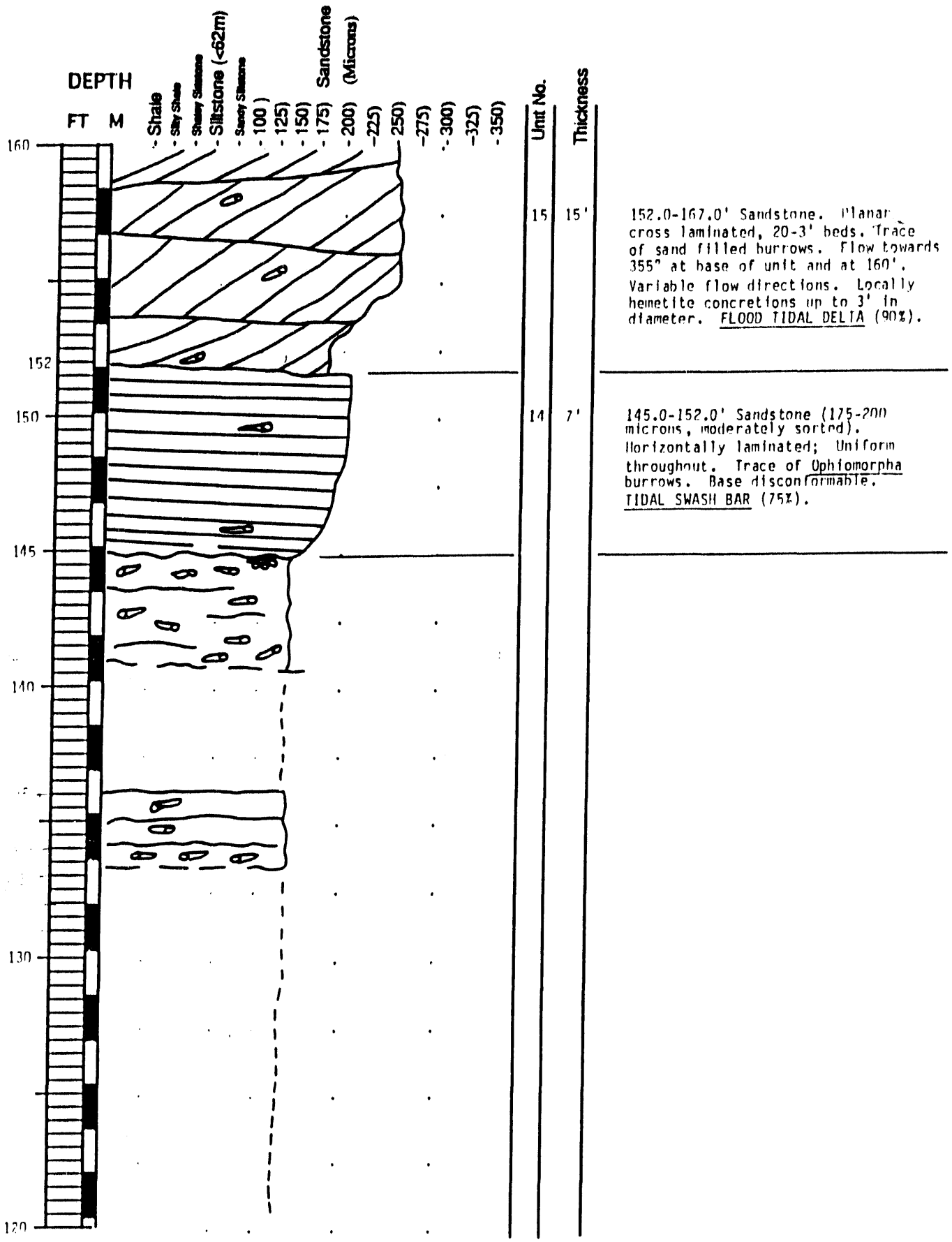

FIGURE 13e Measured section RG-7 Almond Sandstone. SE SW SW sec. 33, T16N, R102W, Sweetwater County, Wyoming. 160 to 200 ft.

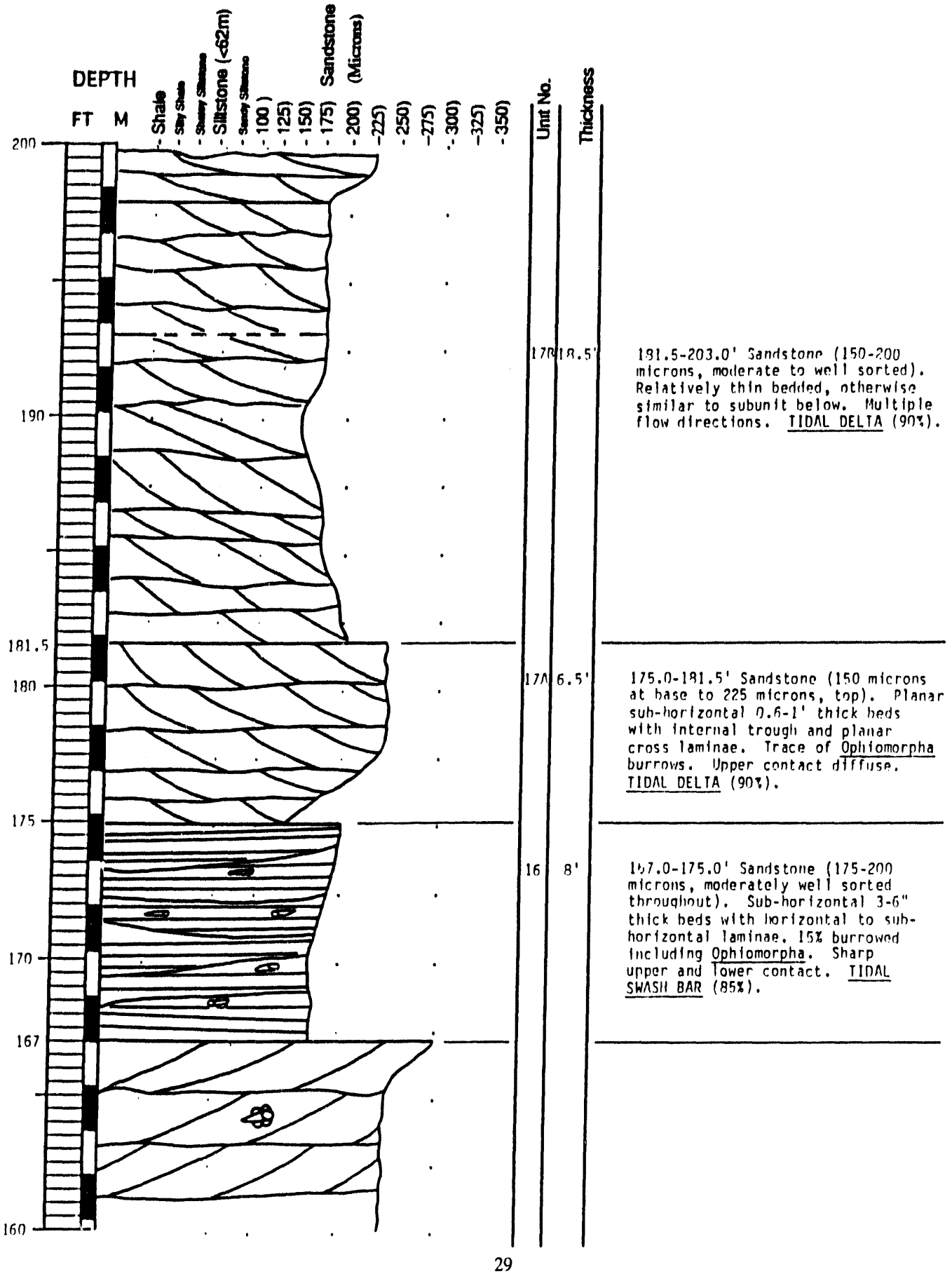

FIGURE 13f Measured section RG-7 Almond Sandstone. SE SW SW sec. 33, T16N, R102W, Sweetwater County, Wyoming. 200 to 240 ft.

[Note: Description and interpretation above 216' is incomplete as of 6/21/91.]

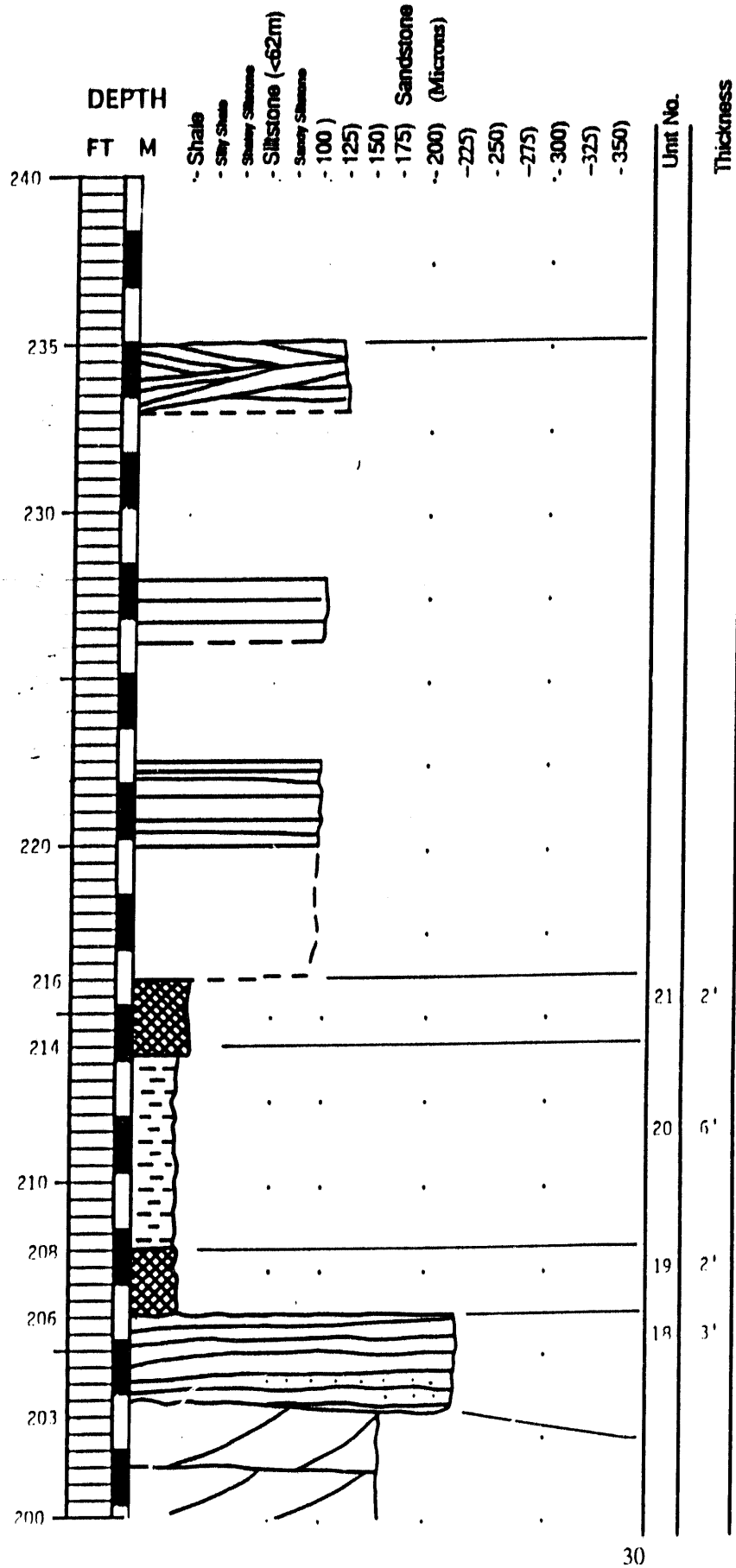

Unit No.	Thickness	
		Top of Outcrop in westernmost fault block.
		216.0-235.0' Sandstone (100-125 microns). Mostly covered along line of measured section. Two sandstones outcrop 50' to west of covered interval. Sandstones light brown, hard platy, calcareous cemented. Small scale HCS. 2% burrowed. INNER SHELF (90%).
21	2'	214.0-216.0' Coal, black vitreous. MARSH (90%).
20	6'	208.0-214.0' Carbonaceous dark gray shale. MARSH (75%).
19	2'	206.0-208.0' Coal, black, vitreous. MARSH (90%).
18	3'	203.0-206.0' Sandstone (225 microns, moderately well sorted). Sub-horizontal to horizontal laminae and beds; swash deposit. Rooted (30% at top. TIDAL SWASH BAR (90%).

FIGURE 13g Measured section RG-7 Almond Sandstone. SE SW SW sec. 33, T16N, R102W, Sweetwater County, Wyoming. 240 to 260 ft.

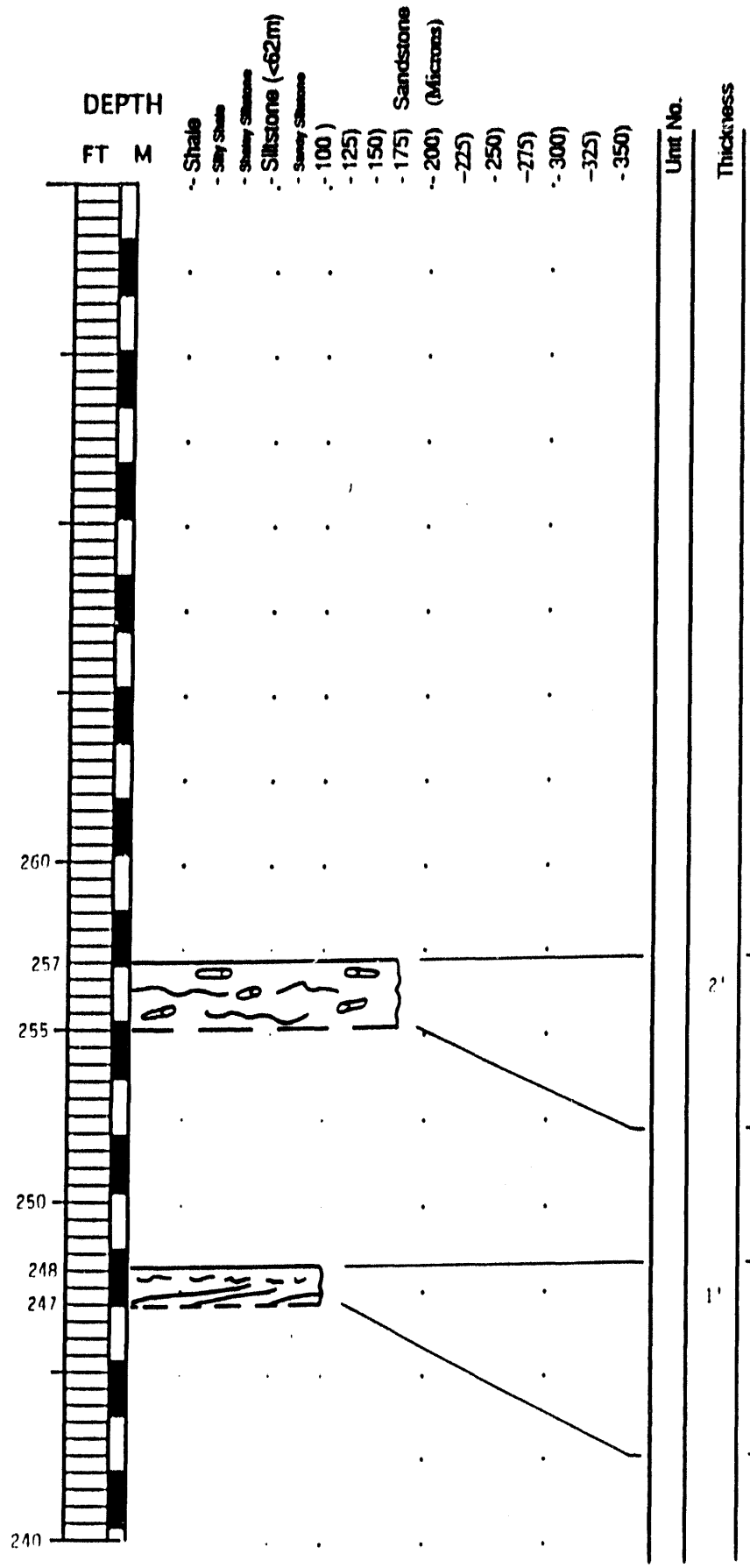

Thickness	
2'	255.0-257.0' Sandstone (175 microns, moderately well sorted). Thin 0.1' thick irregular bedded. Burrowed. Includes Ophiomorpha. Probably bioturbated. MIDDLE TO LOWER SHOREFACE (75%).
1'	247.0-248.0' Sandstone (100 microns). Rippled, non-burrowed. Laterally from measured section sub-horizontal to HCS. In measured section above 235' moved 1/8 mile northeast used dip of 5° on traverse of 100°. INNER SHELF (65%)/

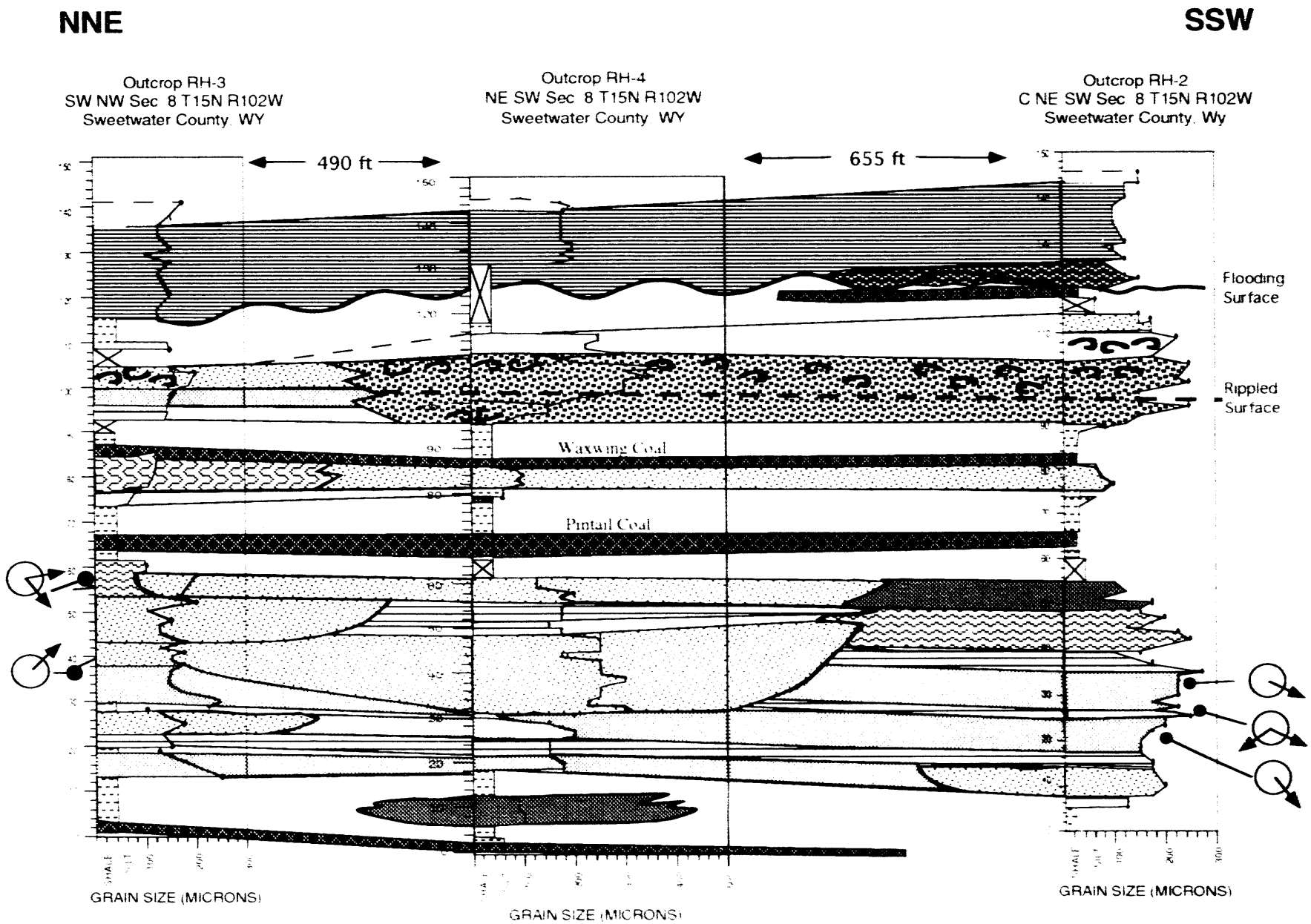

FIGURE 14 Cross section of outcrops RH-2, RH-3 and RH-4, Sweetwater County, Wyoming. Paleocurrent directions indicated by arrows within circles. See figures 2 and 3 for outcrop location and figure 15 for legend.

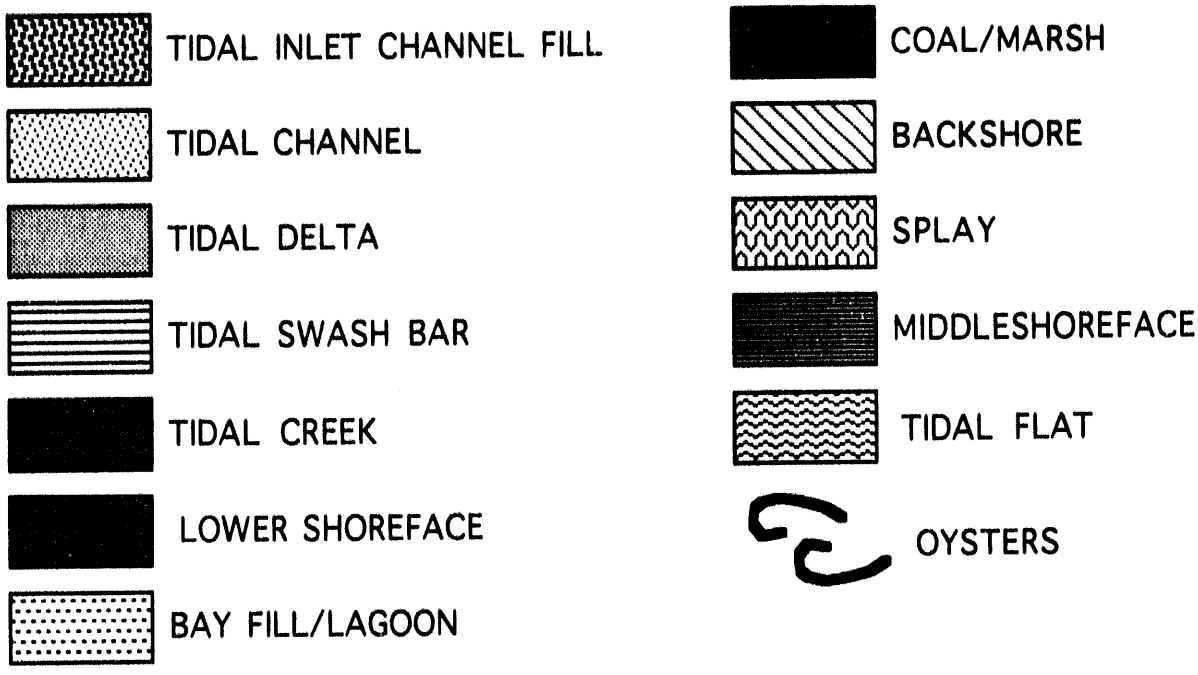

FIGURE 15 Legend for facies represented in Figure 14.

III Petrographic, Permeability and Porosity Data

Mineralogical Composition of the Almond Formation

Whole rock X-ray diffraction (XRD) analysis in weight percent was performed on five samples from outcrop RG7 (Table 3). Total carbonate in analyzed outcrop samples ranges from less than 1 to 4%, although visual examination of additional outcrop samples indicates that some, particularly oyster-rich beds, may be extensively calcite cemented. Dolomite was present in the outcrop sandstones (mean of 0.9%). Ferroan dolomite was present only in some subsurface samples, particularly those that were the most tightly cemented. A comparison of framework composition, mineralogy and grain-size in outcrop and Patrick Draw field subsurface samples is presented by Schatzinger et al., 1992.

The total feldspar content of Patrick Draw sandstones averages 4.8% based on our data, and is in close agreement with 5% determined by Keighin et al., (1989). In addition, our data in Table 3 indicate that there is about twice the feldspar content in outcrop Almond sandstones as those from Patrick Draw field. Thin sections indicate that both in outcrop and in the subsurface considerable detrital feldspar has been removed by dissolution and some has been replace by carbonate minerals. Potassium feldspar (dominantly orthoclase) is more common in upper Almond sandstones at depths less than 6,000 ft in contrast to plagioclase feldspar, which is more common in the more deeply buried upper Almond sandstones (Keighin et al., 1989). Table 3 also indicates that, although there is more feldspar in outcrop Almond sandstones, the proportion of orthoclase to plagioclase feldspar is about equal in both outcrop sandstones and those from Patrick Draw field.

Keighin et al., (1989) found a mean value of 18% total clays from sandstones buried 4,500 to 7,000 ft. Our XRD data (Table 3), however, indicate a mean of only about 3.6% total clays from Patrick Draw reservoir sandstones and 2.2% from outcrop Almond sandstones. These values are generally less than those derived from log analysis (mean of 7-8%) of UA-5 reservoir sandstone at Patrick Draw field. This discrepancy may be explained partly by the selection of a relatively small number of "clean" samples for XRD analysis, which may not be as representative as the "average" values determined by log analysis. Additionally, the amount of clays and carbonate cements varies greatly on the scale of a few millimeters to a few inches. Log-derived clay values may, therefore, be expected to indicate generally more clays than those determined by XRD analysis in this highly heterogeneous type of formation. The mean clay content for shallowly buried upper Almond sandstones given by Keighin et al., (1989) was based on 46 samples collected from over much of the Greater Green River Basin east of the Rock Springs Uplift. Only five of those samples were from Patrick Draw field.

Point count data from 12 thin sections of samples from Patrick Draw field indicate an average of 7.9% total clay, which is in generally close agreement with our log-derived values. Therefore, our petrographic and wireline log analyses indicate on average less than half of the total clay content for reservoir sandstones at Patrick Draw field than Keighin et al., (1989) found based on widespread subsurface data for the upper Almond Formation.

Two other important constituents that may account for the generally low average permeability of reservoir sandstones at Patrick Draw field are rock fragments and carbonate cement. Of 12 thin sections analyzed, the average rock fragment content was 16.1%. One-third to one-half of the rock fragments are of the fine grained sedimentary type with some recognizable metamorphic and igneous (possibly volcanic) types. The types of rock fragments are important because sedimentary fragments and altered volcanic fragments are ductile to extremely ductile (Pittman and Larese, 1991). Obviously, the greater the content of ductile rock fragments, the greater the potential for compaction and reduction of the reservoir pore and throat system. The average total carbonate cement from point counted thin sections was 15.1%, with extreme values of 0.0 and 41.5%. Such abundant yet variable amounts of carbonate cement could have a significant effect on the reservoir rock quality. It is not yet known whether calcite or dolomite is more important with respect to petrophysical properties because the dolomite/calcite ratio varies widely from 1:93 to as much as 25:1.

Keighin et al., (1989) found that kaolinite is the most abundant clay in the shallow reservoir sandstones and that the abundance of kaolinite decreases with increasing depth of burial. Kaolinite is generally not present in upper Almond sandstones buried greater than 9,000 ft. Keighin et al., (1989) also reported that chlorite was not present in any sandstone samples, that illite clays dominated the clay fraction below 9,000 ft, and included discrete illite and illite/smectite. Illite/smectite is of the ordered variety and contains less than 25% expandable layers. Very little smectite is present in either sandstones or shales. Keighin et al., (1989) concluded that even upper Almond rocks that are now at depths as shallow as 4,500 ft may once have been buried to depths where the temperature exceeded 212 °F, or may have experienced a heating event.

Our mineralogical analysis of the upper Almond sandstones (Table 3), both from outcrop and from Patrick Draw field found the same suite of clay minerals as was reported by Keighin et al., (1989). XRD analysis of our

samples indicates that kaolinite is the dominant clay mineral present in reservoir samples and is about equal to mixed layered illite/smectite in samples from the outcrop. Chlorite was not found in any of the samples.

The essential framework components of sandstones are recalculated to 100% and plotted on a quartz-feldspar-rock fragments (Q-F-R) diagram (fig. 16). Almond reservoir sandstones tend to be sublitharenites, litharenites, and feldspathic litharenites low in quartz. Subsurface Almond sandstones tend to have a higher average quartz content than the outcrop Almond sandstones. Almond outcrop sandstones have a higher feldspar content than many Almond reservoir sandstones.

Grain Size and Sorting (Almond Outcrop)

Grain size and sorting (standard deviation of grain-size) were determined from analysis of 30 thin sections from outcrop core plugs by petrographic image analysis. At least 300 point counts per thin section were made. Statistics of the point count data along with permeability and porosity measured from the 1-inch diameter core plugs are listed in Table 4. Analysis of grain size is important in determining the degree of depositional similarity between the outcrop and subsurface rocks, as well as in distinguishing reservoir rock types and their relationship to depositional and diagenetic facies. Subsequent correlations between grain size, pore size distributions, permeability, and other petrophysical properties will be an important component in defining the flow units within the reservoir.

Grain size in sandy facies from the Almond Formation ranges from coarse silt to fine sand (30 - 225 microns). Grain size distribution among combined Almond outcrop and subsurface data falls into two groups (fig. 17). These include a fine-grained group comprising tidal creek and tidal flat facies and a second, relatively coarser-grained group, comprising all of the other facies. Among the coarser-grained group of facies, middle shoreface and some tidal delta samples tend to overlap the finer-grained facies group.

Comparison of mean grain size distribution for facies that are present in thin sections from both the outcrop and the subsurface (fig. 18) indicate that tidal channel grain size distributions are similar. Outcrop tidal delta samples tend to be coarser grained than their subsurface counterparts, as do tidal creek and tidal inlet samples (although there is only a single subsurface tidal inlet sample). Although only data from subsurface samples is available, tidal flat mean grain size are consistently finer than all other facies.

A good measure of the sorting of framework grains within sandstone is standard deviation of the mean grain size. Higher values of standard deviation reflect less well sorted samples. Comparison of the distribution of outcrop and subsurface Almond sorting data (fig. 19) is similar to that for grain size for respective facies. And, as with grain size, corresponding facies in outcrop and subsurface appear to have somewhat different ranges of sorting values. A possible explanation may be found by looking at the relationship between mean grain size and sorting.

A cross plot of mean grain size versus sorting for the entire Almond data set (fig. 20) shows a linear relationship with a high correlation coefficient ($R = 0.95$) and this same general relationship exists for outcrop as well as for subsurface data sets (figs. 21 and 22). The general trend of increasing grain size with decreasing sorting may represent a fundamental relationship created by the greater availability of a wide range of grain sizes for the coarser samples. The tight cluster of data around the best fit line is an indication of the overall good sorting created by tidal processes which dominated deposition of many of the Almond facies. More poorly sorted sandstones, particularly those from medium to coarse-grained samples from other depositional systems (such as fluvial sands), might be expected to show a much greater divergence from the best fit line as one proceeds toward coarser grain size. Further work, however, would be necessary to confirm such a relationship.

Almond Formation grain-size and sorting data are clustered in facies-dependent groups which are, in turn, somewhat different for subsurface and outcrop samples (figs. 21 and 22). Samples from the subsurface at Patrick Draw field may be divided into two groups. In the first group, tidal delta, tidal channel, and tidal inlet facies have coarser grain size and poorer sorting. In the second group, tidal flat and tidal creek facies have finer grain size and better sorting. Some tidal delta data overlap the second group, as does a single point from the tidal channel facies. These relationships are generally expected because the tidal channel, tidal inlet, and tidal delta facies were deposited in higher energy setting than were the tidal flat and tidal creek facies.

There is a wide range of energy across the tidal delta, which could account for the overlap with the finer grained samples. Most of the sediments in tidal channels, tidal inlet, and some tidal delta locations would be moved during the period typified by greatest tidal currents. This, in turn, tends to remove the fines and may create lags of coarser materials. Flow across tidal delta ebb shield and asymmetrical oscillating lower energy tidal flow on tidal creeks and tidal flats tend to better sort out finer sediments. Fine sands in the case of most tidal deltas, and very fine sand, silt, and mud in the case of tidal flats are concentrated in the low energy facies (Nichols and Biggs, 1985). On flood tidal deltas the higher sandy portions (ebb shields) are usually coarser than the lower flood ramp areas (DaBoll, 1969).

Data from the Almond Formation outcrops (fig. 22) can also be divided into three groups. Tidal inlet fill and tidal delta facies consistently contain the coarsest and least sorted (greatest standard deviation) sands while middle shoreface, tidal creek and tidal channel facies contain the finest sandstones with the best sorting (lowest standard deviation) A poorly-defined group of data from swash bar and oyster bed facies generally contain intermediate grain size and intermediate standard deviation values. The association of outcrop tidal channel sandstones with the finest, best sorted samples is generally the opposite of the relationship noted in the subsurface Almond Formation data, but is more like the relationship defined in the Parker River Estuary, Massachusetts (Da Boll, 1969). It should be noted that there is virtually no overlap, however, between the tidal channel data and that from the middle shoreface and tidal creek sandstones. It may be that the relative grain size and sorting of tidal channel sandstones in shoreline barriers is related to the tidal energy flux, sources of sand, and channel configuration, all of which may differ between various barriers. The grain size and sorting relationships of the subsurface Almond Formation appear to be more like those exemplified by the modern Georgia coastal barriers, while those of the outcrop Almond Formation appear to be more like those of the tidal sands from the Parker River Estuary, Massachusetts.

For all facies that were recognized in both outcrop and the subsurface, the grain size and standard deviation (sorting) "field" values overlap; however, outcrop samples from the tidal delta and tidal inlet fill facies all lie among the coarsest and least sorted overall values, outcrop tidal channel samples are among the finest and best sorted overall values, and outcrop tidal creek facies occur in the middle of the overall data set. Because the measurements were from framework grains, most of which are quartz, it is unlikely that the differences between outcrop grain size and sorting are related to different diagenetic histories. Rather, it seems more likely that there were differing intensities of similar processes operating on similar but not identical grain populations in the present Almond Formation outcrop and subsurface (UA-5) shoreline barriers.

Differences in facies grain size and sorting between outcrop and subsurface samples may result, in part, from the spatial distribution of the samples. The subsurface samples were taken from wells over an about 8 square mile area, whereas the outcrop samples are from two outcrop exposures located approximately 4 miles apart. The samples from the outcrop exposures may represent more local conditions while the subsurface samples may represent more average conditions over the barrier system.

Grain Size and Porosity

Porosity data measured from 1-inch diameter cores drilled from Almond Formation outcrop RG profile 7 (RG7) and outcrop RH profile 2 (RH2) is presented in Table 4. Facies interpretations are given for each sample depth.

Outcrop samples tend to have greater porosity (generally between 24 and 33%) than samples taken from the subsurface at Patrick Draw field (generally less than 24%) (fig. 23). Comparison of reservoir and outcrop permeability vs. porosity scatter plots (fig. 24) indicates different trends for subsurface and outcrop data. Outcrop rocks in general tend to be more porous and permeable than subsurface rocks, and this relationship becomes even more obvious when the data are examined on a facies by facies basis. The consistently better permeability and generally better porosity of outcrop rocks from the same facies indicates that although outcrop samples are distinct from the reservoir samples, the petrophysical properties of outcrop samples have all tended to move in the same general direction (relative to porosity and permeability).

When examined individually, tidal channel, tidal creek, middle shoreface, and the oyster bed facies each have a well established relationship between porosity and permeability. In addition, outcrop Almond sandstones from various facies show an obvious trend between increasing porosity and increasing permeability with a high correlation coefficient ($R = 0.91$).

If the six very low permeability subsurface data points in figure 24 are considered separately, it becomes apparent that permeability is independent of porosity for subsurface samples taken together as a group. Because the six very low permeability samples were the result of abundant detrital clays or very abundant calcite cement they appear to reflect different depositional and/or diagenetic processes as compared to the rest of the subsurface samples and probably should be considered independently. Because of the apparent overall lack of dependence between permeability and porosity in subsurface samples, it may be difficult to apply outcrop-derived petrophysical properties to the reservoir units at Patrick Draw field unless the data are examined on a facies by facies basis.

Because of the high correlation between grain size and sorting discussed above, scatter plots of porosity versus grain size and porosity versus sorting (standard deviation of grain size) show similar but highly overlapping facies distributions. Subsurface tidal creek and tidal flat facies, however, consistently tend to have lower porosity, finer grain size, and better sorting than tidal channel and tidal delta samples. Outcrop samples from tidal channel, middle shoreface, and tidal creek facies tend to be slightly less porous, have finer grain size, and better sorting than exhibited by swash bar, tidal delta, tidal inlet, and oyster bed facies. A linear relationship does not exist between porosity and grain size or porosity and sorting for either subsurface or outcrop samples.

Grain Size and Permeability

There is virtually no overlap between the permeability of Almond outcrop samples (fig. 25) with those from the UA-5 sandstone at Patrick Draw field, the outcrop samples having greater permeability. Because of the small number of outcrop samples analyzed and the absence of swamp, tidal flat, and lagoonal facies in the outcrop data set, it is difficult to draw further conclusions about the distinction between outcrop and subsurface facies based on permeability distributions alone.

Because of the close relationship between grain size and sorting (standard deviation of grain size) mentioned above, the scatter plots of permeability versus grain size and permeability versus sorting are very similar. For samples from which thin sections were made, data from these same scatter plots are clustered into facies dependent groups. Outcrop middle shoreface and tidal channel data tend to be finer grained, better sorted, and slightly less permeable than outcrop tidal delta, tidal swash bar, and oyster bed facies. Subsurface facies grain size and sorting appear to be independent of permeability if the same very low permeability samples are treated as a distinct group, as discussed for the porosity versus permeability scatter plots above.

TABLE 3

Whole rock x-ray diffraction analysis in weight percent, for samples from the upper Almond in Patrick Draw field and Rock Springs Uplift outcrops. Numbers in outcrop ID number correspond to measured section depth. (After Jackson et al., 1993)

Well	Depth, ft	Strat. Interval	Quartz	Plagioclase	K-Feldspar	Dolomite	Ferroan Dolomite	Siderite	Pyrite	Calcite	Gypsum	Kaolinite	Illite/Mica	Illite/Smectite
7-18-1	4,945	UA5	61	4	4	–	21	–	3	3	–	3	1	tr
45-14-3	4,450	UA5	5	–	tr	–	tr	–	–	93	–	2	tr	tr
78-14-6	4,305	UA5	78	2	3	5	tr	2	1	5	–	2	2	tr
49-1-3	4,615	UA-6	69	–	2	10	15	–	1	1	–	2	2	t
Arch 120	4,942.4	UA5	52	1	2	1	–	–	4	36	–	2	1	1
	4,944.6	UA5	66	3	3	19	–	–	2	3	–	3	1	tr
	4,948.7	UA5	82	2	4	1	–	–	3	4	–	3	1	--
	4,949.5	UA5	88	3	3	tr	–	–	1	1	–	3	1	tr
	4,962.4	UA5	91	3	2	tr	–	–	tr	tr	–	4	tr	tr
	4,962.5	UA5	86	3	4	–	–	tr	2	tr	–	4	1	tr
	4,966.5	UA5	85	3	2	4	–	–	3	tr	–	tr	2	1
Outcrop Samples														
G7-26B			89	2	3	3	–	–	–	--	–	1	1	--
G7-47			95	1	2	tr	–	–	–	tr	–	1	1	--
G7-91			83	5	8	tr	–	–	–	tr	–	1	1	--
G7-174			89	4	4	tr	–	–	–	--	tr	2	1	--
G7-191			90	3	4	1	–	tr	–	--	–	1	1	--

TABLE 4

Permeability, porosity and grain-size data measured from coreplugs drilled horizontally from Almond outcrop RG (profile 7) and RH (profile 2) localities. Grain-size data were obtained by image analysis of thin sections prepared from the coreplugs.

					GRAIN SIZE, microns							
Outcrop	Footage*	Facies	Permeability	Porosity	Minimum	Maximum	Number of points	Mean	Median	Standard Deviation	Variance	Trask Coefficient
RG7	9	Middle Shoreface	149.90	23.40	34.06	295.02	304	106.49	99.66	42.47	1803.30	1.28
RG7	11.5	Middle Shoreface	401.70	30.30	25.26	260.02	300	105.15	98.62	37.30	1391.40	1.22
RG7	15	Middle Shoreface			17.75	273.08	304	100.21	97.86	38.51	1482.80	1.26
RG7	24	Tidal Channel	749.40	27.50	5.27	328.15	301	135.48	126.66	51.31	2632.60	1.25
RG7	26	Tidal Channel			33.63	288.24	300	136.35	132.65	48.98	2399.40	1.30
RG7	28	Tidal Channel	719.50	27.80	7.94	326.49	301	134.22	128.10	50.87	2588.10	1.26
RG7	33	Tidal Channel	770.10	30.00	0.00	375.27	300	127.30	119.62	51.52	2654.60	1.38
RG7	37.5	Tidal Channel	340.00	24.50	36.52	247.10	300	116.25	111.72	42.33	1792.10	1.34
RG7	45	Tidal Creek	437.80	25.80	26.13	253.38	300	97.18	92.81	34.93	1220.10	1.27
RG7	47	Tidal Creek	104.90	24.70	0.00	256.27	300	85.89	81.55	34.26	1173.80	1.28
RG7	64	Tidal Channel	288.90	21.00	29.66	225.96	300	104.90	101.65	29.30	858.51	1.19
RG7	81	Oyster Bed	1,681.70	32.50	5.56	554.32	300	149.19	138.42	78.68	6191.20	1.35
RG7	85	Oyster Bed	1,336.80	30.70	33.70	363.66	300	155.63	153.83	66.53	4426.00	1.34
RG7	91	Oyster Bed			38.39	296.25	300	141.22	136.29	53.47	2859.00	1.32
RG7	94	Tidal Delta	393.40	27.20	41.06	407.97	300	168.92	156.57	74.38	5532.10	1.37
RG7	95	Tidal Delta	412.90	29.40	35.65	531.52	300	194.27	182.15	84.91	7210.10	1.39
RG7	105	Middle Shoreface	2.10	13.70	0.00	269.19	300	89.85	84.33	36.28	1315.90	1.30
RG7	107.3	Middle Shoreface	257.60	28.90	21.36	290.55	304	103.14	101.94	42.48	1804.40	1.36
RG7	115	Middle Shoreface	414.20	28.10	26.77	364.95	310	95.87	89.31	44.23	1955.90	1.32
RG7	121	Middle Shoreface	617.00	29.90	21.94	230.43	300	109.22	105.00	36.46	1329.20	1.24
RG7	142	Middle Shoreface			37.89	314.80	300	119.90	113.09	51.53	2655.30	1.30
RG7	170	Tidal Swash Bar	1,775.40	31.80	25.40	554.54	301	182.48	182.59	80.15	6423.90	1.34
RG7	174	Tidal Swash Bar	957.80	32.30	44.46	303.32	301	122.70	117.56	40.20	1616.10	1.23
RG7	191	Tidal Delta	1,243.00	31.30	25.62	535.63	300	157.04	146.07	66.84	4467.30	1.32
RG7	200	Tidal Delta	1,652.90	32.70	45.18	664.45	303	180.20	162.96	82.73	6844.60	1.34
RG7	204	Tidal Swash Bar	937.20	31.90	27.71	972.54	300	174.36	169.70	77.58	6017.90	1.27
RH2	11.5	Tidal Channel	234.70	27.80	17.68	309.02	300	130.15	120.20	55.97	3133.10	1.37
RH2	95	Tidal Inlet Fill			35.58	523.29	300	162.29	153.86	68.65	4712.30	1.30
RH2	101.5	Tidal Inlet Fill	36.10	18.30	59.90	741.38	300	220.40	209.18	93.63	8765.70	1.27
RH2	105	Oyster Bed	276.70	27.00	39.55	462.81	300	165.40	158.48	63.54	4036.90	1.28

* Footages correspond to those in the outcrop measured sections.

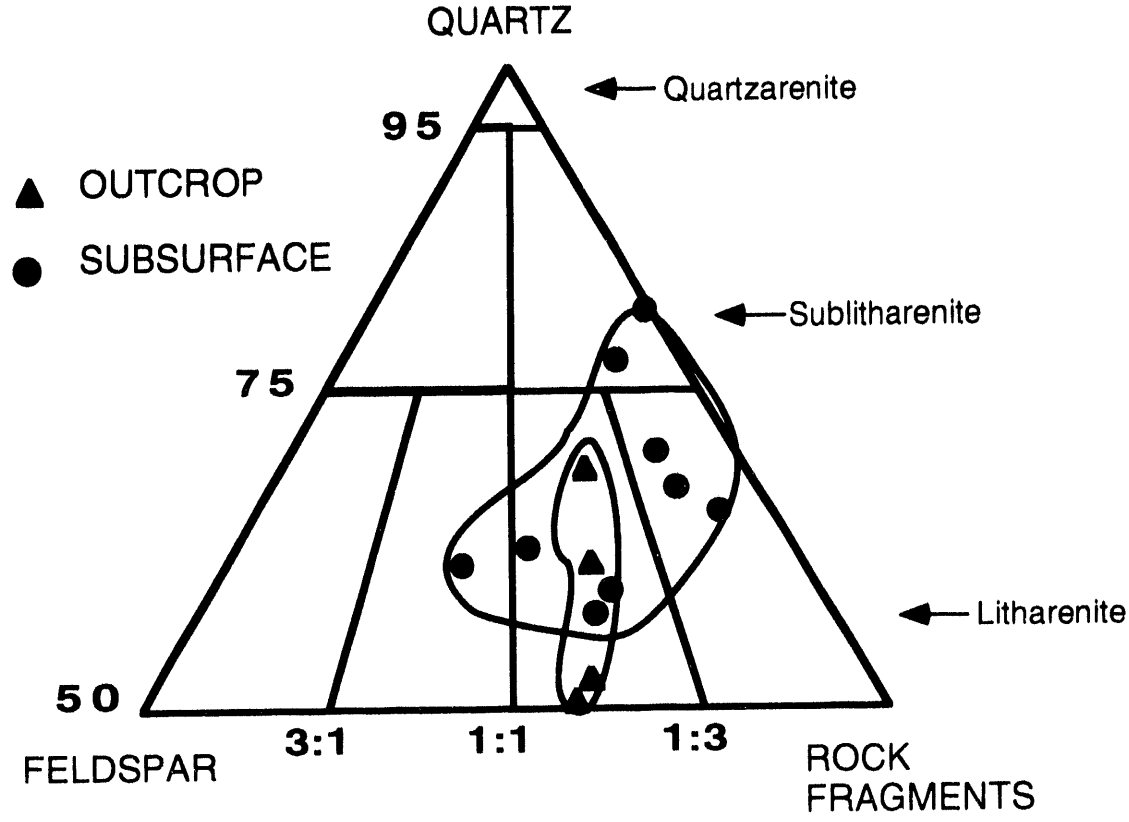

FIGURE 16 Ternary plot of quartz-feldspar-rock fragment composition of outcrop and subsurface Almond Formation. (After Schatzinger et al., 1992)

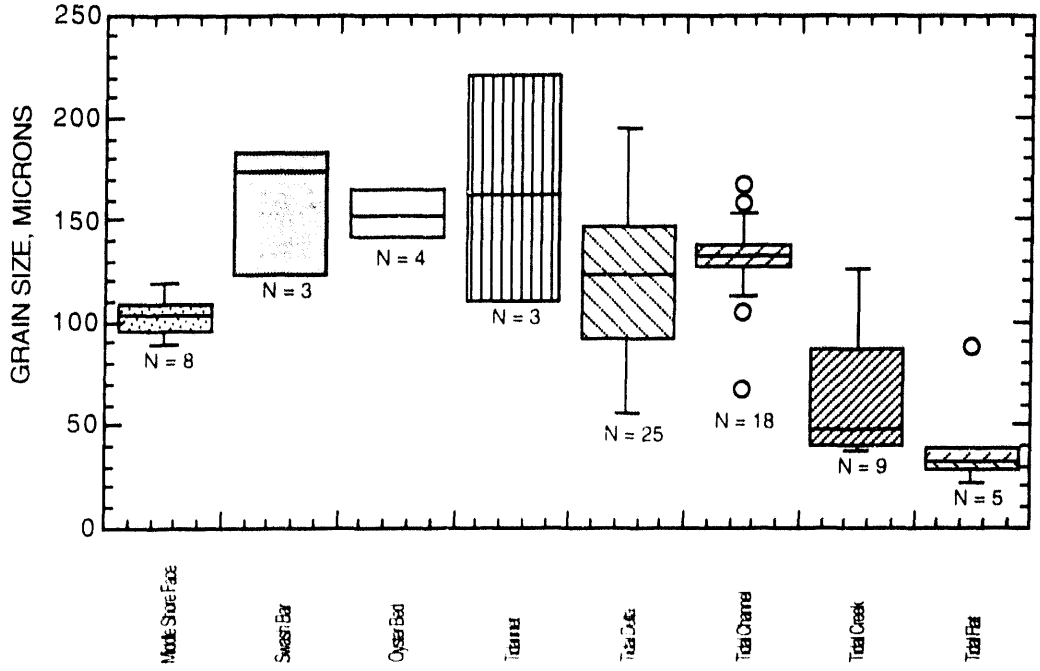

FIGURE 17 Grain size distribution for combined outcrop and subsurface facies in the Almond Formation. Boxes represent the second and third quartiles, whiskers indicate ranges of data to 5th and 95th percentiles, circles indicate data outliers beyond the 5th and 95th percentiles. N represents number of samples in each class of data. (After Schatzinger et al., 1992)

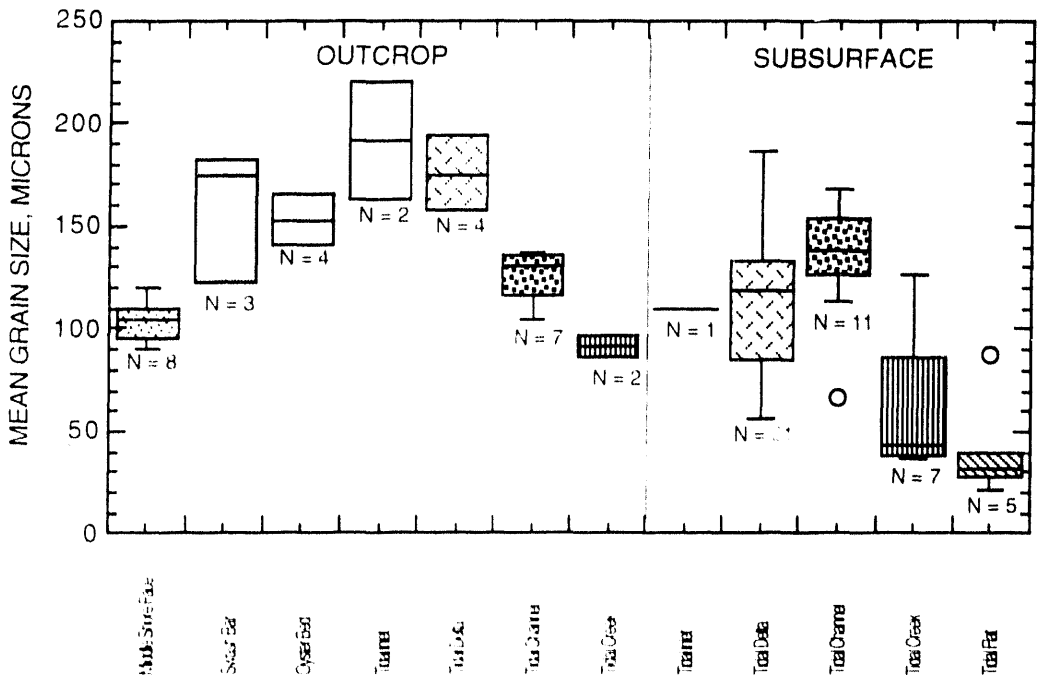

FIGURE 18 Comparison of outcrop and subsurface grain size distribution for various facies in the Almond Formation. For explanation of symbols see Figure 17. (After Schatzinger et al., 1992)

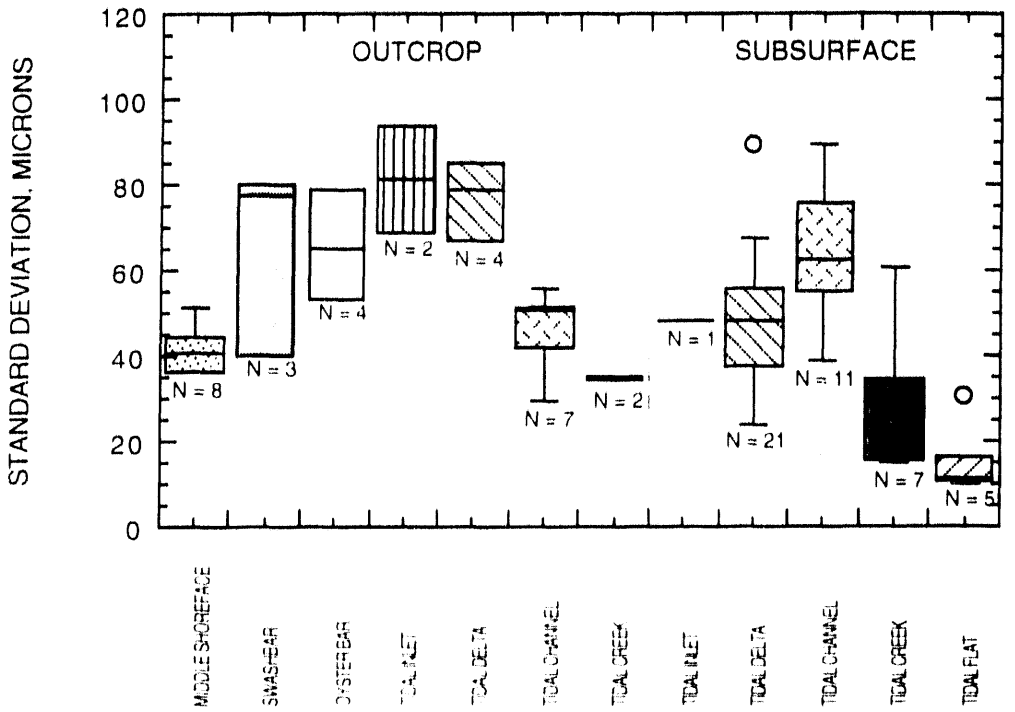

FIGURE 19 Standard deviation (sorting) for various outcrop and subsurface facies in the Almond Formation. For explanation of symbols see Figure 17. (After Schatzinger et al., 1992)

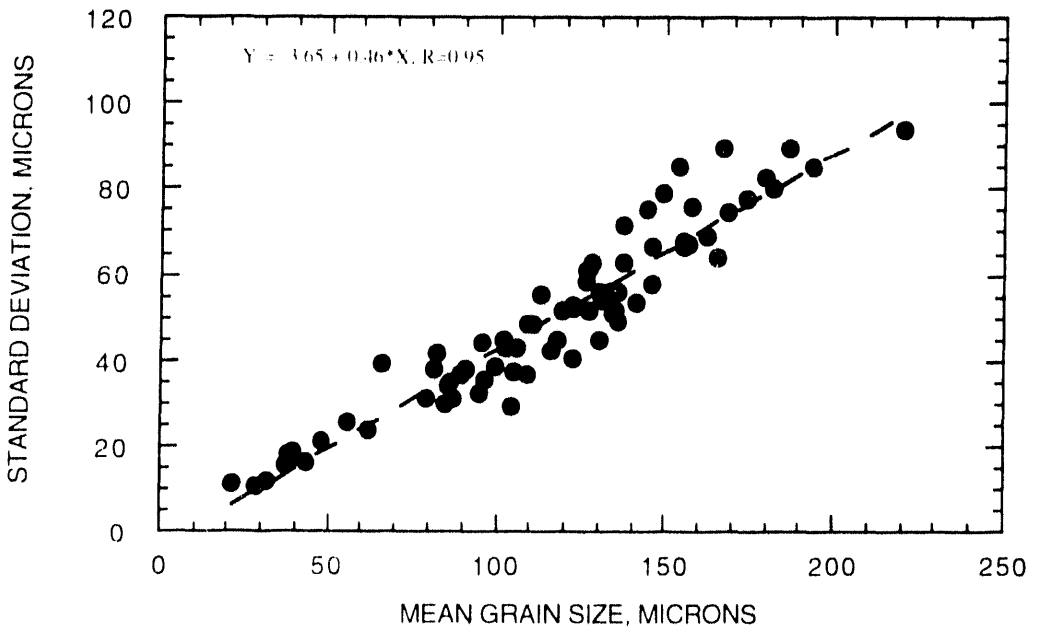

FIGURE 20 Standard deviation (sorting) versus mean grain size for outcrop and subsurface Almond Formation. Based on image analysis of 300 points for each thin section. (After Schatzinger et al., 1992)

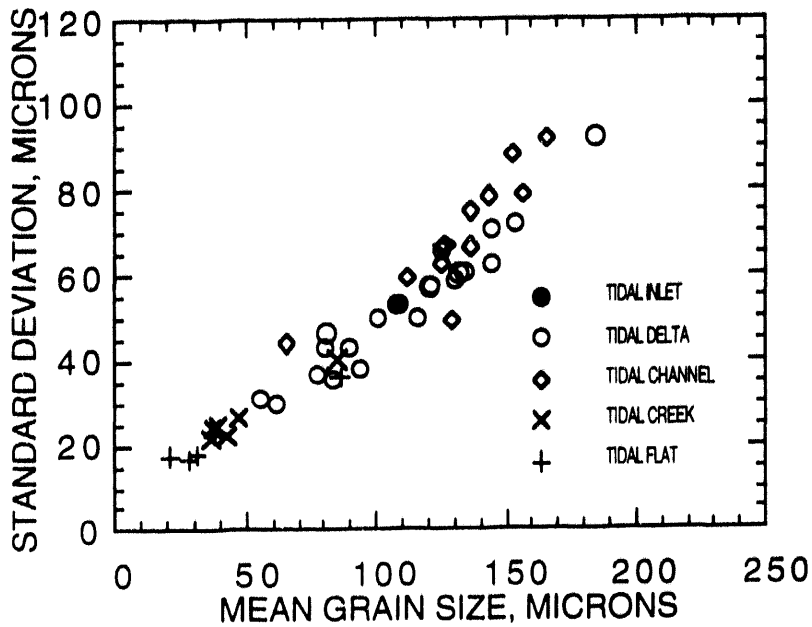

FIGURE 21 Standard deviation (sorting) versus mean grain size for subsurface Almond Formation facies. Based on image analysis of 300 points for each thin section. (After Schatzinger et al., 1992)

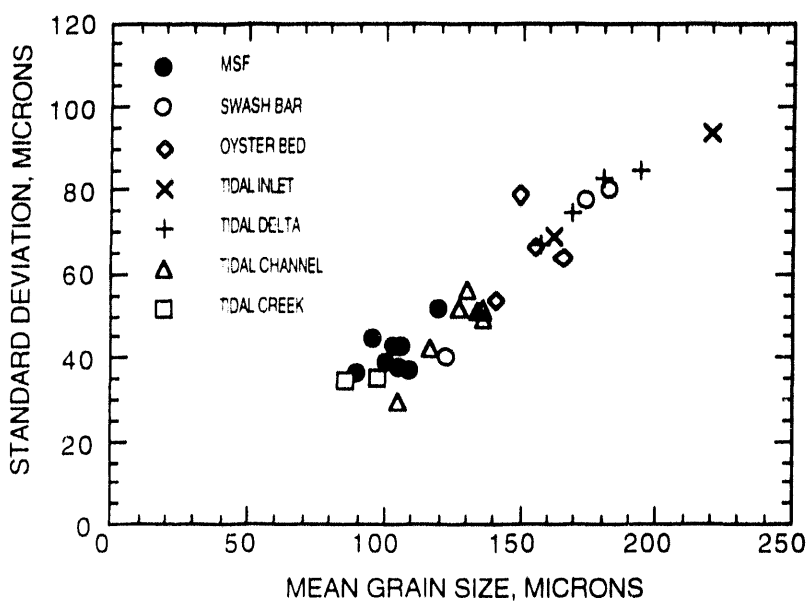

FIGURE 22 Standard deviation (sorting) versus mean grain size for outcrop Almond Formation facies. Based on image analysis of 300 points for each thin section. (After Schatzinger et al., 1992)

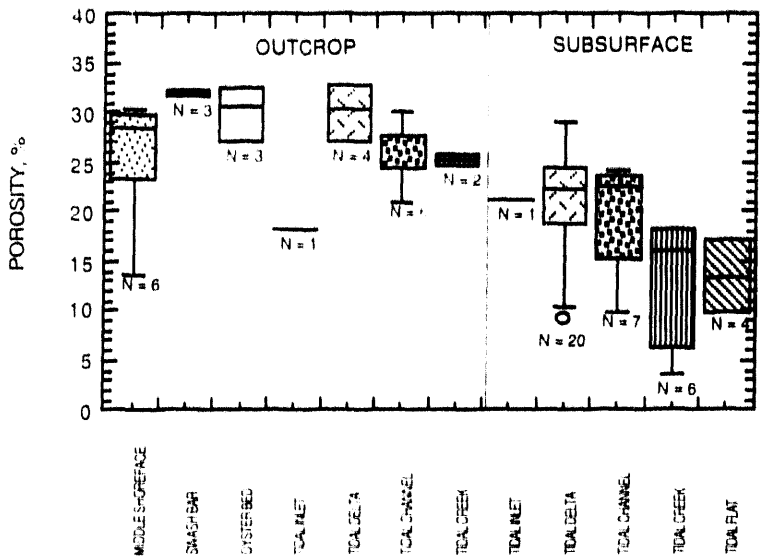

FIGURE 23 Comparison of subsurface and outcrop facies porosity, Almond Formation. For explanation of symbols see Figure 17. (After Schatzinger et al., 1992)

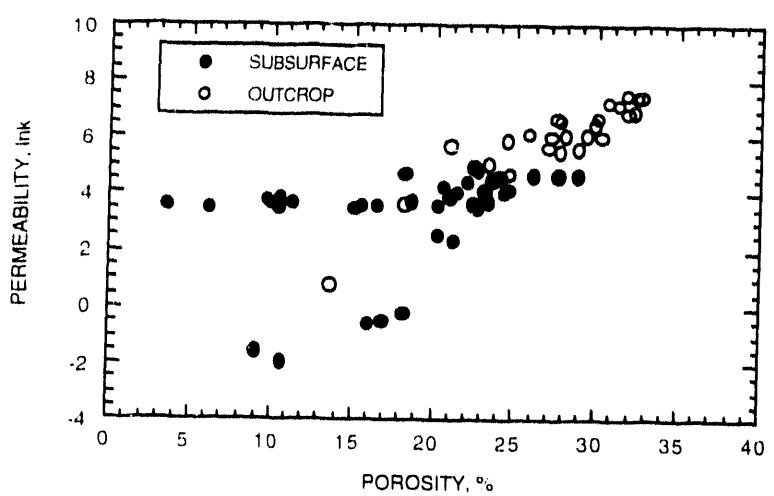

FIGURE 24 Natural log of permeability versus porosity for outcrop and subsurface Almond Formation. (After Schatzinger et al., 1992)

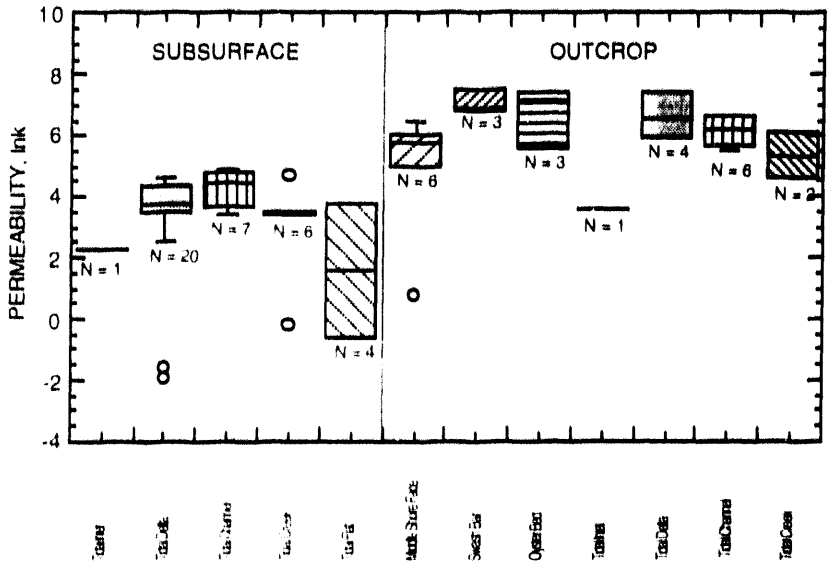

FIGURE 25 Comparison of subsurface and outcrop permeability distribution for Almond facies. For explanation of symbols see Figure 17. (After Schatzinger et al., 1992)

IV Fracture Azimuth Measurements

The lack of information on fracture characteristics in Patrick Draw field and the role of natural fractures in hydrocarbon production prompted the study of fracture distribution (orientation, continuity, and spacing) in the outcrops of the Upper Almond Formation on the east flank of the Rock Springs Uplift. Measurements of 918 fracture azimuths from outcrops RG and RH were taken (fig. 26). Fracture azimuths were measured at three major sandstone horizons along lateral distances of 800 to 1,500 ft. The approximate vertical continuity and lateral spacing were also recorded. Obvious weathering or gravitational fractures were eliminated from the record. Indications of minor faults were observed in a few cases. Fracture azimuth distribution according to facies is presented in figures 27-30.

The predominant major fractures in studied outcrops are usually vertical or near vertical and tend to cut the entire sandstone sequence formed by the same sedimentary process (facies) or several facies, at vertical distances of several feet to tens of feet. The fractures tend to die out in siltstone and shales such as lagoonal or bay facies but may re-appear in the under- or overlying sandstone sequences. Minor sets of fractures usually cut an individual sandstone layer at a vertical distance of several inches or a few feet. The spacing of major fractures vary greatly from a couple of feet to tens of feet, while minor fracture spacing usually varies from inches to a few feet.

Outcrop fractures are exposed to atmospheric conditions and are predominantly open, although calcite or gypsum fillings also were occasionally observed. The abundance of well preserved shells in the upper Almond deposits which are commonly observed in the outcrops, the two cores from holes drilled behind the outcrops, and the cores from Patrick Draw field, provide evidence that at the time of deposition and during post-depositional history the sediments were exposed to formation fluids in thermodynamic equilibrium or oversaturated with respect to calcite and possibly dolomite. This leads to the conclusion that the rock matrix, as well as fractures and faults in subsurface, might have been subjected to extensive cementation or sealing. Engineering processes, however, such as acidization of wells and flooding with water incompatible with original formation fluids could dissolve the precipitate. Planned injection of carbon dioxide to stimulate oil flow certainly would magnify the dissolution process. Also, the hydraulic fractures tend to develop along completely or partially sealed natural fractures and may re-open the original channels to flow. The geochemical and engineering aspects of the Almond Formation reservoir strengthen the importance of studying natural fractures in the system to predict the fluid flow pattern in Patrick Draw field.

There are two major sets of fractures characteristic for all outcrops in the studied area; 20° to 80° and 110° to 160°. Computed mean orientation of the prevailing set is near 130°, while the 95% confidence interval is about 23°(fig. 26). The differentiation between the systematic and nonsystematic joints has not been attempted at this stage of the fracture study in the Almond outcrops. Typically, the greatest local or regional permeability would be along the systematic joints (Kurlander et al., 1991). Therefore, the rose diagrams of cumulative fracture frequency may not adequately reflect the preferential directions of fluid flow suggested by orientation of the longer rose petals.

The orientation of measured fracture sets in outcrops and the calculated means vary somewhat among sandstone horizons and among individual outcrops located one to three miles apart (fig. 27). In most cases, however, the two nearly perpendicular directions of fractures, i.e., 30° to 40° and 130° to 140° definitely prevail in most of the outcrops studied and in the individual sandstone horizons (figs. 26, 27 and 28).

Orientation of dominant fractures in most of the studied outcrops and sandstone horizons does not correspond well with dominant fault directions and orientations of some photolinear features (70° to 80°) mapped in Patrick Draw field area (Greer et al., 1987; Richers et al., 1982) and in the Almond outcrops located north of the ones studied. It does correspond, however, with dominant fault directions (30° to 40°) on the crest of the Rock Springs Uplift, west and northwest of measured outcrops as shown on the Greer et al., (1987) map.

Few fracture measurements from outcrops located north along the Rock Springs Uplift indicate a prevailing orientation of 60° to 70° which is fairly close to the dominant fault direction in the study area (70° to 80°) (fig. 29a). Surprisingly, fracture sets measured in sandstone bodies overlying bar G in outcrop RG (e. g. "White Sands" fig. 29b), as well as the "White Sands 2" and "Major White Sands" (fig. 30a) exposed north and northeast of outcrop RG, reveal two predominant fracture orientations of 130° to 160° and near perpendicular orientation of 70° to 80°. The latter coincides with dominant fault directions in Patrick Draw field and in adjacent outcrop area north of the study area studied by Van Horn (1979). Similar fracture orientations were revealed in sandstones underlying the marine sequence of the bar G in outcrop RH (fig. 30b) which may belong to the Lower Almond (continental) sedimentary sequence. This indicates a possibility that the predominantly marine sediments forming bar G might have been subjected to a different fracturing episode of the Laramide orogenesis than the older and the younger sediments.

Fracture characteristics from outcrop RG may not be a good analog for fracture characteristics in Patrick Draw reservoir horizons. They may apply even less to the Arch Unit in the northern part of the field. The reason is that the outcrop area studied and Patrick Draw field belong to different tectonic blocks outlined by domain

boundaries of the predominant orientation of systematic fractures. There also is a possibility that the two areas were subjected to different fracturing episodes resulting in generation of differentiated patterns of the superimposed fracture sets.

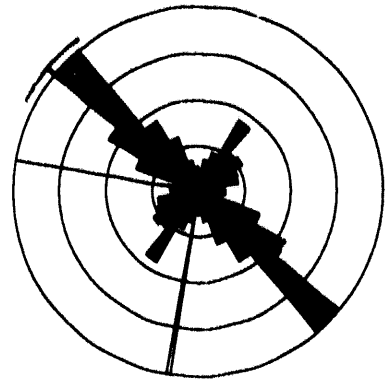

a.

Outcrops RG, RH and VH8-all data
N = 923 Cumulative Length = 0.0
Class Interval = 10 degrees
Maximum Percentage = 19.1
Mean Percentage = 5.56
Standard Deviation = 4.07
Vector Means = 309.5
Conf. Angle = 11.74

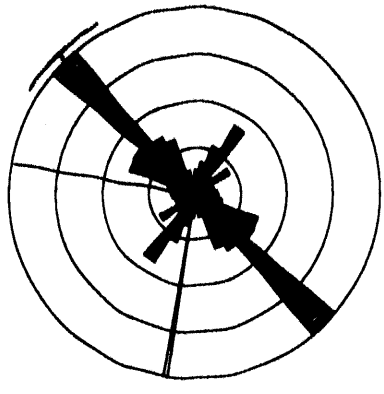

b.

Outcrop RG-all data
N = 434 Cumulative Length = 0.0
Class Interval = 10 degrees
Maximum Percentage = 22.1
Mean Percentage = 5.56
Standard Deviation = 4.75
Vector Mean = 315.9
Conf. Angle = 13.91

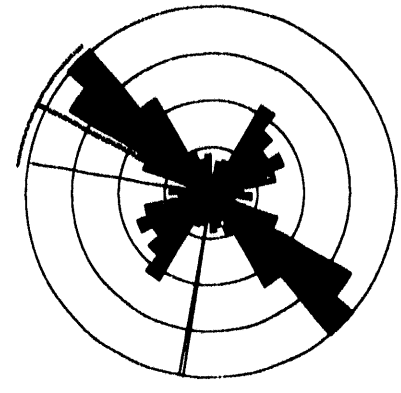

c.

Outcrop RH-all data
N = 422 Cumulative Length = 0.0
Class Interval = 10 degrees
Maximum Percentage = 15.4
Mean Peracentage = 5.56
Standard Deviation = 3.86
Vector Mean = 297.7
Conf. Angle = 20.22

FIGURE 26 Rose diagrams of fracture orientations and related statistics for: a) all outcrops measured in this study; b) all sandstone intervals in outcrop RG; and c) all sandstone intervals in outcrop RH. (After Schatzinger, et al., 1992)

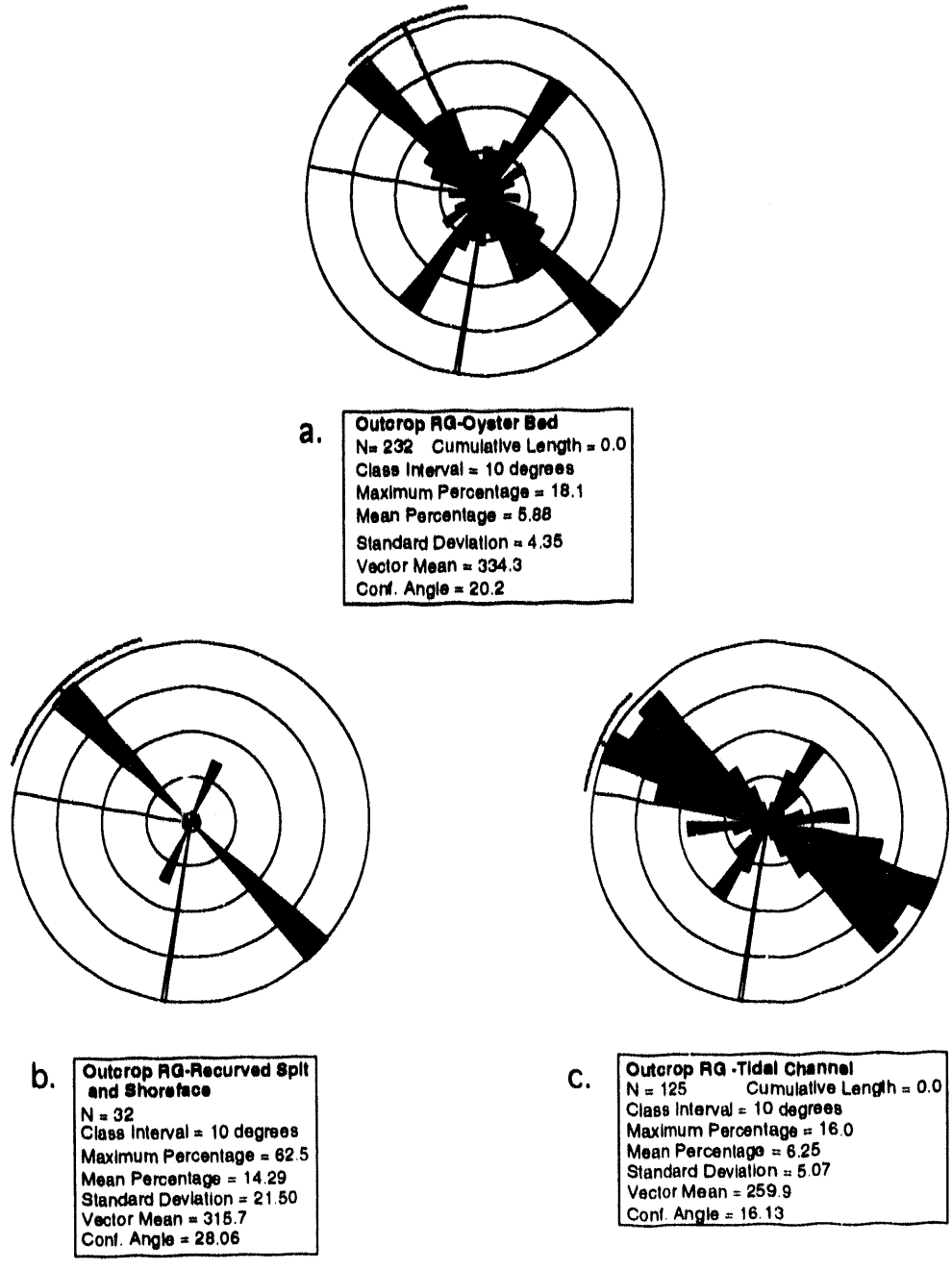

FIGURE 27 Rose diagrams of fracture orientations and related statistics for various facies in outcrop RG: a) Oyster Bed; b) Recurved Spit and Shoreface; and c) Tidal Channel facies. (After Schatzinger et al., 1992)

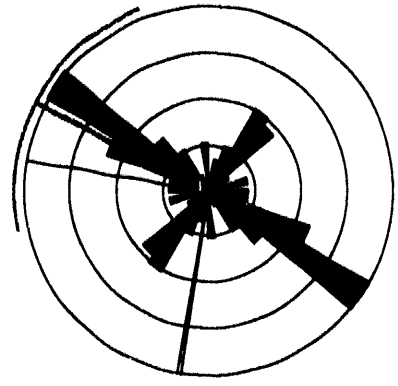

a. **Outcrop RH3-Flood Tidal Delta, Tidal Inlet, and Tidal Channel**
N = 116 Cumulative Length = 0 0
Class Interval = 10 degrees
Maximum Percentage = 20.7
Mean Percentage = 6.25
Standard Deviation = 4.88
Vector Mean = 297.7
Conf. Angle = 40.32

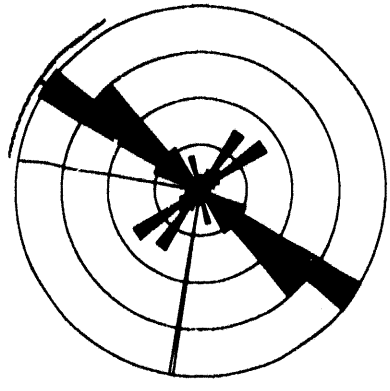

b. **Outcrop RH-Tidal Channel Tidal Delta**
N = 105 Cumulative Length = 0.0
Class Interval = 10 degrees
Maximum Percentage = 25 7
Mean Percentage = 6.67
Standard Deviation = 7 01
Vector Mean = 304.3
Conf. Angle = 25 19

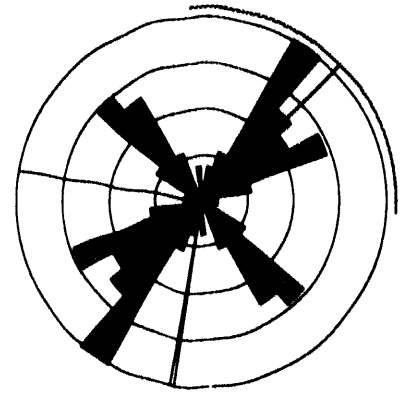

c. **Outcrop RH-Tidal Flat and Tidal Channel**
N = 66 Cumulative Length = 0 0
Class Interval = 10 degrees
Maximum Percentage = 16.7
Mean Percentage = 6 67
Standard Deviation = 4 70
Vector Mean = 44 8
Conf. Angle = 48 59

FIGURE 28 Rose diagrams of fracture orientations and related statistics for three major sandstone facies in outcrop RH: a) Flood Tidal Delta, Tidal Inlet and Tidal Channel; b) Tidal Channel and Tidal Delta; and c) tidal Flat and Tidal Delta. (After Schatzinger et al., 1992)

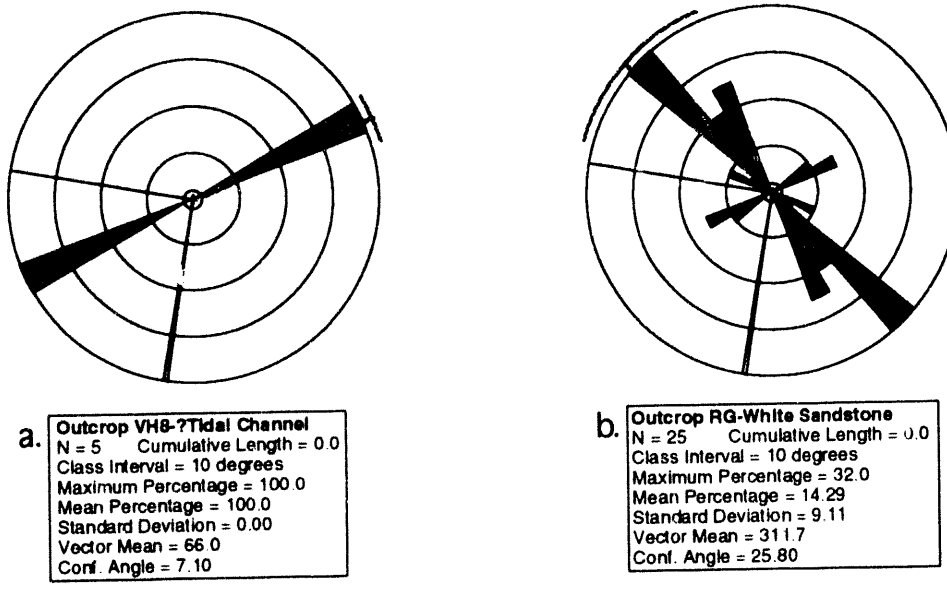

FIGURE 29 Rose diagrams of fracture orientations and related statistics in: a) outcrop VH8; and b) "white sands" overlying bar G in outcrop RG. (After Schatzinger et al., 1992)

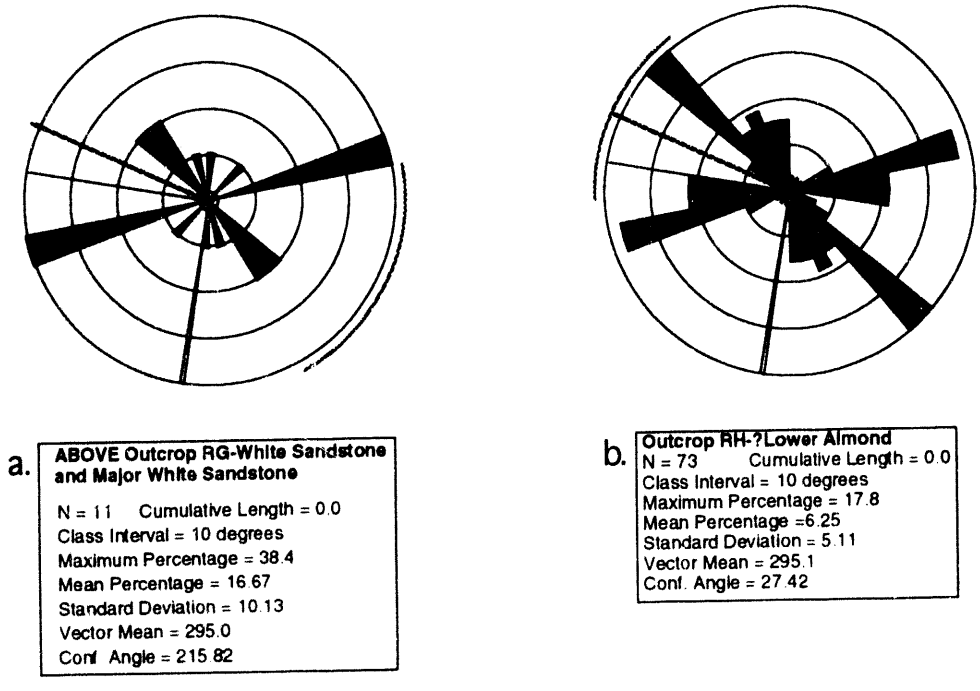

FIGURE 30 (a) Rose diagram of fracture orientations and related statistics in: a) White Sandstone and Major White Sandstone northeast and north of outcrop RG; and b) sandstone (?Lower Almond) underlying the marine sequence of the Upper Almond in outcrop RH. (After Schatzinger et al., 1992)

REFERENCES

Asquith, D. O., 1975. Petroleum Potential of Deeper Lewis and Mesaverde Sandstones in the Red Desert, Washakie and Sand Wash Basins, Wyoming and Colorado. Rocky Mountain Association of Geologists Symposium, p.159-162.

Bernard, H. A., C. F. Major, Jr., and B. C. Parrott, 1959, The Galveston Barrier Island and Environs: A Model for Predicting Reservoir Occurrence and Trend. Transactions of the Gulf Coast Association of Geological Societies, v. IX, p. 221-224.

Cuevas, M. M., E. Donselaar, and S. D. Nio, 1985, Eocene Clastic Tidal Deposits in the Tremp-Graus Basin (Provs. of Lerida and Huesce), in Mila, M. D., and J. Rosel, eds., 6th I.A.S. European Regional Meeting. Excursion Guidebook. Institut D'Estudis Illerdens (Lleida), p. 215-266.

DaBoll, J. M. 1969, Holocene Sediments of the Parker River Estuary, Massachusetts. Contrib. No. 3-CRG, Dept. of Geology, Univ. of Massachusetts, 138 p.

Davies, J. L., 1964, A Morphogenetic Approach to World Shorelines: Zeits. fur Geomorph. v. 8, p. 127-142.

Donselaar, M. E., 1984, Flood Tidal Delta Sedimentation in the Late Cretaceous Menefee Formation (Mesaverde Group), San Juan Basin, Northwest New Mexico. Geologie en Mijnbouw, v. 63, p. 323-331.

Donselaar, M. E., 1990, Facies and Geometry of Fossil Flood-Tidal Deltas (Abs.), *in*, Davis, R. A. Jr., D. Nummedal, and R. W. Tillman, conveners, Tidal inlet and Related Sand Bodies: Modern and Ancient-Abstracts of Technical Program. SEPM Research Conference, San Juan Basin, New Mexico.

Fitzgerald, D. M., S. Penland, and D. Nummedal, 1984, Control of Barrier Island Shape by Inlet Sediment Bypassing: East Frisian Islands, West Germany. Marine Geology, v. 60. Elsevier Science Publishers B. V., Amsterdam-Printed in The Netherlands, p. 355-376.

Flores, R. M., 1978, Barrier and Back-Barrier Environments of Deposition of the Upper Cretaceous Almond Formation, Rock Springs Uplift, Wyoming. The Mountain Geologist, v. 15, no. 2, p. 57-65.

Greer, P. L., J. K. King, and A. J. Ver Ploeg, 1987, Prelilminary Map of Known Surficial Structural features for the Rock Springs 1° x 2° Quadrangle. USGS Open File Report 87-1N.

Hale, L. A., 1950, Stratigraphy of the Upper Cretaceous Montana Group in the Rock Springs Uplift, Sweetwater County, Wyoming. Wyo. Geol. Assoc. Guidebook, 5th Ann. Field Conf., p. 49-58.

Hayes, M. O., and W. J. Sexton, 1989, Modern Clastic Depositional Environments, South Carolina. Field Trip Guidebook T-371, 28th International Geological Congress, American Geophysical Union, p. 1-85.

Hoyt, J. H., and V. J. Jenry, Jr., 1965, Significant of Inlet Sedimentation in the Recognition of Ancient Barrier Islands. *in* R. H. DeVoto and R. K. Bitter (Eds.) Sedimentation of Late Cretaceous and Tertiary Outcrops, Rock Springs Uplift, Nineteenth Field Conference., Wyoming Geological Association, p. 190-194.

Jacka, A. D., 1970, Sediment Economics of Upper Cretaceous Sandstones Rocky Mountain Region. Wyo. Geol. Assoc., 22nd Ann. Field Conf. Guidebook, p. 187-219.

Jackson, S. R., et al., 1993, Integration of the Geological/Engineering Model with Production Performance for Patrick Draw Field, Wyoming. DOE Report, NIPER-634, 122 p.

Jackson, S. R.,1992, Summary of Reservoir Characteristics of Shoreline Barrier Reservoirs. DOE Report, NIPER-651, 24 p.

Keighin, C. W., B.E. Law, and R. M. Pollastro, 1989, Petrology and Reservoir Characteristics of the Almond Formation, Greater Green River Basin, Wyoming. *in* Coalson, E. B., ed., Petrogenesis and Petrophysics of Selected

Sandstone Reservoirs of the Rocky Mountain Region, The Rocky Mountain Association of Geologists, Denver, Colorado, p. 281-298.

Kurlander, B. R., S. Dean and B. Ward, 1991, AAPG Applied Fracture Analysis Workshop. Sept 9-13, 1991, Hagerstown, MD, Course Manual, 458 p.

Lang, H. R., W. H. Alderman, and F. F. Sabins, Jr., 1984, Section 11-Patrick Draw, Wyoming, petroleum test case report. *in* Abrams, M. J., J. E. Conel, and H. R. Lang, eds., The Joint NASA/Geostat Test Case Project, Final Report, AAPG, Tulsa, OK, p. 11-1 -11-112.

Law, B. E., 1984, Relatiohships of source-rock rock, thermal maturity, and overpressuring to gas generation and occurrence in low-permeability Upper Cretaceous rocks, Greater Green River Basin, Wyoming, Colorado and Utah. *in* J. Woodward, F. Meissner, and J. Clayton, eds., Rocky Mountain Assoc. Guidebook, Hydrocarbon Source Rocks of the Greater Rocky Mountain Region, p. 469-476.

Martinsen, R.S., and G. Christiansen, 1992, A stratigraphic and Environmental Study of the Almond formation, Mesverde Group, Greater Green River Basin, Wyoming, *in* Mullen, C.E. ed., Wyoming Geological Association Guidebook, Rediscover the Rockies, p.171-190.

McCubbin, D. G. and M. J. Brady, 1969, Depositional environments of the Almond reservoirs, Patrick Draw Field, Wyoming. The Mountain Geologist, v. 6, p. 3-26.

Meyers, W. C., 1977, Environmental analysis of Almond Formation (Upper Cretaceous) from the Rock Springs Uplift, Wyoming. Ph.D. Dissertation, University of Tulsa.

Moslow, T. F. 1980, Stratigraphy of Mesotidal Barrier Islands. Ph.D Dissertation, Dept. of Geology, University of South Carolina, 187 p.

Nichols, M. M., and R. B. Biggs. 1985, Estuaries. *in* Davis, R. A. Jr., ed., Coastal Sedimentary Environments, Springer-Verlag, NY, p. 77-186.

Pittman, E. D., and R. E. Larese. 1991, Compaction of Lithic Sands: Experimental Results and Applications. AAPG Bull., v. 75, p. 1279-1299.

Rawn-Schatzinger, V., 1993. Field Guide to Muddy Formation Outcrops, Crook County, Wyoming. DOE Report NIPER-713, 109 p.

Rawn-Schatzinger, V. and R. A. Schatzinger, 1993, Annotated Bibliography of Selected References on Shoreline Barrier Island Deposits with Emphasis on Patrick Draw Field, Sweetwater County, Wyoming. DOE Report, NIPER 622, 67 p.

Reinson, G. E., 1984, Barrier Island and Associated Strand Plain System. *in* R. G. Walker, ed., Facies Models, Geoscience Canada, Reprint Series, No. 1, p. 119-140.

Richers, D. M., J. R. Reed, K. C. Horstman, G. D. Michels, R. N. Baker, L. Lundell, and W. Marrs, 1982, Landsat and Geochemical Study of Patrick draw Oil Field, Sweetwater County, Wyoming. AAPG Bull., v. 66, p. 903-922.

Roehler H. W., 1988, The Pintail Coal Bed and Barrier Bar G - A Model for Coal of Barrier Bar - Lagoon Origin, Upper Cretaceous Almond Formation, Rock Springs Coal Field, Wyoming. U.S. Geological Survey Professional Paper 1398, p.1-60.

Roehler, H. W. 1979, Paleogeography and Lithofacies of Barrier Bar G and Associated Rocks, Almond Formation, Southeast Rock Springs Uplift, Wyoming. Rocky Mountain Section SEPM Field Trip - Cretaceous of the Rock Springs Uplift, Wyoming, p. 2-21.

Schatzinger, R. A., M. J. Szpakiewicz, S. R. Jackson, M. M. Chang, B. Sharma and M. K. Tham, 1992, Integrated Geological-engineering Model of Patrick Draw Field and Examples of Similarities and Differences among various Shoreline Barrier Systems:. DOE Report, NIPER-575, 146 p.

Sha Li Ping, 1990, Sedimentological Studies of the Ebb-Tidal Deltas Along the West Frisian Islands, The Netherlands. Geologica Ultraiectina, no. 64, p 160.

Sneider, R. M., C. N. Tinker, and N. D. Sullivan, 1984, Sandstone Reservoir Models from Recent Deposits, Texas Gulf Coast. Geology and Geological Engineering Field Trip Guide, SPE-AIME 59th Annual Technical Conference, Houston, TX. R. M. Sneider Exploration, Inc.

Szpakiewicz, M. and A. G. Collins, 1985, Hydrochemical Study of the Upper Cretaceous and Lower Tertiary Formations in the Uinta, Piceance and Green River basins: Implications for Oil- and Gas-Related Problems. DOE Report, NIPER 95.

Szpakiewicz, M., R. Schatzinger, S. Jackson, B. Sharma, A. Cheng, and M. Honarpour, 1991, Selection and initial characterization of a second barrier island reservoir system and refining of methodology for characterization of shoreline barrier reservoirs. DOE Report NIPER-484, 170 p.

Szpakiewicz, M., S. Jackson and R. Tillman, 1986, NIPER's Geologicla Field Observations; Mustang and Padre Islands, Texas, December Open File.

Szpakiewicz, M., S. Jackson, R. Schatzinger and R. Tillman, 1990 and 1991, NIPER's Geological Field Observations; Almond Formation Outcrops, East Flank of the Rock Springs Uplift, Wyoming, Open File.

UPRC, 1965, Isobaric map of Patrick Draw Field, sweetwater County, Wyoming.

Van Horn, M.D., 1979, Stratigraphy of the Almond Formation, East-Central Flank of the Rock Springs Uplift, Sweetwater County, Wyoming: A Mesotidal Shoreline Model for the Late Cretaceous. M.S. Thesis, Colorado School of Mines, 150 p.

Weimer, R. J., 1961, Uppermost Cretaceous rocks in central and southern Wyoming and Northwest Colorado. Wyoming Geological Assoc., 16th Ann. Field Conf., Symposium of Late Cretaceous Rocks, Green River, Washakie, Wind River and Powder River Basins, p. 17-28.

Weimer, R. J., 1966, Time-stratigraphic analysis and petroleum accumulations, Patrick Draw Field, Sweetwater County, Wyoming. AAPG Bulletin, v. 50, p. 2150-2175.

Weimer, R. J., K. W. Porter, and C. B. Land, 1985, Depostional modeling ot detrital rocks with emphasis on cored sequences of petroleum reservoirs. SEPM Core Workshop No. 8, Golden CO, 252 p.

Weimer, R.J., 1960, Upper Cretaceous stratigraphy, Rocky Mountain area: AAAPG Bulletin, v.44, p 1-20.

Weimer, R. J., 1970, Rates of Deltaic Sedimentation and Intrabasin Deformation, Upper Cretaceous of Rocky Mountain Region. *in* Morgan, J. P., ed., Deltaic Sedimentation Modern and Ancient, SEPM, Spec. Pub. 15, p. 270-292.

White, E. J. O. C. Baptist, and C. S. Land, 1963, Physical properties of the Almond sands in the Patrick Draw area, Wyoming. U. S. Dept of the Interior, Bureau of Mines, Report of Investigations, p. 1-19.

APPENDIX A

GREATER GREEN RIVER BASIN INCLUDING PATRICK DRAW FIELD

This annotated bibliography on shoreline barrier deposits within the Greater Green River Basin is extracted from a larger bibliography on shoreline barrier deposits (Rawn-Schatzinger and Schatzinger, 1993). The emphasis is on the geology, dynamic processes and hydrocarbon recovery of barrier island reservoirs.

The Greater Green River Basin is a large area in southern Wyoming, northwestern Colorado and northeast Utah. The basin is bounded on the west by the Wyoming Thrust Belt and on the north by the Wind River Thrust Belt. The eastern boundary is formed by the Sierra Madre and Park Range uplifts. The southern boundary is the Axial Basin Uplift and the Uinta Mountain Thrust Fault. Five smaller subbasins within the Greater Green River Basin include; Hoback, Green River, Great Divide, Washakie and Sand Wash. Structural features within the Greater Green River Basin that separate the individual basins are the Rock Springs Uplift, Moxa Arch, LaBarge Platform, Pinedale Anticline, Wamsutter Arch and Cherokee Ridge. The area covers more than 51,000 km^2 (Law, 1984).

Rocks in these areas encompass Cambrian through Tertiary sedimentary deposits. Characteristic fill includes Permian age Phosphoria Formation, Triassic-Jurassic Nuggett Formation, Upper Cretaceous Mesaverde Group and equivalent age rocks topped in some areas by the Paleocene Fort Union Formation and Eocene deposits.

Annon., 1973, Oil Characteristics in the Greater Green River Basin: Wyoming Geol. Assoc. Guidebook, 25th Field Conf., p. 12-18.

Tables give field name, location (township and range), county, formation, depth, number of wells, color of sediments, API oil gravity, viscosity, and percentages of sulfur, carbonate, and nitrogen, cumulative oil, and cumulative gas production.

Arp, G. K., 1992, An integrated interpretation for the origin of the Patrick Draw oil field sage anomaly: AAPG Bull. 76, no. 3, p. 301-306.

Remote sensing methods have been used at Patrick Draw Field, Wyoming for nearly 10 years. Patrick Draw is a stratigraphic trap. The surface is covered with sage brush. Remote sensing has detected an anomaly in the growth of the sage over Patrick Draw. The controversy is whether this anomaly, first observed in 1978, is related to the underlying oil field. Sage die-out results from the upward migration of injected gases and water. The soil becomes high pH, high in salinity, and toxic to the sage.

Asquith, D. O., 1966, Geology of Late Cretaceous Mesaverde and Paleocene Fort Union oil production, Birch Creek, Sublette County, Wyoming: AAPG Bull., v. 50, p. 2176-2184.

South Birch Creek is located on the La Barge Arch in western Green River Basin, northwest of the Rock Springs Uplift. It is part of the Big Piney-La Barge producing complex. The close association of oil and most of the gas production from the Paleocene Fort Union shales suggests that this shale is the source of hydrocarbons for the associated reservoirs. Close association of production in Mesaverde reservoirs with an unconformity above it at the overlying shale, absence of distinct chemical differences in oils between Cretaceous and Paleocene reservoirs, and lack of significant production from areas lacking or with poorly developed Paleocene shale suggests that the source of hydrocarbons produced from Mesaverde reservoirs may be the Paleocene lacustrine shales rather than the underlying Cretaceous marine shale and siltstone.

Asquith, D. O., 1968, Origin of large kaolinite crystals in the lower Almond Formation in southwest Wyoming: Jour. Sed. Petrol., v. 38, p. 948-949.

Large kaolinite books, up to 3-mm in diameter from near Rock Springs (WY) are present as a 1-3 in. underclay in the lower nonmarine portion of the Almond. Grain size, crystallinity, and lack of abrasion of books indicate diagenetic rather than detrital origin.

Asquith, D. O., 1975, Petroleum potential of deeper Lewis and Mesaverde sandstones in the Red Desert, Washakie and Sand Wash Basins, Wyoming and Colorado: RMAG Symposium, p. 159-162.

Almond (Upper Mesaverde) was deposited during a local regression in the overall transgression of the marine Lewis Shale over the Mesaverde. Production trend includes Patrick Draw, Table Rock, and Desert Springs fields on the western flank of the Washakie Basin and Red Desert Basin.

Baptist, O. C., E. J. White, and C. S. Land, 1964, Laboratory predictions of water sensitivity compared with field observations of well damage - Patrick Draw, Wyoming: SPE Paper 839 (preprint), 6 p.

Actual formation damage due to invasion of fresh water is estimated from interpretation of DST's and rates of injection into two pilot waterflood wells where fresh water was injected into 1 well and brine into the other.

The results are indecisive. Damage ratios from DST are high for gas sands, but damage is rapidly removed by production. Damage ratios are less in oil sands than in gas and are even less in water sands. Injection rates for fresh water were about the same as for brine. Rates of brine injection are close to those calculated from laboratory relative-permeability curves.

Barlow, J. A., Jr., 1961, Almond Formation and Lower Lewis Shale, east flank of Rock Springs Uplift, Sweetwater County, Wyoming: *in* Wyoming Geologic Association Symposium of Late Cretaceous Rocks, 16th Ann. Field Conf. Green River, Washakie, Wind River and Power River Basins, p. 113-115.

The Almond Formation is the uppermost formation of the Mesaverde Group. The relationship of the Almond to the overlying Lewis Shale and other associated strata is analyzed with stratigraphic correlations, cross sections and maps.

Brock, W. G. and J. Nicolaysen, 1975, Geology of the Brady Unit, Sweetwater County, Wyoming: Rocky Mountain Assoc. Geol. Symposium, *in* Deep Drilling Frontiers of the Central Rocky Mountains: eds. D. W. Bolyard, p. 225-237.

Initial drilling into a deep seismic structure west of the Washakie Basin has produced hydrocarbons from multiple pay zones. Production has been from the Upper Cretaceous Dakota Formation, the Jurassic Entrada and Nugget formations, the Permian Phosphoria Formation and the Pennsylvanian Weber Formation.

The Dakota sandstones are fluvial and distributary channel deposits. The Entrada and Nugget sandstones are the most porous and continuous reservoirs at Brady Unit. Thin carbonate facies in the Phosphoria limits production. The porosity and permeability of the Weber and Phosphoria formations are discontinuous and cause problems in production.

The structural feature at the Brady Unit reflects Precambrian faulting in the basement rocks. A thick sedimentary layer is draped over the fault, dying out in the higher stratigraphic layers.

Bryant, W. A., 1984, Paleoenvironmental interpretation based on foraminifera of coal-bearing Almond Formation, Little Snake River Coalfield, Wyoming (abst.): AAPG, Bull., v. 68, p. 933.

The Almond is about 450 ft thick and divided into two informal members, both of which contain coal. Coals in the upper 100 ft of the upper member are thin; however, coals in the lower member include several thick beds. Coal-bearing portions of both members are characterized by repetitive coarsening-upward bay-fill deposits of mudstone and sandstone, commonly overlain by coal. A major coarsening-upward sequence in the lower part of the upper member is capped by sandstone interpreted as marine shoreface.

Fine grained rocks in both members contain forams. The three foram assemblages are: (1) low diversity agglutinated benthic assemblage interpreted as a hyposaline saltmarsh fauna from fine grained rocks of the lower member, (2) a high diversity mixed agglutinated and calcareous benthic assemblage interpreted as a hyposaline bay to lagoonal fauna in shales in the lower part of the upper member, (3) a moderate-diversity agglutinated benthic assemblage in fine-grained rocks in the upper part of the upper member interpreted as a hyposaline salt marsh to interdistributary bay fauna.

Burton, G, 1961, Patrick Draw area, Sweetwater County, Wyoming: Wyoming Geol. Assoc., 16th Ann. Field Conf., p. 276-279.

An early field analysis of Patrick Draw Field and nearby Table Rock Field. Patrick Draw oil field is approximately 8 miles long and 3 miles wide. Oil is coming from stratigraphic traps in the Almond Formation. Seismic data collected thus far revealed no structural configuation conducive to hydrocarbon accumulation.

Cox, J. E., 1962, Patrick Draw area, Sweetwater County, Wyoming: Billings Geol. Soc., Paper no. 1, p 1-17.

A detailed field study of Patrick Draw Field. The geology is based on core data, and expressed in maps and cross sections.

Davis, J. R., 1966, Stratigraphy and depositional history of upper "Mesaverde" Formation of Southeastern Wyoming: Ph.D. thesis, The University of Wyoming, 124 p.

The Mesaverde Formation outcrops in the Laramie, Carbon, Hanna, and Kindt basins of Wyoming. The sequence in these basins includes the Steele Shale, Pine Ridge Sandstone, and the Almond. The Mesaverde is overlain by the Lewis Shale. Descriptions of the depositional environments include details on the marine fossils, sedimentary structures, grain size analyses, and facies. The Almond Member was deposited as a barrier bar during a early transgressive phase of the Lewis Sea. The Almond becomes progressively thicker (600 ft) in the western

portions of the basins. Several transgressive-regressive cycles are represented by the Almond, and a long period of stable strandlines allowed for diverse transitional environments.

Dickinson, R. G., 1992, Table Rock Field-Frontier Formation, an overpressured reservoir: Wyoming Geol. Assoc. 43rd Field Conf. Guidebook, p. 139-144.

Data from a test well in the Table Rock unit of the Frontier Formation drilled in 1991 is presented and analyzed. Initial gas production was 4,300 MCFD from highly overpressured layers. The bottom hole pressure at 14,400 ft is 11,100 psi. The sandstones of the Nugget, Weber and Madison units have greater porosity and permeability than those drilled into the Frontier. Formation The effective permeability and the hydrostatic pressure are major factors in continuing gas production from the Frontier Formation in the Table Rock Field.

Douglas, W. B., Jr., and T. R. Blazzard, 1961, Facies relationships of the Blair, Rock Springs, and Ericson formations of the Rock Springs Uplift and Washakie Basin: Wyoming Geol. Assoc., 16th Annual Field Conf. Guidebook, p. 81-86.

This paper suggests revisions for nomenclature in the Rock Springs Uplift: rocks formerly correlated with the Rock Springs Formation are shown to be laterally equivalent with the Ericson Formation. From bottom to top the formations of the Mesaverde Group are Blair, Rock Springs, Ericson and Almond.

Finley, R. J., 1983, Comparison of depositional systems and reservoir characteristics of selected blanket-geometry tight gas sandstones (abst.): AAPG Bull., v. 67, p. 460-61.

The upper Almond Formation of the eastern Greater Green River Basin may contain more shallow marine and offshore bars than barrier strand-plain facies. The upper Almond occurs at depths of 6,000-15,000 ft, with a net pay of 14-18 ft.

Flores, R. M., 1978, Barrier and back-barrier environments of deposition of the Upper Cretaceous Almond Formation, Rock Springs Uplift, Wyoming: The Mountain Geologist, v. 25, p. 57-65.

Depositional environments identified in the upper Almond of Rock Springs Uplift include shoreface, barrier island, tidal inlet, tidal delta, washover fan, tidal flat, lagoon, tidal creek, overbank, pond, and marsh. Tidal delta, tidal-inlet-channel, washover fan, and tidal-creek deposits significantly affected back-barrier accretion and lagoon filling. The complete filling of the lagoon led to coalescing of marsh on the back side of the barrier island with the marsh on the landward side of the lagoon. Thin, discontinuous coal beds that rapidly grade into carbonaceous shale formed in the marsh in close proximity to the barrier island. Thin to thick, laterally extensive coal beds that locally grade into carbonaceous shale formed in the marsh on emergent levee, overbank, and bayfill deposits at the landward side of the lagoon. Deposition of the above detrital deposits, as well as tidal-creek channel sandstones, caused splitting and merging of the coal beds.

Garcia-Gonzalez, M. and R. C. Surdam, 1992, Coal as a source rock of petroleum: a comparison between the petrology of the Mesaverde Group coals, in burial and hydrous pyrolysis: Wyoming Geol. Assoc. Guidebook, 43rd Field Conf., p. 237-244.

The composition and textural changes in coal were studied at different stages of maturation from samples taken from the Almond Formation coals in the Greater Green River Basin of Wyoming. Samples were taken from the surface to a depth of 11,000 ft. Samples of Lance Formation coal were studied at different temperatures under hydrous pyrolysis. Composition and textural changes brought about by burial show a pattern. First there is a loss of the original laminated texture, followed by formation of a porous texture which evolves to a vesicular texture. At greater burial depth and pressure quantities of exsudatinite (a precursor to petroleum) is formed. Micrinite forms from liptinite while at the same time desmocollinite becomes homogenized, and the semifusinite and fusinite content increases with temperature increase related to burial depth. Charts and tables explain and compare the coal maceration stages, and compare samples from different outcrops and core depths.

Gosar, A. J., and J. C. Hopkins, 1969, Structure and stratigraphy of the southwest portion of the Rock Springs Uplift, Sweetwater County, Wyoming: *in* Lindsay, J.B., ed., Geologic Guidebook of the Uinta Mountains, Utah's Maverick Range, 16th Ann. Field Conf., Intermountain Association of Geologists, p. 87-90.

A short summary of the stratigraphy of the area with structural interpretations is presented.

Greer, P., J. K. King, and A. J. VerPloeg, 1987, Preliminary map of known surficial structural features for the Rock Springs 1 x 2 Quadrangle: Wyoming Geol. Surv., Open File Report 87-1N.

Includes a listing of all the reference maps used to compile the Rock Springs Quadrangle map.

Hawkins, C. M., 1980, Barrier bar sands in the Second Frontier Formation, Green River Basin, Wyoming: Stratigraphy of Wyoming: 31st Ann. Wyoming Geol. Assoc. Field Conf. Guidebook, p. 155-161.

Results are based on logs and core cuttings from the gas production area on the crest and flanks of the Moxa Arch at 7,000 to 12,000 ft. Presents interpretation of a classical upward coarsening, marine, shoreface, foreshore, dune, lagoonal package. This was a subsurface study of a gas productive barrier.

Heasler, H. P. and R. C. Surdam, 1992, Pressure compartments in the Mesaverde Formation of the Green River and Washakie Basins, as determined from drill stem test data: Wyoming Geol. Assoc. 43rd Field Conf., p. 207-220.

Drill stem tests were used to study the pressure in the Mesaverde Formation of the Green River and Washakie basins. Initial and final shut in pressures were graphed to analyze the relationships and evaluate pressure zones. Anomalous pressure zones were mapped on potentiometric surface maps. These anomalous pressure zones in both the Green River and Washakie basins are on the scale of individual oil fields.

Hendricks, M. L., 1983, Stratigraphy and tectonic history of the Mesaverde Group (Upper Cretaceous), east flank of the Rock Springs Uplift, Sweetwater County, Wyoming: unpublished Ph.D. thesis, Colorado School of Mines, Golden, Colorado, 213 p.

The Mesaverde Group in southwestern Wyoming includes 4000 ft of sediments of the Blair, Rock Springs, and Ericson Formations. The Upper Blair is a prodelta sequence of shales and thin sandstones. The Rock Springs Formation is a cyclic deposit of marine and non-marine sandstones, shales and coals. The Lower Ericson is a thick unit of fluvial sandstones interbedded with thin carbonaceous shales.

The Rock Springs Formation was deposited as a wave-dominated delta. Two faults in the Rock Springs Formation indicate penecontemporaneous movement during deposition. Coal layers in the Rock Springs Formation are associated with prograding delta lobes. Illustrated with numerous photos of textural features, and maps showing structural and stratigraphic developments.

Irwin, D., 1976, Arch and Monell Units, Patrick Draw-Table Rock area, Sweetwater County, Wyoming-upper Almond Sandstone study: *in* Unpublished Union Pacific Resources Co. Data Files.

This report separates the Almond Formation at Patrick Draw in four sandstone units. They are in descending order UA-5, UA-6, UA-7, UA-8. These sandstone units are separate by marine shales. Units UA-5, UA-6, and UA-7 are subdivided into A and B, and unit UA-6 sometimes has a C. These units are recognizable on log and in core analysis. The sandstones were deposited as shallow water and barrier beach sands along the edge of the Cretaceous sea. Units UA-5 and UA-6 are less than 40 ft. thick and have been deformed somewhat.

Unit UA-5 is the primary producing zone Patrick Draw Field for both the Arch and Monell areas. UA-5B is an excellent reservoir and is 35 ft. thick in the center of Patrick Draw Field. A Y-shaped tidal channel dissects the UA-5 sandstone. The sand isolith map indicates that Table Rock was present as a paleostructure influencing patterns at the time of deposition. A coal unit underlies unit UA-5, and marine shales overlie it.

Irwin, D. C., 1986, Upper Cretaceous and Tertiary cross sections, Moffat County, Colorado: Rocky Mountain Assoc. Geol. Symposium, p. 151-155.

Three cross sections across the Sand Wash Basin in the southern part of the Greater Green River Basin are presented. The Sand Wash Basin is bounded on the south by the Uinta Mountains, in the north by the Cherokee Arch (along the Colorado-Wyoming state border), on the east by the Park Range and on the west by the Hiwatha Sugar Loaf Anticline. Over 30,000 ft of sedimentary deposits from Cambrian to Tertiary age fill the basin. The cross sections were chosen to display Upper Cretaceous facies relationships and show the correlations of Tertiary formations. The source for the Mesaverde Group rocks in the basin is suggested as southerly to southwesterly based on core data.

Iverson, W. P., 1992, Oil and gas production and reserves, Mesaverde Group, Green River Basin, Wyoming: Wyoming Geol. Assoc. 43rd Field Conf. Guidebook, p. 245-252.

A summary and analysis of hydrocarbon production from the Mesaverde Group in the Greater Green River Basin. Over 11% of the gas produced in Wyoming comes from the Greater Green River Basin which contains only 5% of the state's wells. Production decline curves are calculated based on current production and a 575 Bcf gas reserve is estimated. Fracturing has aided production from tight gas sands by connecting the numerous sands.

Jacka, A. D., 1965, Depositional dynamics of the Almond Formation, Rock Springs Uplift, Wyoming: Wyoming Geol. Assoc., 19th Field Conference Guidebook, p. 81-100.

Upper Almond cycles display the following sequence of deposits from the base upward: (1) marine and/or lagoonal shale, (2) barrier-island sandstone, (3) marsh or mudflat deposits, and 4) lagoonal-bay deposits. These

sequences reflect the lateral shifting of three contemporaneously existing depositional entities: (1) marine environment in which surfzone and infra-surfzone sands, and offshore muds accumulated; (2) the barrier-island environment consisting of foreshore beach, backshore beach, and fringing marsh or mudflat deposits; (3) the lagoonal-bay environment in which predominantly fine-grained sediment, carbonaceous shale, and oyster reefs accumulated.

Evidence indicates that seaward growth of barrier islands was accompanied by expansion of lagoons that resulted in a progressive flooding of the landward margins of the barrier. Thus, positions previously occupied by a barrier island were successively blanketed with lagoonal deposits. As the distance between a seaward-advancing barrier island and the mainland increased, a threshold limit was approached beyond which the volume of sand supplied to the seaward face was insufficient to permit further seaward growth. The operation of negative processes (subsidence, compaction, erosion, and possibly an independent rise in sea level) soon brought about the submergence or drowning of an abandoned barrier island.

Jacka, A. D., 1970, Principles of cementation and porosity-occlusion in Upper Cretaceous sandstones, Rocky Mountain Region: Wyoming Geol. Assoc, 22nd Ann. Field Conf. Guidebook, p. 265-285.

Upper Cretaceous sediments from the Rockies were chosen because they constitute good models for humid-subhumid climates, swampy coastal plain, barrier island-lagoon-bay, and deltaic facies with established structural and geological histories; and, outcrops and subsurface data which may be compared.

Vadose cementation is restricted to hot arid and semi-arid regions where carbonate (caliche) is concentrated, and hot regions with wet-seasons. Rapid, evaporation-triggered precipitation of carbonates, hydroxides, and oxides results in initial precipitation of finely crystalline grain coating cement films, which separate grains, causing an expanded or floating fabric, and which later replace terrigenous grains to form concretions.

Cementation below the water table in fresh or sea water occurs slowly resulting in coarsely crystalline cement that tends to fill pore bodies. Soon afterward, burial silica is precipitated as syntaxial overgrowths on quartz grains at shallow to moderate depths under conditions of low temperature, and slightly acidic pH. At greater depths, silica cementation is followed by calcite precipitation and replacement of quartz under higher temperature and pH. Silica, mobilized at depth by replacement and solution of quartz, diffuses upward and carbonate diffuses downward where it precipitates on prior calcite "seeds". Transportation of cementing material by opposing diffusion gradients occurs slowly through nearly static interstitial waters which overcome inadequacies inherent in supposition of transport by abnormally large volumes of water (as required by water from compacting clays).

Jacka, A. D., 1970, Sediment economics of Upper Cretaceous sandstones Rocky Mountain Region: Wyoming Geol. Assoc., 22nd Ann. Field Conf. Guidebook, p. 187-219.

The Upper Cretaceous in the Rocky Mountains commonly display the following sequence: (1) marine and/or lagoonal shale; (2) barrier island sandstone; (3) marsh-mudflat deposits; (4) lagoonal-bay deposits; (5) alluvial-coastal plain sediments. The sequence displays seaward progradation of coastal plain in response to a large sediment supply. The Gulf Coast Barrier Island/Coastal plain is proposed as an analogue for Upper Cretaceous (especially Almond Formation) in the Rocky Mountains.

The paper is based primarily on investigation of environments, paleogeography and depositional history of the Upper Cretaceous Almond Formation of the Rock Springs Uplift.

Jackson, S., et al., 1993, Integration of the Geological/Engineering Model with Production Performance for Patrick Draw Field, Wyoming: DOE Report NIPER-634, 122 p.

An integrated geological/engineering model for production performance is based on barrier island reservoirs from Patrick Draw Field, Wyoming and Bell Creek Field, Montana. The objectives were: (1) to identify heterogeneities that influence the movement and trapping of fluids within the reservoirs; (2) to characterize methods to quantify reservoir architecture and to predict mobile oil saturation distribution for application to Enhanced Oil Recovery processes; and (3) to summarize reservoir and production characteristics of shoreline barrier systems.

Hydrogeochemical analytical techniques were found to be an inexpensive reservoir characterization tool. Formation water salinity in Patrick Draw Field varies across the field and can cause errors is the estimation of oil saturation. CO_2 flooding was more successful in the Monell Unit at Patrick Draw Field than in the Arch Unit. Horizontal drilling is has the best potential for additional oil recovery in the Arch Unit.

Keighin, C. W., B. E. Law, and R. M. Pollastro, 1989, Petrology and reservoir characteristics of the Almond Formation, Greater Green River Basin, Wyoming: *in* Coalson, E.B., et al., eds, Petrogenesis and Petrophysics of Selected Sandstone Reservoirs of the Rocky Mountain Region, RMAG, Denver, p. 281-298.

Production through 1986 was 100 MM bbl oil and seven TCF gas. SEM and thin section analyses indicated that pores in fine to very fine Almond Formation sandstones are small (< 20μ) and formed in part by dissolution of

framework grains and authigenic cements. Intergranular micropores occur between crystals of authigenic clay. Sandstone contains 15 to 30% clay, which is dominantly illitic. Local concentrations of kaolinite occur, but chlorite is rare. Smectite clay minerals were not detected. Distribution of cements, as well as detrital feldspars, is variable.

Not only porosity, permeability, and depth, but also vitrinite reflectance seem to be related in both conventional and unconventional (tight) Almond reservoirs It may be possible to define an approximate depth at which overpressuring may occur based on these data.

Krueger, M. L., 1960, Occurrence of natural gas in the western part of Green River Basin: Wyoming Geol. Assoc. 15th Annual Field Conference Guidebook, Overthrust Belt of Southwestern Wyoming and Adjacent Areas, p. 195-209.

The Green River Basin is one of the largest of the Rocky Mountain intermountain basins. Its maximum north-south dimension is approximately 180 miles; its maximum east-west dimension, near its southern end, is 90 miles. The basin is bounded on the northeast by the Gros Ventre-Wind River Mountain Range, on the east by the Rock Springs Uplift, on the south by the east-west trending Uinta Mountains, and on the west by the east thrust fault (Disturbed Belt) of the Hoback-Wyoming Range. Production data on the gas fields in the Green River Basin is presented in tables.

Krystinik, L. F., 1990, Characteristics of cores from a wave-dominated barrier/tidal inlet deposit: Cretaceous Almond Formation, south-central Wyoming (abst.): *in* Davis, R.A., D. Nummendal, and R. Tillman, eds., Tidal Inlet and Related Sand Bodies Modern and Ancient: SEPM Research Conference San Juan Basin, New Mexico, pages unnumbered.

East of Table Rock Field in Sweetwater County, the UA-8 sandstone is a north-south trending barrier/lagoon complex which has been cored at several localities in barrier and back-barrier facies. In the Union Pacific Railroad Corporation Robinson Siding No. 1 well (11-19N-97W), a 59-ft continuous core was cut through a sandstone body interpreted to be a tidal inlet deposit. The tidal inlet is laterally equivalent to wave-dominated shoreface deposits along strike and to back-barrier lagoonal deposits to the west.

The tidal inlet deposit is a 45 ft thick, blocky- upper-fine to lower-medium-grained sandstone body. The inlet has a sharp basal scour on older lagoonal deposits, and the inlet fill is composed of a basal oyster-shell lag which grades upward into clean, massive to medium-scale trough cross-stratified sandstone. A number of oyster-shell lags occur within the cross-stratified inlet fill, and these slightly inclined horizons may mark lateral accretion surfaces, as observed in field exposures of Almond formation inlets. The cross-stratified sandstone becomes more massive to planar-laminated toward the top 3 ft of the sandstone body and may record foreshore deposition as spit accretion filled the inlet. The upper 6 ft of the core is composed of *Ophiomorpha*-burrowed sandstone which grades upward into a transgressive unit composed successively upward of burrowed argillaceous sandstone, gritty mudstone and black silty mudstone.

Land, C. B. Jr., 1972, Stratigraphy of Fox Hills Sandstone and associated formations, Rock Springs Uplift and Wamsutter Arch area, Sweetwater County, Wyoming: A shoreline-estuary sandstone Model for the Late Cretaceous: Quarterly of the Colorado School of Mines, v. 67, no. 2, 69 p.

The Upper Cretaceous Fox Hills Sandstone which outcrops on the east flank of the Rock Springs Uplift is a regressive sequence of sandstone and siltstone which was deposited along a barrier island coastline in littoral, shallow neritic, and estuarine environments. It overlies and intertongues with marine Lewis Shale; and it is overlain by, and intertongues with, the nonmarine Lance Formation. Depositional environments: An earlier report by Weimer interpreted the Fox Hills as a barrier island sequence similar to the modern barriers along the Gulf Coast. Weimer interpreted the shoreline to have been generally north-south oriented with lagoons and coastal swamps to the west and a deeper neritic environment to the east. Land is generally in agreement, but points out some minor differences of interpretation:

1. Sands deposited in migrating estuaries was important in Fox Hills. The scour at base of Weimer's upper "G" sandstone is the base of migrating estuary channel.
2. Lenses of *Ostrea* are reinterpreted as lag deposits in estuary channels.
3. Subsequent subsurface control indicates that shoreline trend is northeast-southwest.
4. Weimer (1961) compared Fox Hills environments to the Gulf Coast Barriers- where the barriers are separated by broad lagoons that are filling with clay and silt deposits.

Land finds better analogy with the modern Georgia coast (brought to his attention by Weimer). The Georgia coast has about 7-ft tides, and the barrier chain is separated from the mainland by a saltmarsh-estuary channel complex. The high-energy environments of sand deposition in these estuaries is believed to be similar to the postulated Fox Hills environments.

Lanham, R. E., 1980, Petrography and diagenesis of low-permeability sandstones of the lower Almond Formation, Southwestern Wyoming: M.S. Thesis, Univ. of Colorado, 113 p.

Petrographic study of the lower Almond sandstones in the Tierney Gas Field, in the Wamsutter Arch area of southwestern Wyoming; the sandstones are fine-grained sublitharenites containing chert fragments and little or no feldspar. Sandstones average 9% porosity and have very low permeabilities, averaging 0.10 mD. Compaction and quartz cementation have reduced both k and ø; dissolution of unstable minerals has created varying amounts of secondary porosity.

Quartz cement averages 15% of rock volume and has inhibited compaction, but also occluded porosity and reduced permeability. In many instances, cementation by quartz was hindered by detrital and authigenic clays. Where clay is common, quartz cement is less abundant and intergranular microporosity is widespread.

Based on thin section analyses, up to one-half of existing porosity of some sandstones is secondary, having been formed by dissolution of detrital and authigenic minerals. Much of the porosity was created by dissolution of siderite and possibly dolomite-ankerite. Some of the resulting pores were subsequently filled by authigenic quartz and kaolinite. (A complete solid solution between dolomite and ankerite appears to exist). Dissolution of chert grains also appears to have created a significant amount of secondary porosity. Chert dissolution first produces a microporous mass but with continued leaching results in grain-size voids. Leaching of biotite, and possibly feldspar, created minor amounts of secondary porosity. Formation of secondary porosity was hindered by the presence of matrix, which inhibited access of leaching fluids to potentially soluble minerals. Good photomicrographs and SEM images illustrate the text.

Law, B. E., 1984, Relationships of source-rock, thermal maturity, and overpressuring to gas generation and occurrence in low-permeability Upper Cretaceous rocks, Greater Green River Basin, Wyoming, Colorado and Utah: *in* J. Woodward, F. Meissner, and J. Clayton, eds, Rocky Mt. Assoc. Guidebook, Hydrocarbon Source Rocks of the Greater Rocky Mountain Region, p. 469-476.

Most of the hydrocarbon production from Upper Cretaceous and Lower Tertiary reservoirs in the Greater Green River Basin is gas. The basin covers areas of southern Wyoming, northwestern Colorado and northeastern Utah. Gas deposits are found interbedded with coal and carbonaceous rocks. Gas accumulations are associated with overpressuring. Overpressuring is caused by thermal generation of gas. Gas migrates limited distances of less than several hundred feet. Large volumes of gas in the Greater Green River Basin occur at temperatures of 190° to 200° F with a vitrinite reflectance of about 0.8.

Law, B. E., 1992, Paleofluid flow paths - Evidence from thermal maturity mapping, Greater Green River Basin, Wyoming and Utah (abst.): AAPG Ann. Convention Program, Calgary, Alberta, page unnumbered.

Thermal maturity mapping is used to reveal unusually high and low areas resulting from thermal perturbations associated with ascending and descending fluids. An area of high thermal maturity is coincident with Patrick Draw Field, Wyoming, and an area of low thermal maturity is coincident with the Bridger Lake and Lucky Ditch oil fields near the Moxa Arch. Vitrinite reflectance values for the Almond Formation at a depth of 5,000 ft range from 0.48 to 0.68. Faults are the suggested pathways for the hot fluids. In contrast, the southern end of the Moxa Arch has a low thermal maturity and a low thermal gradient.

Law, B. E., C. W. Spencer, and N. H. Bostick, 1980, Evaluation of organic matter, subsurface temperature and pressure with regard to gas generation in low-permeability Upper Cretaceous and Lower Tertiary sandstones in Pacific Creek area, Sublette and Sweetwater counties, Wyoming: The Mountain Geologist, v. 17, p. 23-35.

The area for this report is 35 miles directly north of the Rock Springs Uplift. The onset of overpressuring occurs about 11,600 ft, at the base of the Upper Cretaceous Lance Formation. Generation of wet gas is apparently one of the main processes related to overpressuring. Reversal of SP curves near the top of overpressuring is related to reduction of formation water salinity. Small amounts of water produced during thermochemical decomposition or organic matter and the dehydration of clays during clay transformation may provide enough low-salinity water to effectively dilute the original formation water.

Total organic content (TOC) averages 1.38% (range 0.25 to 7.84). The top of overpressuring and beginning of important wet-gas generation occurs at vitrinite reflectance values of 0.74 to 0.86.

Lawson, D. C., and C. W. Crowson, 1961, Geology of the Arch Unit and adjacent areas, Sweetwater County, Wyoming: WGA Guidebook, 16th Ann. Field Conf., p 280-299.

The Arch Unit at Patrick Draw field is 10 miles long and 4.5 miles wide. The first oil well was drilled in early 1959. A history of the production and initial geology is presented. Patrick Draw Field is located on the crest of the Wamsutter Arch on the east flank of the Rock Springs uplift. Stratigraphic units are the early Tertiary

Wasatch Formation, and Upper Cretaceous Lance, Fox Hills, Lewis Shale, and Almond formations. Oil production is from sand bodies in the Almond.

Leckie, D., and L. F. Krystinik, 1989, Is there evidence for geostrophic currents preserved in the sedimentary record of inner to middle-shelf deposits?: J. Sed. Petrol., v. 59, p. 862-870.

Wave-ripple crests in the Almond trend generally N-S, parallel to regional shoreline, while other shoreline indicators and humocky cross stratiation (HCS) beds trend E-W, normal to shoreline orientation.

Lewis, J. L., 1961, The stratigraphy and depositional history of the Almond Formation in the Great Divide Basin, Sweetwater County, Wyoming: Wyoming Geological Assoc., Symposium of Late Cretaceous rocks Green River, Washakie, Wind River and Powder River Basins; p. 87-95.

The Almond Formation crops out on the east flank of the Rock Springs uplift, the structural divide between the Great Divide Basin to the east and the Lesser Green River Basin to the west. The Almond outcrops are characterized by cuestas with low west facing escarpments. The Almond outcrop is bordered on the west by the steep escarpment of the Ericson Sandstone and on the east by a long strike valley into the Lewis Shale. Three major environments of deposition are recognized; (1) coastal swamp in the lower shale, (2) beaches or sandbars and sandspits created by waves and currents, (3) shallow marine to non-marine deposits from lagoons and coastal swamps.

Martinsen, R. S. and G. Christensen, 1992, A stratigraphic and environmental study of the Almond Formation, Mesaverde Group, Greater Green River Basin, Wyoming: Wyoming Geological Assoc. Guidebook, Rediscover the Rockies; p. 171- 190.

The Almond Formation was selected to study the origin and characteristics of tight gas sands in the Mesaverde Group. The Almond Formation in the Rock Springs Uplift area of Wyoming is divided into upper and lower members. The lower Almond in fresh to brackish water deposition. The upper Almond is marine and estuarine and deposited as a series of landward-steping strandline sandstones. These strandlines were deposited as part of an barrier island system. The Almond reservoirs in the Washakie Basin have been highly productive. The Dripping Rock field further south was deposited as a storm sequence. Regional tectonics and localized movement along basement block faults are controlling agents in Almond deposition. Production tables show the field characterists and production statistics for several units in the Rock Springs area. Stratigraphic maps, structural contours and paleogeographic reconstructions are used to define the geologic setting of the Almond Formation and its production.

McCubbin, D. G., and M. J. Brady, 1969, Depositional environment of the Almond reservoirs, Patrick Draw Field, Wyoming: The Mountain Geologist, v. 6, no. 1, p. 3-26.

This study supports Weimer (1966) that the main reservoir sandstone is a composite shoreline deposit, at least partly replaced updip by lagoonal shales.

UA-5 at Patrick Draw consists of a western bar and a younger eastern bar that partly overlaps the western bar. The western bar and, in places, the eastern bar rest with sharp contact on a widespread coal that forms the uppermost unit of the underlying cyclic sequence. Both sandstone bodies contain transported bivalves and some forams and show burrows including rare *Ophiomorpha*. Both sand bodies show a vertical sequence of stratification types interpreted as deposition in nearshore-marine and beach environments on a seaward-prograding shoreline. Lateral changes in stratification types suggest that the seaward direction was to the east. Vertical and lateral variations in grain size of this record an initial transgression, followed by deposition in progressively more shallow environments during shoreline progradation.

The lagoonal facies that overlies the western bar and appears to be at least partly equivalent to the eastern bar consist of silty to sandy shales and some thin sandstones. Oysters are common and are a major constituent of coquina beds. The occurrence of large, whole, randomly oriented oyster valves in a shale matrix indicates that these oysters are in their original place of growth. Some of the shales contain a microfauna of arenaceous forams. Structures formed by burrowing animals are abundant in the silty or sandy shales.

McDonald, R. E., 1973, Big Piney-La Barge Producing Complex, Sublette and Lincoln Counties, Wyoming: Wyoming Geol. Assoc., 25th Field Conf., p. 57-77.

A gas producer since 1956, and major oil producer since 1960. Cumulative gas production is over 1.2 tcf, total oil produced is about 65 MMBBL. The producing complex is on and around the flanks of a Laramide anticlinal fold that was formed subjacent to a salient along the Disturbed Belt, west of Wind River Mountains., in the northern part of the Green River Basin.

Meyers, W. C., 1977, Environmental analysis of Almond Formation (Upper Cretaceous) from the Rock Springs Uplift, Wyoming: Ph.D. Dissertation, University of Tulsa, 280 p.

Micropaleontology and photos of two 5-in diameter cores drilled 1/2 mile downdip from the outcrop face exposed in the Rock Springs Uplift (T20N, R101W)were studied. There were 150 palynological species were recorded.

Mieras, B. L., 1992, Sequence stratigraphy, Frontier Formation, south-central Wyoming: esutatic and tectonic influences: Wyoming Geol. Assoc. 43rd Field Conf. Guidebook, p. 51-60.

An erosional unconformity 90 million years old forms the boundary between the Greenhorn Cycle and the Niobrara Cycle in the Western Interior Basin. The boundary is marked by sandstone poor deposits of the underlying Bell Fourche Member. The Wall Creek Member is the sand-rich upper member of the Frontier Formation. The Emigrant Gap Member lies between the Wall Creek and Belle Fourche in a discontinuous pattern. The Frontier Formation overall is a coarsening upward succession. The sequence boundary of the Greenhorn and Niobrara Cycles falls in the Upper Wall Creek Member. The transgressive phase of the Niobrara Cycle suggests local tectonic control of the late Frontier deposition.

Unconformaties as observed in sequences and marine deposits vary from place to place within the geographic and stratigraphic locations of the Frontier Formation. This paper reconstructs the chronostratigraphic sequences of the Frontier Formation using textural features, lithology and maps for the correlations.

Miller, F. X., 1977, Biostratigraphic correlation of the Mesaverde Group in Southwestern Wyoming and Northwestern Colorado: Rocky Mountain Assoc. Geol., Symposium, p. 117-137.

The Mesaverde Group consists of Upper Cretaceous marine strata in eastern Wyoming and Colorado and non-marine strata in north-central Utah. Biostratigraphic units are based on paleontologic data on the marine faunas. Faunal samples are from cores and outcrop. Formation names within the Mesaverde Group are difficult to correlate and differ from basin to basin. The purpose of this paper was to place all the regional formations in proper chronostratigraphic order. Numerous maps and correlation charts are used to illustrate the stratigraphy.

Myers, R. C., 1977, Stratigraphy of the Frontier Formation (Upper Cretaceous), Kemmerer Area, Lincoln County, Wyoming: Wyoming Geol. Assoc. Guidebook, 25th Annual Field Conference, p. 271-292.

The Frontier Formation of Turronian age on the west side of the Green River Basin, Wyoming, is a nearshore sequence of marine and nonmarine bentonites, shales, siltstones, sandstones, conglomerates, and coals. These strata represent two cycles of clastic shoreline progradation along the western fringe of the Cretaceous Seaway in the western interior of the United States.

Newman, H. E., 1981, Greater Green River Basin stratigraphy as it relates to natural gas potential: SPE/DOE 9845, Presented at SPE/DOE Low Permeability Symposium, Denver, Colorado, pages unumbered.

The 21,000 square miles of the Greater Green River Basin encompasses the Green River Basin proper, the Rock Springs Uplift, the Red Desert and the Washakie and Sand Wash Basins. Drilling for hydrocarbons reaches depths of 20,000 ft. Natural gas is found in tight sands from the Mesaverde Group, Lewis, Lance, Fort Union, and Wasatch formations.

Five lithofacies maps of the basin are presented, and a geological analysis of potential gas reservoirs is given. The Almond was deposited in transitional coastal plain and nearshore environments during a transgression; however, the barrier island sediments were deposited during stillstands or local regressions of the Lewis Sea. The Almond barrier may have advanced seaward as much as 20 miles (Jacka, 1965).

Pryor, W. A., 1961, Petrography of Mesaverde sandstones in Wyoming: Wyoming Geol. Assoc., 16th Ann. Field Conf. Guidebook, p. 34-46.

This study was based on a systematic sampling of outcrops from uppermost, middle, and lower sandstone bodies in the Mesaverde section from a number of formations including the Almond. Textural classification of the Almond as a lithic graywacke (immature chert arenite) with 25% chert: Q58F12R30. Heavy minerals comprise less than 0.8% by weight of Mesaverde sandstone samples. Much of the report dwells on species and interpretation of heavy minerals

Richers, D. M., 1990, Patrick Draw Oil Field: Unpublished review copy. Submitted to AAPG.

Discovered in 1959, the estimated reserves are 200 to 250 MMBBL oil. Patrick Draw is just one of many Cretaceous oil fields in Wyoming that produce from elongate sand bodies that were distributed along the margin of the Upper Cretaceous Sea. The field is divided into three producing units: (north to south) Patrick Draw North, Arch, Monell. Production is from Almond, although localized pay or shows in Lewis, Fox Hills, and Lance

formations (Cretaceous), as well as from the Paleocene Fort Union and Eocene Wasatch formations. Patrick Draw like, most fields in the area, is a stratigraphic trap. The Almond is felt to represent near-shore barrier bar and beach front sands. As a result, reservoirs tend to be several miles long and less than 4 miles wide.

The field is located on the eastern flank of the Laramide Rock Springs Uplift, and on the southern limb of the Wamsutter Arch. Present axis of the arch is about 10 miles north of the original axis formed at the end of the Cretaceous. Vitrinite reflectance data and thermal modeling indicate that Patrick Draw is currently in the oil window; the Lewis Shale several miles east of Patrick Draw could have entered the oil window 18-20 million years ago.

The Almond represents near-shore barrier bar and/or ancient shorelines, with some shallow tidal-flat facies. Generally, the producing sandstone bodies are less than 2 miles wide and some are up to 20 miles in length. Lateral facies changes are abrupt, resulting in extreme porosity differences over a very small distance. Updip seal for stratigraphic traps is provided by facies change into less permeable coastal plain shales and siltstones. Overlying seal is provided by the Lewis Shale. UA-6 is productive only in the northern portion of the field, about 10-ft below the UA-5. UA-5 and UA-6 are generally separated by a dark gray shale and silty shale.

Tidal flats are represented as fine-grained, laminated and rippled mudstones and sandstones. Burrows are common. Evidence for small tidal creeks includes deformed and slumped features.

Marsh environments are evidenced by dark, organic-rich very fine grained sand and mudstone. Some coal is also present.

Oil samples had API gravity of 44.4 and a density of 0.7977 g/cc at 25° C; and a GOR between 600:1 to 1554:1 for Almond production. Whole oil chromatogram shows preponderance of lighter n-paraffin components generally indicative of maturity because mature oils are generally enriched in the lighter components. Pristane to phytane ratios greater than 3.0 in high wax crude oils and condensates characterize input from terrigenous materials common to lacustrine, fluviatile, and deltaic environments. This assessment fits Patrick Draw. A terrigenous source for Patrick Draw oils is strongly suggested.

Surface geochemical studies support: (1) fractures and faults are the preferred migration pathway of hydrocarbons leaking from the subsurface reservoir to the surface, (2) high surface hydrocarbon anomalies are repeatable over a period of years, (3) geobotanical anomalies exist over the gas cap in western up-dip portions of the field. A stressed sage community is located over the field.

Richers, D. M., V. T. Jones, M. D. Matthews, J. Maciolek, R. J. Pirkle, and W. C. Sidle, 1986. The 1983 Landsat soil-gas geochemical survey of Patrick Draw area, Sweetwater County, Wyoming: AAPG Bull., v. 70, p. 869-887.

Resampling the Geosat test site at Patrick Draw indicated that the 1980 assessment was correct: that faults and fractures visible as linear features on satellite and aircraft imagery provide paths for active microseepage of hydrocarbons from depth to the near surface. This association is particularly true near the earlier described blighted sage zones, where a much wider area of anomalously high free soil gas values and fluorescence was revealed.

Richers, D. M., R. J. Reed, K. C. Horstman, G. D. Michels, R. N. Baker, L. Lundell, and R. W. Marrs, 1982, Landsat and soil-gas geochemical study of Patrick Draw oil field, Sweetwater County, Wyoming: AAPG Bulletin, v. 66, p. 903-922.

Anomalous hydrocarbon concentrations in soil-gas samples appear in those areas near lineaments mapped from Landsat images of the Patrick Draw Field. These lineaments represent extensional faults and fractures produced during development of the Rock Springs Uplift to the west. Several of the lineaments extend to depth and are able to serve as conduits allowing preferential microseepage of hydrocarbons to the surface in the Patrick Draw area, indicating the nature of expected hydrocarbons at depth.

Ritzma, H. R., 1955, Late Cretaceous and Early Cenozoic structural pattern, southern Rock Springs Uplift, Wyoming: Wyoming Geol. Assoc. 10th Annual Field Conference Guidebook, Green River Basin, p. 135-137.

The structure of the Rock Springs Uplift exposes a succession of Late Cretaceous and Early Cenozoic formations east of Rock Springs, Wyoming. The uppermost strata are outcrops of the Green River (Eocene) and Fort Union (Paleocene) formations. The lowermost strata exposed are the Baxter Shale, Blair, and Mancos Shale formations, all Upper Cretaceous. The beds dip to the east onto the Wamsutter Arch into the Red Desert and Washakie Basins exposing the Mesaverde Group, Lewis Shale, and Lance Formation. The numerous unconformities and overlaps give an indication of the great changes brought about by structural movement.

Roehler, H. W., 1965, Summary of Pre-Laramide Late Cretaceous sedimentation in the Rock Springs Uplift area: Wyoming Geol. Assoc. 19th Field Conference Guidebook, Sedimentation of Late Cretaceous and Tertiary Outcrops, Rock Springs Uplift, p. 11-12.

Short descriptions of the late Cretaceous formations in the Rock Springs Uplift accompany a map showing depositional relationships. The section is restored to late Cretaceous view and the extent of Teritary erosion is shown cutting through the Lance, Fox Hill, and Lewis Shale formations to expose underlying units.

Roehler, H. W., 1977, Lagoonal origin of coals in the Almond Formation in the Rock Springs Uplift, Wyoming: 1977 Symposium on the Geology of Rocky Mountain Coal, Colorado Geol. Surv. Resources Series 1, p. 85-89.

Three units are recognized:

Upper 300 ft-coastal lagoon, mixed barrier bar, lagoon, shallow marine; saltwater deposition is indicated by shark teeth, and cephalopods.

Middle 350 ft-brackish water lagoonal environment. Brackish water deposition indicated by oysters and other mollusks.

Lower 200 ft-freshwater coastal swamps. Freshwater environment are indicated by dinosaur, crocodile, turtle, and fish fossils.

Depositional Model: marine coastline with lagoons formed behind barrier island during westward trangsressions of late Cretaceous sea. Evidence for lagoonal origin of coals is: intertonguing and juxtaposition of the coal beds and barrier islands and by presence of fossil oyster beds containing coal-bearing sequences. Eighteen coal beds that range from 25 to 16 ft thick have been mapped in the Almond Formation.

Roehler, H. W., 1977, Geologic map of the Cooper Ridge NE Quadrangle, Sweetwater County, Wyoming: U. S. Geol. Surv., Map GQ-1363.

Roehler, H. W., 1978, Geologic map of the Mud Springs Ranch Quadrangle, Sweetwater County, Wyoming: U. S. Geol. Surv., Map GQ-1438.

Roehler, H. W., 1978, Correlations of coal beds in the Fort Union, Lance and Almond formations in measured sections on the east flank of the Rock Springs uplift, Sweetwater County, Wyoming: U. S. Geol. Surv., Open File Report 78-248.

Fold out stratigraphic column and measured sections of the upper Mesaverde Group formations.

Roehler, H. W., 1978, Correlations of coal beds in the Fort Union, Almond, and Rock Springs Formation in measured sections on the west flank of the Rock Springs uplift, Sweetwater County, Wyoming: U. S. Geo. Surv. Open File Report 78-395.

A fold out stratigraphic column and measured section of the upper Mesaverde Group formations in the Green River Basin.

Roehler, H. W., 1979, Geology and energy resources of the Sand Butte Rim NW Quadrangle, Sweetwater County, Wyoming: U. S. Geol. Surv. Professional Paper 1065-A, A54 p.

The Sand Butte Rim quadrangle is on the east flank of the Rock Springs Uplift in southwestern Wyoming. The underlying 20,000 ft of sedimentary deposits include 28 formations ranging in age from Cambrian to Tertiary. Upper Cretaceous and lower Tertiary rocks outcrop and dip 3 to 6 degrees southeast. Coal resources are estimated at 1 billion short tons in the Fort Union, Lance and Almond formations. Oil was first discovered in Sand Butte Rim quadrangle in 1959 at Patrick Draw Field.

Roehler, H. W., 1979, Geology and mineral resources of the Mud Springs Ranch Quadrangle, Sweetwater County, Wyoming: U. S. Geol. Surv. Professional Paper 1065-C, C35 p.

Mud Springs Ranch quadrangle is located on the southeast flank of the Rock Springs Uplift in southwestern Wyoming. Sedimentary rocks exposed are 5,400 feet thick and are gray sandstone, siltstone, and shale; gray and brown carbonaceous shale and thin beds of coal. The Blair, Rock Springs, Ericson, Almond, and Lewis formations of Cretaceous age and the Paleocene, Fort Union Formation are represented. There are three coal beds in the Fort Union Formation and 15 in the Almond Formation that can potentially be mined. Oil and gas tests have been made, but the structurally controlled stratigraphic trap prospects have not been analyzed.

Roehler, H. W., 1979, Geologic map of the Camel Rock Quadrangle, Sweetwater County, Wyoming: U. S. Geol. Surv., Map GQ-1521.

Roehler, H. W., 1979 Paleogeography and lithofacies of barrier bar G and associated rocks, Almond Formation, southwest Rock Springs Uplift, Wyoming: Rocky Mountain Sec. Soc. Economic Paleo. and Mineralogists, Field Trip, Cretaceous of the Rock Springs Uplift, Wyoming, p. 2-21.

Surface and subsurface investigations of barrier bars in the Almond Formation are discussed.

1. Barrier bars were deposited in interdeltaic areas during the westward transgression of the Lewis Sea in the late Cretaceous.
2. Large brackish lagoons formed behind the barriers
3. As many as ten barriers are stacked along the east flank of the Rock Springs Uplift. The vertical sequences are cyclic:
   a. marine erosion
   b. lagoon and back barrier carbonaceous shale and coal
   c. dune, washover and tidal channel sandstone
   d. upper shoreface sandstones
   e. middle shoreface sandstone
   f. lower shoreface sandstone
   g. marine shale
   h. marine erosion
4. Lithofacies are identified by primary sedimentary structures.
5. The barriers are prograding.
6. The shape, size, and spacing of tidal channels, flood tidal deltas and ebb-tidal deltas suggest a tidal range of 5 to 6 ft.

Roehler, H. W., 1988, The Pintail Coal Bed and Barrier Bar G - A Model for coal of barrier bar-lagoon origin, Upper Cretaceous Almond Formation, Rock Springs Coal Field, Wyoming: U.S. Geological Survey Professional Paper 1398, 60 p.

The early Maastrichtian upper Almond barrier is 60 miles long and 4 miles wide. There are 18 miles of outcrops on the east flank of Rock Springs Uplift.

The study was based on outcrops around Rock Springs Uplift: 104 measured stratigraphic sections plus 14 others that describe lithofacies and primary sedimentary structures were used. Four widely spaced holes were drilled and logged (no cores were taken).

Barrier bar G: mesotidal (4.5-8 ft range); islands 5 to 7 miles long, roughly drumstick-shaped, washover fans present, but not common; numerous tidal inlets; flood-tidal deltas large (up to several miles wide); ebb-tidal deltas moderately large to small.

Divisions of Almond Formation: Upper 100-400 ft-very fine-grained to medium grained; deposited in shallow marine, barrier bar and lagoonal environments; saltwater fauna-marine mollusks, shark teeth, ammonites, numerous trace fossils. Middle 125-250 ft-brown carbonaceous shale and coal, some thin interbedded gray shale and gray, fine-grained crossbedded sandstone deposited in lagoonal environments; brackish water fauna of abundant oysters and brackish mollusks. Lower 100-600 ft-swampy, coastal plain setting: fresh water fauna of dinosaurs, turtles, crocodile, and fish bones.

The Pintail coal bed was deposited in a lagoon, landward of barrier bar G. As the barrier prograded, the back-barrier flat was progressively covered by swamp deposits that include the seaward wedgeout of the coal bed. The coal bed is massive and locally more than 6 feet thick. Splits and partings of carbonaceous shale are interpreted as tidal inlet and tidal creek deposits. The model demonstrates that the barrier and its lagoon evolved through saltwater to brackish-water to freshwater stages, with the times of maximum peat accumulation occurring in the freshwater stage.

Roehler, H. W., 1990, Stratigraphy of the Mesaverde Group in the Central and Eastern Greater Green River Basin, Wyoming, Colorado and Utah: U. S. Geological Survey Professional Paper 1508, 52 p.

The Mesaverde Group comprises 5,000 ft of deposits in the central and eastern Greater Green River Basin. The lower Mesaverde formations; Rock Springs, Blair, Haystack Mountains, Allen Ridge and Iles were deposited in a major eastward regression of the Cretaceous Seaway. A regional uplift of the Rocky Mountains followed the deposition. The upper Mesaverde; Almond and William Fork formations were deposited during a westward transgression of the Seaway.

Environments of deposition in the Mesaverde Group include alluvial plain, floodplain, coastal-plain, barrier plain, tidal-flat, delta-plain, marine shoreline, marine shelf and slope deposits.

Lithologies, sedimentary structures, fossils, water depth and salinity, diagenetic processes and sediment sources are analyzed and illustrated.

Roehler, H, W., J. Horne, R. Levey, M. Hendricks, M. Van Horn, C. Land, and B. Weimer, 1979, Field trip Cretaceous of the Rock Springs Uplift, Wyoming: Rocky Mountain Section, SEPM, Sept. 21-23, 1979, 72 p.

A series of papers on the Cretaceous geology of the region of the Rock Springs Uplift. The three day field trip observed outcrops of the Almond, Blair, Rock Springs, Fox Hills and Ericson formations. Papers discuss the paleogeography, lithology , and stratigraphic relationships of the formations of the Rock Springs Uplift. The papers are well illustrated by maps, cross sections, cores, and paleogeographic reconstructions.

Ryder, R. T., M. W. Lee, W. R. Agena, and R. C. Anderson, 1990, Seismic expression of subtle strat trap in Upper Cretaceous Almond: Oil and Gas Journal, v. 88, no. 51, p. 54-57.

Patrick Draw Field produces oil and gas from a stratigraphic trap in the Upper Cretaceous Almond Formation. Table Rock Field produces from a faulted anticline structural trap from multiple Tertiary, Mesozoic, and Paleozoic reservoirs. The objective of this study was to determine if the stratigraphic trap in the Almond could be detected on a 12-fold common depth point seismic profile. Seismic data was analyzed across the entire Rock Springs Uplift.

Schatzinger, R. A., M. J. Szpakiewicz, S. R. Jackson, M. M. Chang, B. Sharma, M. K. Tham and A. M. Cheng, 1992, Integrated Geological-Engineering Model of Patrick Draw Field and Examples of Similarities and Differences Among Various Shoreline Barrier Systems: DOE Report NIPER-575, 146 p.

Shoreline barrier deposits were studied to determine problems specific to this class of reservoirs and to develop methods to characterize shoreline barriers. Prediction of residual oil saturation on interwell scales and improvement of flow patterns of injected fluids was an important goal.

Four main areas studied were: (1) development of a quantitative geological and engineering model for Patrick Draw Field, Wyoming; (2) comparison of the mesotidal barrier island system at Patrick Draw Field to the microtidal barrier island system at Bell Creek Field, Montana; (3) application of geostatistical analysis to determine interwell properties at Patrick Draw Field; (4) continued development of methodologies to characterize shoreline barrier reservoirs.

Later compartmentalization is indicated at Patrick Draw Field by; (1) anomalous production zones, (2) precipitous changes in formation water salinity, and (3) large decreases in formation pressure during primary production. Channeling and poor waterflood sweep efficiency in the Arch Unit may be caused by fractures.

The comparison and contrast between Patrick Draw Field and Bell Creek Field show that both reservoirs are compartmentalized. Initial production is influenced by the internal architecture of the reservoir. Secondary and tertiary production are more influenced by structural and diagenetic features. Faults in both fields contribute to poor sweep efficiency. Diagenetic changes were more significant at Bell Creek in the early stages of leaching, at Patrick Draw the later stages of cementation by carbonates and clays had more significant effects.

Shapurji, S. S., 1978, Depositional environments and correlation of the Mesaverde Formation, Wind River Basin, Wyoming: Wyoming Geol. Assoc. 30th Field Conf. Guidebook, p. 167-180.

The Upper Cretaceous Mesaverde Formation is widespread in the central Rocky Mountain area. In the Wind River Basin facies include marine and nonmarine sandstones, siltstones, shales and coals. The multiple transgressions and regressions caused intertonguing of marine and nonmarine deposits and confused the stratigraphy. The Wind River Basin is a structural basin bounded on the west by the Wind River Mountains, on the north by the Owl Creek and Big Horn Mountains, on the east by the Casper Arch, and on the south by the Granite Mountains. The Mesaverde Formation has extensive exposures on the flanks of the Casper Arch. A number of well logs and cores were correlated to describe and interpret the complex stratigraphy of the Mesaverde Formation in the Wind River Basin. The coal and hydrocarbon potential for the Mesaverde Formation is discussed. At the time of publication coal was of greater significance than oil or gas.

Sharma, B., 1992, A new technique to estimate vertical variability of rock properties for reservoir rock evaluation: SPE 24724, Soc. Petroleum Eng., 67th Ann. Tech. Conf., Washington, D. C., p. 637-652.

Examples from Patrick Draw Field, Wyoming and Bell Creek Field, Montana are presented to demonstrate a new technique for description of vertical variability within a reservoir. Information on rock properties used to verify the technique includes: geological description of cores, XRD analysis, SEM and CT-scan data, porosity, air permeability, primary and waterflood oil production data.

The vertical distribution of reservoir rock properties available as a function of depth is transformed into functions of frequency (cycles per foot) by the application of standard time series analysis techniques. Estimation of vertical variability is computed by a 'power spectra' of core measured permeability, and digitized gamma ray, sonic, density and neutron logs. The 'power spectra' for a clean sandstone decayed very rapidly at higher frequencies if there was no thin bed stratification. Sandstones with variable reservoir properties showed slower decay in the 'power spectra'. Kaolinite clay filled sandstones showed very low amplitudes at higher frequencies. The study of decay spectra may provide quantitative information on variations in cement content and types and volumes of clays in reservoir rocks.

Smith, L. K., and R. C. Surdam, 1992, Cyclic CO_2 enhanced oil recovery in Wyoming Cretaceous fields: Wyoming Geol Assoc. 43rd Field Conf. Guidebook, p. 145-166.

A number of CO_2 projects have been attempted in the Cretaceous oil reservoirs of Wyoming. Both reservoir geology and fluid geochemistry affect the success of CO_2 projects. Five case studies from Wyoming are presented and analyzed and recommendations given. The five reservoirs tested are from four Cretaceous formations in Wyoming; Dakota, Muddy, Cody and Frontier.

The major problems in the CO_2 projects have come from confinement, loss of CO_2 and scale damage or precipitation. The confinement of the CO_2 to near the well-bore is essential to maintain contact with residual oil and to move the oil. This loss of confinement is usually due to high permeability, heterogeneity of the reservoir, fractures and the spacing of nearby injection or production wells. Scale problems are not as common with cyclic CO_2 projects, but cause severe damage when they occur. Shortening the duration of CO_2 soak time will lessen scale problems. Other causes of scale damage are abundant calcite in the reservoir and large pressure drops into the wellbore.

Stearns, D. W., W. R. Sacrison, and R. C. Hanson, 1975, Structural history of southwestern Wyoming as evidenced from outcrop and seismic: Rocky Mountain Assoc. Geol. Symposium, *in* Deep Drilling Frontiers of the Central Rocky Mountains, ed. D. W. Bolyard, p. 9-20.

The study area in southwestern Wyoming includes the Red Desert, Green River and Wind River Basins. The Western Wyoming thrust belt lies just west of the study area. The mountain ranges in the area were produced during the Laramide Orogeny. Early structural deformation began in the Precambrian rocks of the Sierra Madra, Medicine Bow, Wind River and Owl Creek mountains. The widespread Cambrian sandstones were deposited on a peneplaned Precambrian surface. Later deformations occurred in the Ordovician and Devonian. During the Pennsylvanian the region was a sedimentary depocenter. Shallow marine and continental sedimentary deposits of the Mesozoic indicate a relatively stable area. Movement was a slow continuous downwarping with 30,000 ft of Cretaceous rocks deposited. The elongate Moxa Arch formed in the Cretaceous. Seismic evidence for the Cretaceous downwarping and crustal movements in southwestern Wyoming is discussed in detail.

Stone, D. S., 1975, A Dynamic analysis of subsurface structure in northwestern Colorado: Rocky Mountain Assoc. Geol. Symposium *in* Deep Drilling Frontiers of the Central Rocky Mountains, ed. D. W. Bolyard, p. 33-40.

Northwestern Colorado subsurface structure is extensively folded and faulted. The fold-fault trends are consistent with regional tectonic trends which effect the central Rocky Mountains. The structural trends and anticlinal folding in northwest Colorado are very complex and confusing. They were formed by northeast-southwest compression extending from the Precambrian through the Laramide. Numerous maps and cross sections are used to illustrate the stages discussed. Northward in the Green River Basin the wrench faults of northwestern Colorado become deeply buried and die out in the Upper Cretaceous rocks (Almond and Lewis formations).

Surdam, R. C., 1992, Sandstone geometries, petrophysical characteristics, and pressure regimes, Mesaverde Group, Green River Basin, Wyoming: Wyoming Geol. Assoc. 43rd Field Conf. Guidebook, p. 167-169.

A summary of the lithology, petrophysical characteristics and pressure of the tight gas sands of the Mesaverde Group in the Green River Basin, Wyoming. The Mesaverde ranges from 2,000 to over 5,000 feet in thickness and covers 19,000 sq. miles within the Green River Basin. Hydrocarbon production is primarily from tight gas sands. The sandstone beds consist of multiple stacked wedges of deltaic deposition into the Western Interior Seaway. Two major regressions, two regional transgressions and numerous local events encompass a period of 13 million years. These sea level changes have compartmentalized the basin into shoreline, nearshore and offshore sandstones which interfinger with each other.

Szpakiewicz, M. and A. G. Collins, 1985, Hydrochemical Study of the Upper Cretaceous and Lower Tertiary Formations in the Uinta, Piceance and Greater Green River Basins; Implication for Oil and Gas Related Problems: DOE Report NIPER-95, 70 p.

Formation waters from Upper Cretaceous and Lower Teritary strata in the Uinta, Piceance and Green River basins were analyzed for hydrogeochemical components. Oil and gas reservoirs in these basins are organic-rich, non-marine rocks of lacustrine, paludal, and alluvial origin.

Chemical analysis of the samples reveals zones within the rocks depend on proportions of meteoric, ancient marine, and diagenetic fluids. Anaerobic bacteria has caused biochemical degradation in some zones. Isolated, biologically inactive low-temperature zones are favorable for oil survival. Formation waters may be diluted or enriched by bicarbonates, by thermal decarboxylation of organic acids, or by thermometamorphism of the carbonates.

Szpakiewicz, M. J., R. Schatzinger, S. Jackson, B. Sharma, A. Cheng, and M. Honarpour, 1991, Selection and Initial Characterization of a Second Barrier Island Reservoir System and Refining of Methodology for Characterization of Shoreline Barrier Reservoirs: DOE Report NIPER-484, 170 p.

Patrick Draw Field, Wyoming and Bell Creek Field, Montana represent a combination of end-member models of shoreline barriers developed under different hydrodynamic conditions. The hydrodynamic conditions primarily involve changes in sea level and the dominant tide and wave regime of a coastline. The Muddy Formation in Bell Creek Field consists of fine-grained littoral and neritic sandstones deposited as shoreface and foreshore facies in a shoreline barrier system. The Almond Formation in Patrick Draw Field has two units; fine- to medium-grained estuarine sandstone deposited in a tidal channel/tidal delta environment with associated migrating tidal inlets, and fine to very fine grained littoral and shallow neritic sandstones. The similarities and contrasts between the microtidal (Bell Creek) and mesotidal (Patrick Draw) types of shoreline barrier deposits is used to improve the generalized shoreline barrier model. A study of the engineering and geological data is used to correlate the heterogeneities with log signatures, pressure, injection, production characteristics, and fractual distribution.

Thomas, G. E., 1973, Evanston Lineament Green River Basin, Wyoming: Wyoming Geol. Assoc. 25th Annual Field Conference Guidebook, Symposium and Core Seminar on the Geology and Mineral Resources of the Greater Green River Basin, p. 93-95.

ERTS imagery in the Green River Basin area of southern Wyoming shows a prominent tonal alignment which is here named the Evanston lineament. The Evanston lineament is parallel to the Sweetwater River lineament defined in 1971. The outcrop pattern in the photographs shows that the lineament extends southeasterly into Colorado between the Washakie Basin and the Uinta Mountains.

Thomas, J. B., 1978, Diagenetic sequences in low-permeability argillaceous sandstones: Journal of the Geological Society of London, v. 135, p. 93-99.

Based on Cretaceous sandstones from the Rockies, a regular sequence of mineral paragenesis is observed in low permeability sands. Diagenetic sequences in the coarser sandstones do not match the order of free energies of formation. This implies that early precipitation in very fine-grained sandstones probably occurs under nearly static conditions, whereas constant fluid throughput in coarser-grained rocks leads to a markedly different diagenetic sequence. Thus, two potential sandstone reservoirs, one coarse and one very fine, commonly will have different authigenic mineral suites even though their original pore waters were broadly identical.

The author uses examples from the Almond Formation; contrasts upper Almond (coarser, cleaner) with lower Almond (finer grained, tighter).

Tillman, R. W., 1990, Tidal channels in Almond barrier islands sandstones, Patrick Draw Field, Wyoming (abst.): *in* Davis, R.A. Jr., D. Nummendal, and R. W. Tillman, Conveners, Tidal Inlet and Related Sand Bodies: Modern and Ancient; SEPM Research Conference, San Juan Basin New Mexico, May 5-10, pages unnumbered.

The reservoir produces from tidal channel sandstones designated as UA-5, that consist of a western barrier island and a younger overlapping eastern barrier island. In parts of the fields, the barrier islands have been thoroughly dissected by what are interpreted as tidal inlet channels. The UA-4 and UA-5 reservoirs include tidal inlets, while the UA-6 sandstone may be predominantly tidal creeks. The western barrier, and in places the eastern barrier, rests with sharp contact on a widespread coal that forms the uppermost unit of the underlying cyclic sequence.

The tidal channel fill typically is coarsest grained and includes abundant transported oysters at the base. Oysters also are scattered throughout the lower half of the inlet fill. Current structures, including cross-lamination and asymmetrical ripples, dominate the inlet fill. *Ophiomorpha* and other burrows are scattered throughout the sandstone fill of the inlet.

Van Horn, M. D., 1979, Stratigraphy of the Almond Formation, East-Central flank of the Rock Springs Uplift, Sweetwater County, Wyoming: A mesotidal-shoreline model for the Late Cretaceous: M.S. Thesis, Colorado School of Mines, 150 p.

The Almond Formation was deposited as a mesotidal barrier island coastline on a fluvial-coastal plain, with estuarine, open-marine littoral, and shallow neritic environments. The lower Almond is fluvial deposits of small, lenticular, channel sandstones; levee, overbank, and floodplain sandstones, siltstones, mudstones; and carbonaceous shales and coals. The upper Almond is a sequence of coals deposited in fresh water coastal-marsh environments; carbonaceous shales, mudstones, siltstones, and thin sandstones deposited in salt marsh-tidal flats in an estuarine setting. A detailed analysis of the sediments, fossils, and sedimentary structures of the Almond Formation is covered. Surface and subsurface studies of Patrick Draw Field indicate that the oil is trapped by a stratigraphic trap

of combined facies changes and westward truncation. The overlying Lewis Shale provides an impermeable seal for the migration of hydrocarbons.

Van Horn, M. D., 1979, Stratigraphic relationships and depositional environments of the Almond and associated formations east-central flank of the Rock Springs Uplift: Rocky Mountain Sect. Soc. Economic Paleontologists and Mineralogists, Field Trip, Cretaceous of the Rock Springs Uplift, Wyoming, p. 50-63.

The upper Ericson, Almond and lower Lewis Formations are nonmarine to marine deposits of the final transgression of the Cretaceous Seaway. They were deposited along a mesotidal barrier-island coastline in fluvial-coastal plain, estuarine, and marine environments.

The lower Almond has fluvial-related deposits of small lenticular channel sandstones, levee, overbank, and floodplain sandstones, siltstones, mudstones carbonaceous shales and coal beds. The upper Almond unconformably overlies the lower Almond. It has two distinct units of fine to medium-grained estuarine sandstones and fine to very fine grained littoral and shallow neritic sandstones. The estuarine sandstones were deposited in migrating tidal inlets associated with a barrier-island coastline.

The large oil accumulation in the upper Almond is attributed to early placement of the Patrick Draw sandstones in a structurally high position on the incipient Wamsutter Arch by downwarping to the west.

Ver Ploeg, A. J., R. H. DeBruin, R. L. Oliver, and M. Clark, 1983, Almond and Frontier tight gas sand cross sections, Greater Green River Basin, Wyoming: Geol. Surv. Wyoming, Open File Report 83-5, 22 p.

The Almond and Frontier formations in southeast Wyoming account for most of the tight gas sand production in Wyoming. The deposits range from continental deltaic to barrier and offshore bar sands.

The Almond Formation is composed of fine to medium grained sandstones interbedded with shales, silty shales, and coal units. The environments are barrier island, marsh-mudflat, and lagoonal-bay. The upper Almond facies migrate upward stratigraphicly in a westerly direction approaching the Rock Springs Uplift. The overlying Lewis Shale represents the last major marine invasion of the Upper Cretaceous sea.

Wach, P. H., 1977, The Moxa Arch, an overthrust model?: Wyoming Geol. Assoc. Guidebook, 29th Annual Field Conf., p. 651-664.

Moxa Arch is a major north-south structural feature extending from Bridger Lake, where it is over ridden by the North Uinta Thrust Fault, to at least the Big Piney-La Barge Platform, where it becomes lost in thrust faulting and attendant strike-slip faulting. The Moxa Arch may serve as a model for buried or scalped arches in the Overthrust Belt.

Wanner, J. J., D. A. Chesnut, and D. O. Cox, 1979, Gas production from tight Mesa Verde sands in Wyoming-A field case history: SPE 7934, p. 233-237.

Barrel Springs Field, Washakie Basin, Wyoming is described. Production is from Almond and Ericson sands in the Upper Mesaverde.

Weaver, C. E., 1961, Clay mineralogy of the Later Cretaceous rocks of the Washakie Basin, Wyoming: Wyoming Geol. Assoc. 16th Annual Field Trip Guidebook, Symposium of Late Cretaceous Rocks, p. 148-154.

This is one of the earliest papers dealing with the subsurface mineralogy of the Mesaverde Group. X-ray diffraction analyses of the clay size fraction of well cutting from Upper Cretaceous rocks in the Washakie Basin were used to determine that clay minerals in the Almond Formation are comprised of kaolinite, montmorillonite, chlorite, illite, and mixed-layer illite-montmorillonite. Weaver reported that montmorillonite (smectite) does not occur at depths greater than 10,000 ft because of its presumable conversion to mixed-layer illite-montmorillonite. Weaver did not attempt to distinguish authigenic from detrital clays but did mentioned that some of the kaolinite might be of diagenetic origin.

Weimer, R. J., 1961, Uppermost Cretaceous rocks in central and southern Wyoming and northwest Colorado: Wyoming Geological Assoc. 16th Ann Field Conf. Symposium of Late Cretaceous Rocks, Green River, Washakie, Wind River and Power River Basins, p. 17-28.

Upper Cretaceous stratigraphy is very complex and the nomenclature is often confused. Changes from marine to non-marine, as the Lewis Sea transgressed and regressed the area, are correlated across the region, not just in local basins. Maps show regional restorations of the stratigraphy from the Rock Springs Uplift east to the Denver Basin and south toward Grand Junction, Colorado. Petrographic samples from a wide area of localities in Wyoming and Colorado were analyzed and are presented in tables.

Weimer, R. J., 1966, Time-stratigraphic analysis and petroleum accumulation, Patrick Draw Field, Sweetwater County, Wyoming: AAPG Bull., v. 50, p. 2150-2175.

Patrick Draw Field was discovered in 1959. Although several sandstone reservoirs produce at Patrick Draw, the principal productive interval consists of two sandstone bars at the top of the Almond Formation. Spatial dimensions, lithologic character, and stratigraphic framework of the bars suggest that they are barrier-bar sandstone bodies deposited along the margin of the Lewis sea. The bars are linear and grade updip into impermeable shale and sandstone that was deposited in a swamp and lagoonal environment. A second important productive interval is approximately 40-ft below the top of the Almond Formation. The areal distribution, lithologic character, and stratigraphic framework of the sandstone in this interval suggest that it was deposited as a tidal delta in a lagoon. Each of the three major productive sand bodies have different oil-water contacts.

Weimer, R. J., and R. W. Tillman, 1982, Sandstone Reservoirs: SPE 10009, Pres. at the International Petroleum Exhibition and Technical Symposium of the SPE, Bejing, China, p. 1-5.

Patrick Draw Field was discovered in 1959. Approximately 56 MMBBL oil and 11 TFC gas have been produced (22 years). Reserves in place are estimated at 200-250 MMBBL oil. The upper 60 ft of Almond Formation consists of two sands: UA-5 (upper sandstone), UA-6 (lower sandstone).

UA-6 Sandstone: Productive in West Desert Springs Field and northern part of Patrick Draw. Gray, very fine to fine grained calcareous sandstone, ranges from 0 to 25 ft; Average thickness 12 ft. Interpreted as tidal creek channels and tidal flats west of a shoreline sand trend based on erratic distribution of production, fine grain size, close association above and below with coal beds and lagoonal shale.

UA-5 Sandstone: Main producing zone in Patrick Draw. Overlain by marine Lewis Shale, by oyster coquina layers or by 5-10 ft of carbonaceous shale and impermeable sandstone. The sandstone is quartzose, gray, fine to medium grained, calcareous and contains abundant dark gray to black chert grains and minor amounts of feldspar, quartz 64%, chert 32%, feldspar (mostly plagioclase) 4%; trace amounts of biotite, muscovite, chlorite and zircon. Cements are dominantly silica, calcite, dolomite and clay minerals (kaolinite). Thickness is 0-30 ft, lateral extent of sandbody is 20 miles long, 6 miles wide. UA-5 pinches out updip at the western margin of Patrick Draw into impermeable coal-bearing shale and siltstone.

Depositional Model: UA-5 is a shoreline sand deposit based on sedimentary structures and geometry. Unit has characteristics of prograding barrier island shoreline deposit: coarsening upward texture with burrowed sandstone near base, overlain by trough crossbeds in sets 1 to 2 ft thick with laminae of clay or carbonaceous material within the cross lamina. *Ophiomorpha* trace fossils indicate near normal marine salinity. The mesotidal range (4 to 8 ft) is based on widespread occurrence and thickness of the channel sands.

White, E. J., O. C. Baptist, and C. S. Land, 1963, Physical properties of the Almond sands in the Patrick Draw area, Wyoming: U. S. Bureau of Mines, Rept. of Invest., p. 1-19.

The Almond sandstone samples were included in part of a long term study of the relationship between the clay mineral content of reservoir rocks and water damage. The physical properties and clay content of the Almond sandstone were analyzed in the laboratory. Samples were included from a wide area of Patrick Draw Field. Susceptibility to water damage was estimated and the injectivity to water of the Almond sandstone inferred from the samples.

Wiloth, G. J., 1961, Symposium on Late Cretaceous Rocks, Wyoming and adjacent areas: *in* Wiloth, G. J. ed, Wyoming Geol. Assoc. 16th Ann. Field Conf. Green River, Washakie, Wind River and Power River Basins, 347 p.

Seven regional papers and forty papers on local basins, formations, and oil and gas fields are presented. A road log of the three-day field trip is given along with numerous maps.

Winn, R. D., Jr., S. A. Stonecipher, and M. G. Bishop, 1984, Sorting and wave abrasion: Controls on composition and diagenesis in Lower Frontier sandstones, Southwestern Wyoming: AAPG Bull., v. 68, p. 268-284.

The lower Frontier Sandstone on Moxa Arch was deposited in wave-dominated, multi-river delta plain which prograded eastward into the Cretaceous Interior Seaway. Depositional hydrodynamics largely controlled diagenesis. Fluvial sandstones contain a greater percentage of rock fragments and have less quartz than equivalent marine sandstones owing to the combined effects of sorting and wave abrasion. The coarsest sands and gravels, which were trapped on the delta plain, were initially richer in rock fragments than finer-grained sands that were passed to the shoreline. These latter sands had a significant portion of unstable grains, including chert, destroyed by wave abrasion. Quartz-rich permeable marine sandstones were cemented early by silica (that preferentially formed as monocrystalline quartz), whereas primary porosity in quartz-poor fluvial sandstones was largely preserved through this stage. Fluvial sandstones were affected more by grain dissolution, calcite replacement, calcite precipitation in open pores, and by subsequent carbonate dissolution. Fluvial sandstones generally have the best porosity and

permeability mostly due to creation of secondary porosity. Compaction in finer-grained sandstones destroyed permeability by squeezing clays into open spaces. Other major diagenetic processes are late-stage growth of kaolinite and continued precipitation of silica.

Wyoming Geological Association, 1973, Symposium and core seminar on the geology and mineral resources of the Greater Green River Basin: Wyoming Geol. Assoc. 25th Ann. Synposium and Core Seminar, Casper, Wyoming, 178 p.

A description of proper core handling and labeling techniques used for core is discussed in this paper. A map of the Greater Green River Basin designates where the samples cores were collected. Sample cores from 20 localities are shown. The cores are logged and shown with accompanying photographs. Information was donated by a number of petroleum companies from wells in the Greater Green River Basin.

Wyoming Geological Association, 1979, Wyoming Oil and Gas Fields, Greater Green River Basin (2 vols): Wyoming Geol. Assoc. Symposium, 428 p.

A complete survey (through 1978) of oil fields drilled in the Greater Green River Basin, Wyoming is presented. Each field is listed alphabetically and data is given in tabular form. The discovery well is named and dates of discovery and drilling are given. Data for each field includes; range and township location; general field data on type of trap, number and type of wells; reservoir data on formation, lithology, oil statistics and cumulative production; and structure maps. A short discussion on the history or any unique features of a field is given in a summary paragraph.

Yin, P., J. Liu, and R. C. Surdam, 1992, Petrographic and petrophysical properties of the Almond sandstone in the Washakie Basin: Wyoming Geological Assoc. Guidebook, p. 191-205.

The Almond sandstones of the Waskakie Basin are described as sublitharenite, litharenite and lithic arkose. The sands are well-sorted and fine- to very-fine-grained. Differences in framework composition, authigenic minerals, and porosity and permeability occur above and below 8,000 ft and these are defined in detail. The resulting variations in types of hydrocarbon reservoir are explained. The diageneitc changes in the Almond sandstones are the affect of durial at depths deepter than their present depth. A reconstruction of the diagenetic changes and burial history of the Almond Formation is presented using data from thin sections; grain size analysis, mineral composition, clay mineralization and cementation, and porosity and permeability profiles.

DATE
FILMED
2/17/94

END